Development of Delivery Strategies Facilitating Broad Application of Messenger RNA Tumor Vaccine

by

Kyle Kok Loong Phua

Department of Biomedical Engineering

Duke University

Date: _____

Approved:

_____

Kam W. Leong, Supervisor

_____

Smita K. Nair

_____

Fan Yuan

_____

William M. Reichert

_____

Mari L. Shinohara

Dissertation submitted in partial fulfilment of
the requirements for the degree of Doctor
of Philosophy in the Department of
Biomedical Engineering in the Graduate School
of Duke University
2014

ABSTRACT

Development of Delivery Strategies Facilitating Broad Application of Messenger RNA Tumor Vaccine

by

Kyle Kok Loong Phua

Department of Biomedical Engineering

Duke University

Date: _____

Approved:

_____

Kam W. Leong, Supervisor

_____

Smita K. Nair

_____

Fan Yuan

_____

William M. Reichert

_____

Mari L. Shinohara

Dissertation submitted in partial fulfilment of
the requirements for the degree of Doctor
of Philosophy in the Department of
Biomedical Engineering in the Graduate School
of Duke University
2014

Abstract

Genetic modification of dendritic cells with plasmid DNA is plagued with low transfection efficiencies because DNA taken up by non-dividing dendritic cells rarely reaches the nucleus. But this difficulty can be overcome by the use of messenger RNA (mRNA), which exerts its biological function in the cytoplasm and obviates the need to enter the nucleus. Since pioneering work of Boczkwoski *et al.*, [1] the *ex-vivo* application of mRNA-transfected dendritic cells as a vaccine has been evaluated in numerous phase I trials worldwide[2, 3] and is still currently being actively optimized in clinical trials.

However, a major disadvantage of using mRNA-transfected DCs as a vaccine is that it requires patients to undergo at least one 4-hour leukapheresis procedure, followed by separation of the peripheral blood mononuclear cells (PBMCs), from which monocytes are isolated and cultured for a week in a defined medium with cytokines. The resulting DCs are matured after being loaded with mRNA and frozen for storage. Aliquots are subsequently thawed prior to administration to patients. This process of harvesting, culturing and loading DCs is more time- and resource-intensive than Provenge, the first FDA approved cell based tumor vaccine in 2011.[4] Recent evidence has confirmed a lack of broad translation of Provenge due to complexity and cost of treatment. This predicates a similar fate for mRNA-transfected dendritic cell vaccine going forward.[5, 6]

This thesis presents alternative delivery strategies for mRNA mediated tumor vaccination. Through the application of synthetic and natural biomaterials, this thesis demonstrates two viable approaches that reduce or eliminate the need for extensive manipulation and cell culture.

The first approach is the direct *in vivo* delivery of mRNA encapsulated in nanoparticles for tumor vaccination. A selected number of synthetic gene carriers that have been shown to be effective for other applications are formulated with mRNA into nanoparticles and evaluated for their ability to transfect primary DCs. The best performing formulation is observed to transfect primary murine and human monocyte derived dendritic cells with an efficiency of 60% and 50% (based on %GFP+ cells) respectively. The *in vivo* transfection efficiency and expression kinetics of this formulation is subsequently evaluated and compared with naked mRNA via various routes of delivery. Following this, a proof-of-concept study is presented for a non-invasive method of mRNA tumor vaccination using intranasally administered mRNA encapsulated in nanoparticles. Results show that intranasally administered mRNA induces tumor immunity only if it is encapsulated in nanoparticles. And anti-tumor immunity is observed in mice intranasally immunized under both prophylactic as well as therapeutic models.

The second approach evaluates whole blood cells as alternative cell based mRNA carriers. A method is developed to encapsulate intact and functional mRNA in murine whole blood cells. Whole blood cells loaded with mRNA not only include erythrocytes but also T cells (CD3+), monocytes (CD11b), antigen presenting cells (MHC class II) as well as plasmacytoid DCs (CD45R-B220). Mice immunized with mRNA-loaded whole blood cells (intravenously) develop both humoral and cellular antigen-specific immune responses, and demonstrate delayed tumor onset and progression in a melanoma therapeutic immunization model (using tyrosinase related protein -2, TRP-2, as an antigen). Importantly, the therapeutic efficacy of mRNA-loaded whole blood cell vaccine

formulation is found to be comparable to mRNA-transfected dendritic cell vaccine (administered intraperitoneally).

In conclusion, this thesis presents new methods to the delivery of mRNA tumor vaccines that reduce or eliminates the need for extensive cell manipulation and culture. Results presented in this thesis reveal viable research directions towards the development and optimization of mRNA delivery technologies that will address the problem of broad translation of mRNA tumor vaccines in the clinics.

Contents

List of Figures

List of Tables

List of Supplementary Figures

Acknowledgements

I will like to thank the National University of Singapore for financial support funded through the NUS-Overseas Graduate Scholarship program (NUS-OGS). Arrangements under the NUS-OGS allowed me to take care of my retired parents without creating financial distress in the family. Without this arrangement, this thesis could not be completed. I will like to thank Dr Kam W. Leong, my thesis advisor, for financial support and scientific guidance throughout the years. As important, I will like to thank Dr Smita K. Nair, my thesis co-advisor and the pioneering investigator in mRNA-transfected dendritic cell vaccine, for her scientific support and guidance. My research career is fortunate enough to have been anointed by two prominent scientists.

I am also grateful to David Boczkwoski, who shares knowledge and experience in tumor vaccination, David Synder who taught me all my animal handling techniques, Ying Zhang who taught me the entire microfluidic chip fabrication process and many others whom I learn the diverse skills needed for multidisciplinary work required in this thesis (Megan Ho, Chai-Hoon, Mike Cook, Beth Harvat, George Pitoc).

Finally, I will like to thank my sisters for taking care of our parents in my absence.

1 Introduction

1.1 Cell Mediated (*ex-vivo*) messenger RNA tumor vaccination

1.1.1 Introduction

Over the past two decades, mRNA has gained attention in medical research as a vehicle to deliver tumor antigens as well as activation stimuli for the induction of immune response against cancer. The advantages of using mRNA for genetic modification of cells is founded on its potential for higher transfection efficiencies in non-dividing cells (no nuclear entry required), rapid expression, predictable kinetics as well as higher safety profile compared to plasmid DNA.[7] As a result, efficient genetic modification of dendritic cells which was previously difficult to achieve is now possible.

Besides higher transfection efficiencies, there are additional advantages of using mRNA as a tumor associated antigen. Firstly, the number of patients that can be treated with RNA-based vaccines is not limited by prior identification of the immunogenic peptides or knowledge of the patient's HLA (human leukocyte antigen) type. Unlike peptides that binds directly to patient's HLA molecules, tumor protein translated by mRNA works through the cellular process to generate peptides in the patient's DCs, some of which will bind to the patient's HLA molecules. Secondly, mRNA encodes the entire tumor antigen thus enabling presentation of all epitopes, instead of just a single epitope, contained within the encoded protein in the context of MHC class I molecules to CD8+ T cells. Thirdly, the use of mRNA leads to improved antigen specificity compared to DNA. [8]

Based on these advantages, the use of ex-vivo mRNA modified DCs as a cancer vaccine has been widely reported. [1-3, 7, 9-19] In 1997, the FDA approved the first clinical trial based on the use of ex-vivo mRNA-transfected DCs to induce an immune response in cancer patients. [3] Over the past decades, vaccines consisting of autologous DCs loaded with

tumor antigen mRNA have proven to be safe, well tolerated and capable of inducing tumor antigen-specific immune responses in a substantial number of vaccinated patients. Although objective tumor regression was not always observed, these clinical trials demonstrated the potential of mRNA-modified DCs for anti-cancer vaccination.

1.1.2 Preparation of mRNA transfected dendritic cell vaccine

The use of transfected DCs as a vaccine is a time- and resource-intensive process that requires that patients undergo at least one 4-hour leukapheresis procedure, followed by separation of the peripheral blood mononuclear cells (PBMCs), from which the monocytes (alternatively $CD34^+$ or $CD14^+$ cells) are isolated and cultured for a week in a defined medium with cytokines (Granulocyte-Monocyte Colony Stimulating Factor, GM-CSF and IL-4). As shown on Figure 1, the resulting DCs are further cultured with TLR agonists to stimulate maturation as mature DCs express higher levels of co-stimulatory molecules, produce greater quantities of cytokines and are superior in the stimulation of cytotoxic T-cell response compared to immature DCs.[9] TLR activators such as lipopolysaccharide (LPS), CD40L, IL-1, IL-6, IFN-γ, TNF-α and prostaglandin E_2 have been used in various combinations by different research groups and are equally capable of inducing DC maturation. [20] Matured DCs are typically frozen and aliquots are subsequently thawed prior to administration to patients.

1.1.3 Ex-vivo application of mRNA transfected DCs for tumor immunotherapy

The concept of using mRNA transfected DCs was first demonstrated in 1996 by Boczkowski *et al.* [1]. In this study, mice vaccinated with DCs pulsed with mRNA (delivered using DOTAP liposomes) from tumor expressing chicken ovalbumin (OVA) or with in vitro transcribed OVA mRNA could be protected from tumor challenge. In the same study, mice that had a primary melanoma tumor removed had significantly fewer lung metastases if they were vaccinated with DCs transfected with melanoma RNA than DCs

transfected with an unrelated RNA. Later studies show that DCs transfected with mRNA using electroporation are more effective T cell stimulators than DCs passively pulsed with mRNA (delivered via DOTAP liposomes).[8] As shown on Table 1, there is accumulating clinical evidence that vaccines consisting of autologous DCs transfected with mRNA encoding tumor associated antigens (via electroporation) are safe, well tolerated and capable of inducing tumor antigen specific immune response. [2, 3] Although objective tumor regression was not always observed, these clinical trials affirm the concept of mRNA-DC tumor vaccination and opens up opportunities for further optimization.

Several optimization approaches to mRNA-DC vaccine have been reported. The first strategy employed is the use of a cytokine cocktail to induce full DC maturation. Fully matured DCs secretes IL-12 (both subunits p40 and p70) that support T cell function, [21] express co-stimulatory molecules such as CD70/80/86,[22] chemokine markers such as CCL19 and CCL21 that increases it migratory capacity towards the lymph node,[23] as well as additional pro-inflammatory cytokines.[21] To date a few maturation cocktails have been established: namely the IL-6/IL-1β/TNF-α/PGE_2 combination, [3] the LPS/IFN-γ combination, [20] or KLH/TNF-α/PGE_2 combination. [3]

The second strategy is co-electroporation of adjuvant molecules alongside antigen encoding mRNA. The rationale of this strategy is to modulate DC function leading to enhanced DC antigen presentation capacities. For example, the co-electroporation of TriMix mRNA (CD70/ constitutiveTLR4/ CD40L) facilitates the full DC maturation without the need for overnight culture of electroporation DCs. [13] DCs can be used for vaccination immediately after their recovery from electroporation procedure. In another approach, DCs were separately loaded with mRNA encoding for anti-GITR (glucocorticoid-induced tumor necrosis factor receptor) antibody. These DCs were mixed with DCs loaded with

mRNA encoding tumor antigen and immunized into mice. GITR, a member of the tumor necrosis factor receptor superfamily, is constitutively expressed on Tregs but it is also expressed at low levels on multiple immune cells, including T cells, natural killer cells and B cells in which it is up-regulated on activation. [24] Several studies have shown that anti-GITR, alone or as an adjunct to active immunization, increases the ability to break immune tolerance. [25-27] Co-delivering DCs transfected with mRNA that encodes for GITR and tumor antigen increases therapeutic efficacy through the modulation of effector T cell suppression, although the exact mechanism has yet been delineated. [10] A third co-delivery approach is to co-electroporation siRNA that targets immunoproteasomes in DCs. Many cancers, including melanoma, exclusively express constitutive proteasomes and are unable to express immunoproteasomes. In contrast, mature DCs used for immunotherapy exclusively express immunoproteasomes. Since proteasomes generate peptides presented by HLA class I molecules, knocking down immunoproteasomes (with siRNA) skews peptide production towards constitutive proteasome. The idea is to increase the quality of antigen presentation leading to enhanced anti-tumor immunity. This approach has been shown to be effective in patients as circulating melanoma cell levels fell, and T cell lytic activity against autologous melanoma was induced. Of two subjects with active disease, one had a partial clinical response, while the other, who exhibited diffuse dermal and soft tissue metastases, had a complete response. [15]

The third optimization strategy is the determination of the route of delivery that will lead to highest lymph node accumulation, immune response or clinical outcome. mRNA transfected DCs need to reach the lymph nodes to induce a potent immune response. Different routes of vaccination such as intradermal (ID), subcutaneous (SC), intranodal (IN) as well as intravenous (IV) administrations have been tested during clinical trials. Labelling of DCs with Indium^{111} and subsequent imaging of their migration has

demonstrated that SC administered DCs rarely reach lymph nodes. Similarly, IV injected DCs does not result in their accumulation in lymph nodes but in an initial accumulation in the lungs and subsequent redistribution to the liver, spleen and bone marrow. [28] In contrast, about 4% of ID administered DCs are recovered from lymph nodes. [29] In addition, DCs were shown to co-localize with T cells efficiently in draining lymph nodes after intranodal administration. [30] Importantly, in a study that compared intranodal and intradermal administration of ex vivo modified DCs in patients with advanced melanoma found that despite a higher number of DCs in lymph nodes after intranodal administration, intradermal injection proved to be superior in inducing functional tumor antigen-specific T cells. [31]

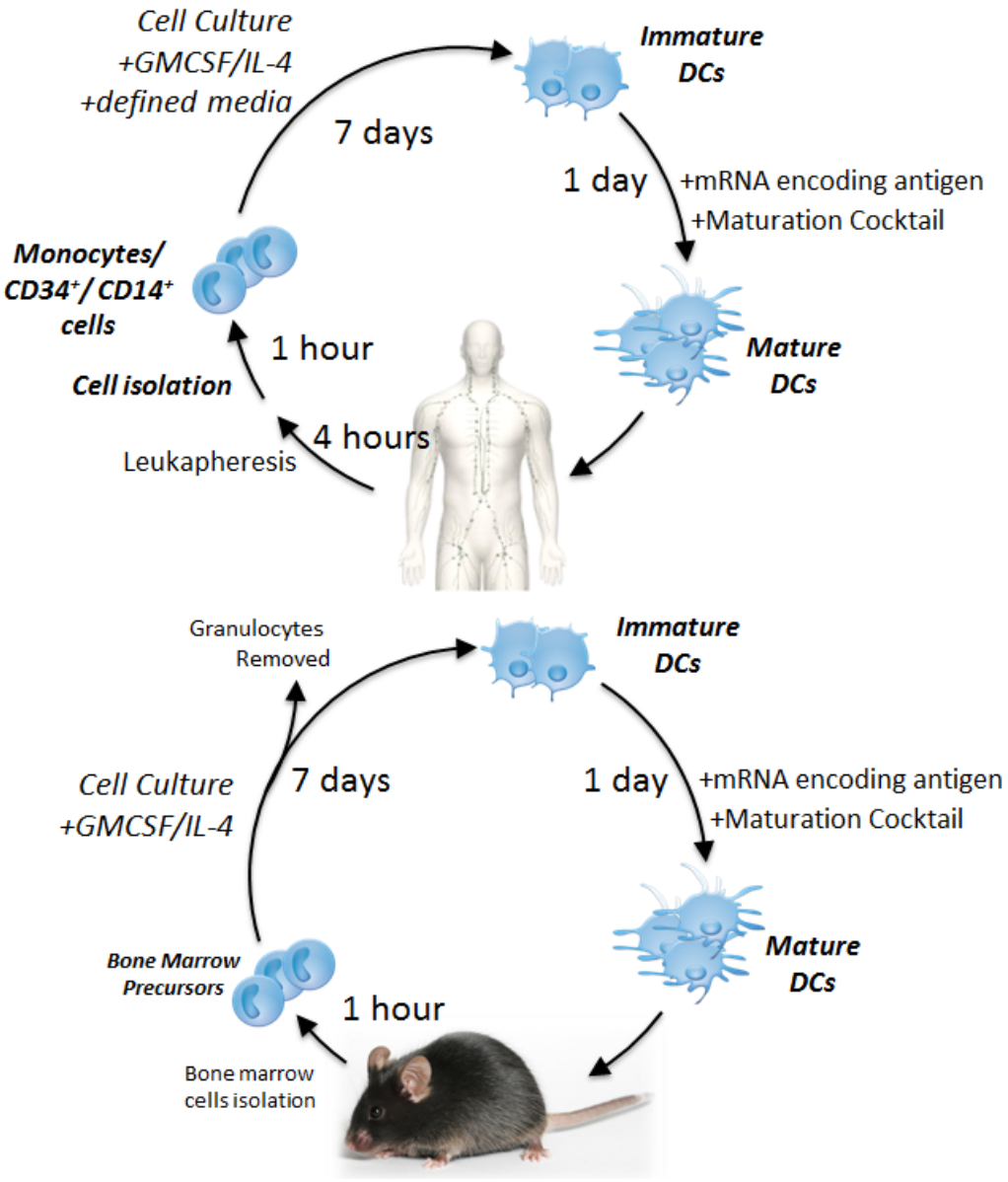

Figure 1. mRNA dendritic cell vaccine preparation process in mouse and humans

Table 1. Clinical efficacy of *ex-vivo* application of mRNA transfected DCs for tumor immunotherapy

Ref	Cancer Type	Route	Vaccination Schedule	Antigen mRNA	Clinical Response	
'03	Colorectal	IV	10^6 DCs pulsed with 25 µg RNA and KLH 4 times at monthly intervals	Total Tumor RNA	No clinical response	
'02	Metastatic Prostate cancer	IV/ID	1-5x10^7 DCs 3 times biweekly with escalating dose and 10^7 given ID	PSA mRNA	Reduced serum PSA levels (6/7), undetectable circulating tumor cells (3/7)	
'03	Renal carcinoma	IV/ID	IV: 1-5x10^7 DCs , ID: 10^7 DCs 3 times biweekly with escalating dose	Total Tumor RNA	7/15 SD	None
'03	Metastatic CEA expressing tumor (lung, breast, colon)	IV/ID	Phase I & II: 10^7–10^8 DCs (IV), 10^6 DCs (ID) 4 times biweekly	CEA mRNA	Phase I: 3/24SD,1/24 CR	Phase I:18/24PD Phase II: 13/19 relapse
'04	Brain cancer	IV/ID	0.5–5×10^7 DC/m^2, 3 times biweekly with escalating dose, 3 times at 3-mo intervals	Total Tumor RNA	4/7 SD	2/7 PD
'05	Neutroblastoma	IV/ID			1/11 SD	-
'05	Prostate Cancer	ID	10^7 DCs, 3 times or 6 times weekly	hTERT hTERT-LAMP1	None	
'05	Renal carcinoma/ovarian cancer	ID	10^7 DCs 3 times biweekly, 18 µg/kg DAB389IL-2 (ONTAK) given prior to vaccination	Total Tumor RNA	-	8/11 PD
'05	Androgen resistant prostate cancer	ID/IN	2x10^7 DCs 4 times weekly		ID:6/9 SD IN:5/10 SD	ID:3/9 PD IN:5/10 PD
'06	Metastatic melanoma	ID/IN			ID: 1/8 SD IN:1/12SD	ID:7/8 PD IN:11/12PD
'10	Acute myeloid leukemia	ID	0.5-2x10^7 DCs , 4 times biweekly	WT-1 mRNA	-	-
'12	Advanced Melanoma	IN	10^7 DCs 3 times biweekly	TriMix,GP100,Tyrosinase	Stage3:12/26 Stage4:5/19	Stage3:1/26 Stage4:1/19
'13	Advanced melanoma	IV/ID	IV/ID: ~10^7 DCs	TriMix,MAGE-A3,C2, Tyrosinase,GP100-DC-LAMP	2/15 CR 2/15 SD	-

Abbrev: i.d., intradermal; i.n., intranodal; i.v., intravenous; KLH, keyhole limpet hemocyanin; DTH, delayed type hypersensitivity; hTERT , human telomerase reverse transcriptase; PSA, prostate specific antigen; CEA , carcinoembryonic antigen; SD, stable disease; CR, complete response; PD, progressive disease; LAM P-1, lysosome-associated membrane protein-1; PGE2, prostaglandin E2; IL, interleukin; TN F, tumor necrosis factor; WT-1, Wilms' tumor-1; TAA , tumor-associated antigen; HLA, human leukocyte antigen; IFN, interferon; TriMix mRNA , a mix of 3 mRNA molecules encoding CD70, CD40L and a constitutive active form of toll-like receptor 4 (caTLR4);

1.2 Nanoparticle mediated (direct *in vivo*) messenger RNA tumor vaccination

1.2.1 Introduction

The attractiveness of mRNA delivery is founded on its potential for higher transfection efficiencies in non-dividing cells (no nuclear entry required), rapid expression, predictable kinetics as well as higher safety profile compared to plasmid DNA.[7] mRNA delivery is gaining attention because of a gradual acceptance from the research community that *in vitro* transcribed mRNA is not as biologically labile as initially thought. Improved understanding on mRNA stability from the basic biological research[32] in the last decade has led to optimized designs of *in vitro* transcribed mRNA. Structural features such as 3' globin UTR, anti-reverse cap analogue, polyA tail as well as use of modified nucleotides have all led to enhanced mRNA translation.[33] Such improvements made an impact in the clinic as dendritic cells (DCs) can be transfected efficiently with *in vitro* transcribed mRNA and subsequently applied as a tumour vaccine. It has also led to the development of alternative cell based approaches[34, 35] as well as direct in vivo injections of mRNA in naked[19, 36] and nanoparticle formats.[37-42]

Besides established clinical infrastructure for the manufacturing and quality control of GMP grade mRNA, the biological stability of mRNA has reached a threshold where mRNA application may be extended even further through biomedical engineering principles. The most common manipulation of mRNA is their encapsulation into nanoparticles for enhanced delivery efficiencies. While there is a handful of published data on mRNA nanoparticle mediated tumour vaccination, there is currently no mRNA nanoparticle vaccine in clinical trials, thus making this is an active area of

research in nanomedicine. There is also growing interest in gene delivery groups who are venturing into the mRNA arena, as well as mRNA vaccinologists who are venturing out in search for effective ways to deliver mRNA to antigen presenting cells *in vivo*. It would seem that after almost two decade of advances made in nucleic acid delivery systems of RNAi and DNA that we would have solved the problem of mRNA delivery to dendritic cells, but we have not, at least not yet. Nevertheless, a good understanding of gene delivery barriers has been achieved in the gene delivery field and many tools have also been developed to address these delivery barriers. In addition, the immunological properties of mRNA, signalling pathways through pattern-recognition receptors (e.g. TLR, RLRs) and their implications on immune responses have also been characterized in recent years. Hence, we are at an appropriate juncture in time where knowledge in engineering sciences can accelerate the clinical translation of mRNA and help fulfil its true potential.

In this chapter we will first discuss whether mRNA is amenable for engineering manipulation. We will then draw on knowledge of gene delivery and mRNA immunotherapy to put together a frame work for mRNA nanoparticle tumour vaccination. This frame work is a set of delivery and biological barriers highlighting rate limiting steps to antigen presentation mediated by mRNA nanoparticle vaccine: gene delivery (extracellular and intracellular), immune activation and MHC presentation (Figure 2). We will describe and discuss these barriers within the context of genetic immunization with examples from published studies on mRNA nanoparticle tumour vaccination and DC transfection. Studies evaluating the optimal application of mRNA nanoparticle vaccination have often been performed in niche

areas (either delivery focused or immunology focused). It is also the aim of this review to put these studies together into an overall picture to help identify bottlenecks to mRNA nanoparticle mediated immunization.

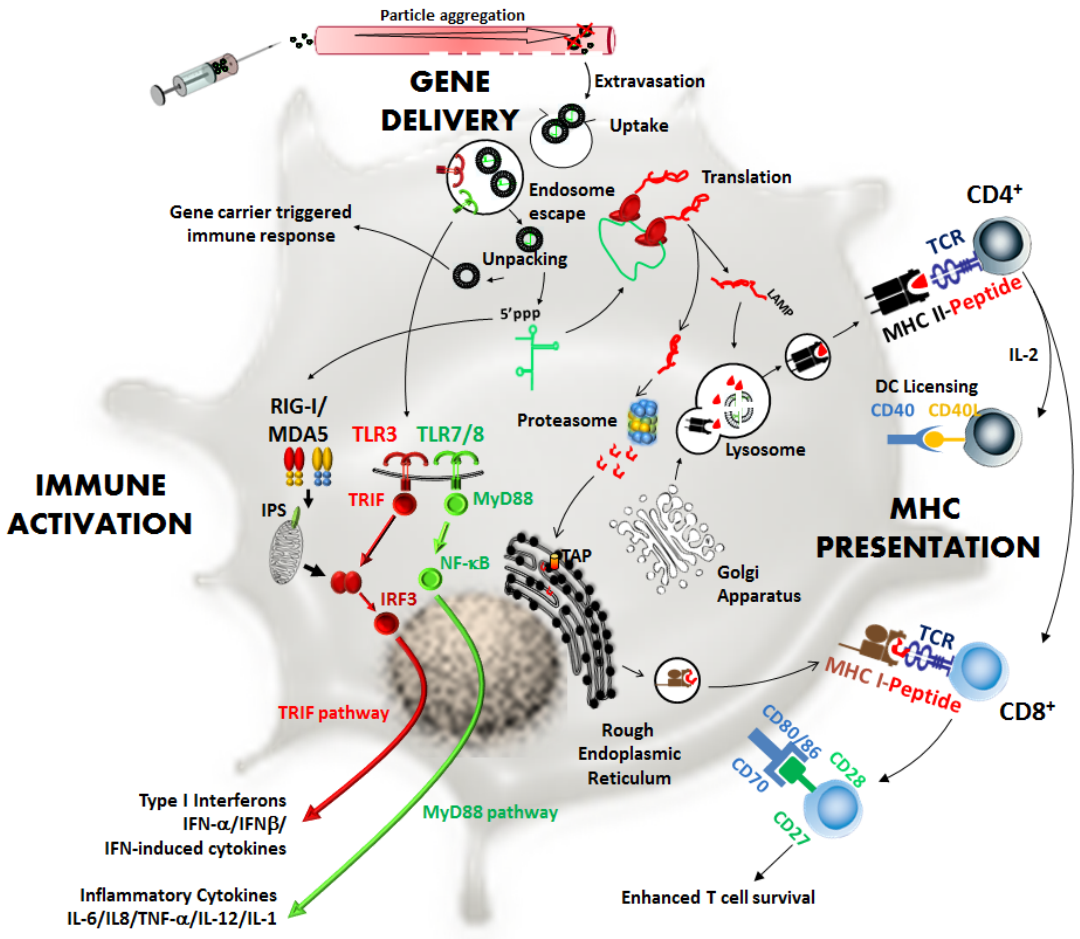

Figure 2. Frame work for mRNA nanoparticle mediated tumor vaccination.
Proposed frame work for mRNA nanoparticle mediated tumour vaccination. A combination of three overlapping processes determines immune response: gene delivery, immune activation, and major histocompatibility complex (MHC) presentation. In this framework, nanoparticles administered into the body have to overcome extracellular barriers from the site of administration to antigen presenting cells. After cell uptake, nanoparticles have to escape the endosome and mRNA has to unpack from the gene carrier and enter the protein translation pathway. At the same time, through pattern recognition receptors, mRNA nanoparticle needs to mediate immune activation (via TLR3,7/RIG-I,MDA5) so that cytokines are secreted for ensuing adaptive immune responses. Protein translated from delivered mRNA molecule needs to enter both the MHC I (via proteasome) and II (via lysosome) processing pathways so that antigen peptides can be presented on both MHC I and II molecules.

1.2.2 Is mRNA stable enough for biomedical manipulation?

From the delivery efficiency perspective, one key advantage of using mRNA for gene therapy is that transfection can be achieved without the need for the gene to enter the nucleus. Consequently transfection of non-dividing cells (e.g. DCs, T cells, neurons), which were previously considered unattractive candidates for non-viral gene therapy, are now actively being investigated[7, 43, 44]. The rationale and other advantages for using mRNA as an antigen encoding molecule have also been well reviewed[11, 17, 18, 45, 46]. It is undeniable that mRNA is built by nature and shaped through evolution to be transient messengers of genetic information. But alongside advances in molecular biology, substantial progress has been made to understand the regulation of mRNA biological stability,[32] and improved understanding on various mechanisms of mRNA degradation has led to a focused effort to optimize the mRNA structure for enhanced intracellular stability and increased protein translation capabilities. These studies demonstrate the importance of an optimized 5' cap analogue, a 3'UTR globin sequence and a sufficiently long poly-A tail in the structural makeup of the mRNA, leading to increased gene expression in dendritic cells.[17] More recently, investigations into the TLR mediated immunogenicity of mRNA have led to the development of modified mRNA. It was initially observed that endogenous RNA are significantly less potent in triggering TLR mediated immune response than *in vitro* transcribed RNA.[47] It was then discovered that modified nucleotides (e.g. pseudouridine) contained within endogenous RNA not only suppressed immune responses, but also enhanced protein translation in mRNA transcribed with these modified nucleotides[48]. The mechanism of enhancement is predominantly caused by a lack of Type I interferon secretion from transfected cells and to a lesser extent modified mRNA's enhanced intracellular stability[48]. The conclusions make sense since

modified nucleotides are also building blocks of structural RNAs such as ribosomes, which are non-immunogenic and relatively resistant to degradation.

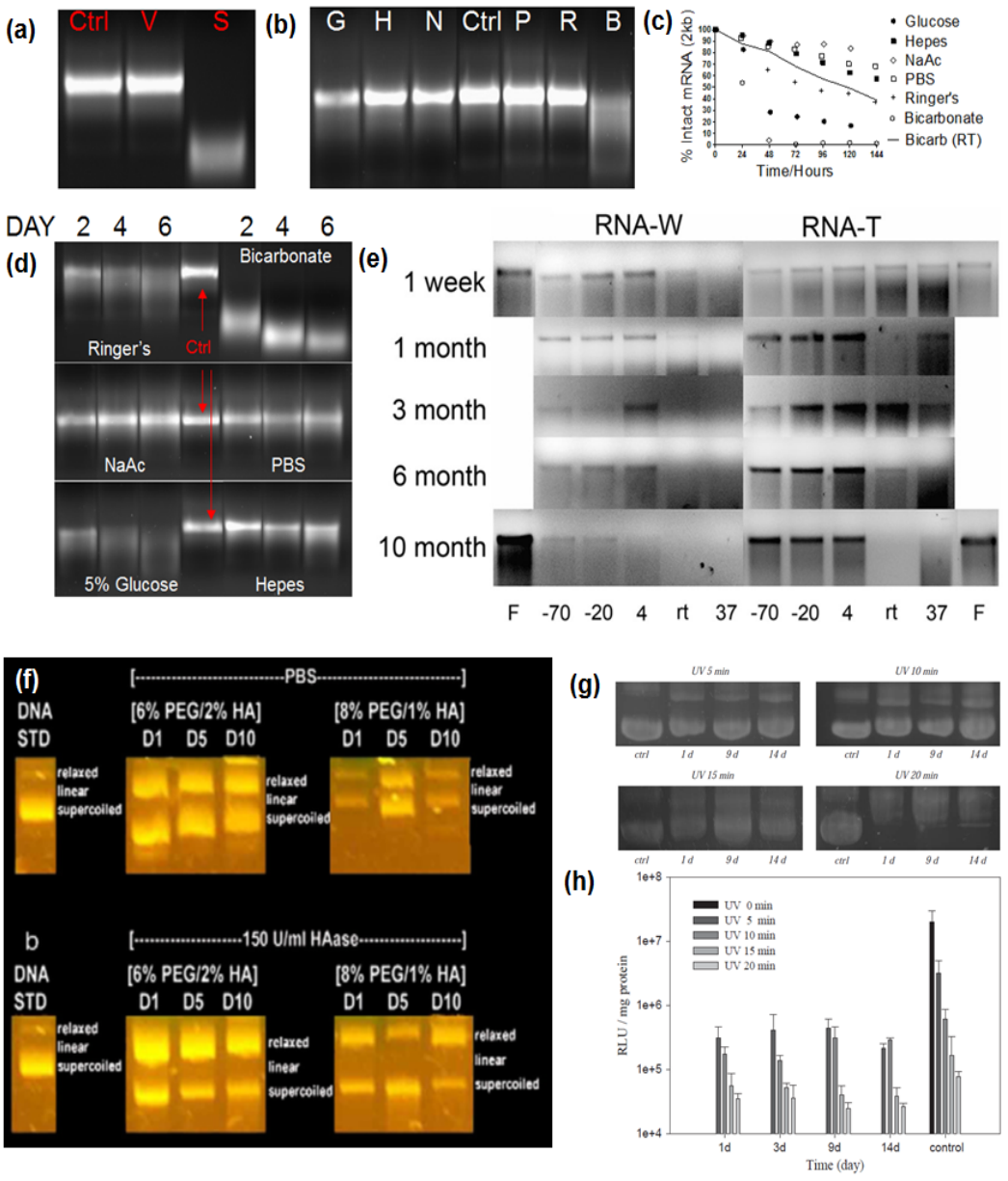

Figure 3. Solution stability of mRNA.

(a) Ctrl: control, V: mRNA vortexed at max speed for 9 minutes and incubated at 4oC overnight, S: mRNA sonicated (bath-type) for 3 minutes.

(b) Agarose gel electrophoresis of mRNA diluted into various buffer (200μg/ml) and incubated at room temperature for 6 days. G: 5% glucose (unbuffered solution), H: 100mM Hepes, N: 100mM sodium acetate, Ctrl: control mRNA stored at -20oC, P: PBS, R: Ringer's lactate, B: 0.75% sodium bicarbonate.

(c) Degradation profiles of mRNA analyzed on agarose gel (quantified with densitometry analysis). mRNA is incubated at 37oC in various buffers (symbols) or at room temperature in sodium bicarbonate (line)

(d) Agarose gel electrophoresis analysis on structural integrity of mRNA incubated at 37oC in various buffers over 6 days (only day 2,4,6 are shown).

(e) Agarose gel electrophoresis of mRNA stored in water (RNA-W) or trehalose (RNA-T) over time. "F" indicates freeze-dried RNA.[49]

(f) Agarose gel electrophoresis analysis of structural integrity of DNA encapsulated in PEG cross-linked hydrogels

(g) Agarose gel electrophoresis analysis of structural integrity of DNA encapsulated in UV-cross-linked hydrogels.[50]

(h) Bioactivity of DNA released from hydrogels cross-linked using different UV intensity.[51]

(a) – (d) are unpublished data. (e)-(h) are reproduced with permission.[49,50,51]

Enhanced biological stability and performance of mRNA *in vivo* attract the attention of biomedical engineers because of the opportunities to incorporate mRNA into medical devices for therapeutic applications. Being a "late bloomer", many devices that have been built for DNA have not been well developed for mRNA, such as nano-/micro-particles, transcutaneous microneedles,[52, 53] hydrogels[50, 51, 54] and other macroformulations[55]. The question then becomes whether mRNA can be physically and/or chemically stable enough to be manipulated under fabrication conditions. Through various publications from biomedical engineering groups, it can be certain that mRNA can withstand conditions associated with nanoparticle formulation. As shown in Figure 3a (unpublished data), mRNA can withstand significant vortex-induced shear stress, but rapidly degrades upon sonication. Freeze dried mRNA and mRNA stored in trehalose at 4°C can remain stable for up to 10 months (Figure 3b).[49] The former is a feasible method to obtain highly concentrated mRNA dissolved in the desired buffer compared to column recovery (e.g. RNeasy cleanup kit). Solution stability of naked mRNA is a key piece of information currently missing in the context of the development of controlled release devices such as hydrogels. Notwithstanding commercially available RNA storage solutions of proprietary nature, to develop encapsulation technologies, biomedical engineers need to know the physical stability of *in vitro* transcribed mRNA in common defined buffers. At present, this information can only be found for pure water and trehalose (Figure 3b).[49] In fact, mRNA can be highly stable at room temperature but degrades with varying degrees at physiological temperature (Figure 3c, 3d and 3e). Degradation is a result of chemical hydrolysis of the phosphodiester bond of mRNA backbone caused by nucleophillic attack from hydroxide ions or 2'-OH group present in the ribose sugar residues of mRNA itself. At 37°C, mRNA remains relatively stable in

Hepes, PBS and sodium acetate, degrades gradually over time in Ringer's lactate and 5% glucose (non-buffered) solution, but degrades rapidly in sodium bicarbonate (Figure 3e). Using densitometry quantification (Image J), degradation profiles in different buffers at 37°C are quantified and plotted on Figure 2c. At room temperature, mRNA remains stable in all buffers except sodium bicarbonate (Figure 3d). At 4°C, mRNA is highly stable in all buffers including bicarbonate (data not shown) and is consistent with published data shown in Figure 3b.

The solution stability of mRNA is indeed lower compared to plasmid DNA. Plasmid DNA's solution stability has been demonstrated in hydrogels. Agarose gel electrophoresis shows that DNA recovered from PEG cross-linked hydrogels remain intact after being left at 37°C for up to 10 days (Figure 3f)[50] and 14 days (Figure 3g)[51], respectively. The proportion of DNA in relaxed conformation increased while the supercoiled conformation decreased over time.[50, 51] This is consistent with stability studies conducted in our lab (data not shown). While UV can inactivate plasmid DNA in a dose dependent manner, changes from coiled to relax conformation did not significantly affect the bioactivity of plasmid DNA released from hydrogels throughout the 14 day duration of the study (Figure 3h).[51]

In summary, mRNA is highly shear resistant and hence it can be mixed more efficiently with gene carriers during formulation to form higher quality particles. In addition, solution stability of mRNA is not a limiting factor in the fabrication of mRNA based biomedical devices because it is compatible with commonly used buffers and can remain stable at room temperature during the fabrication process. However, it will may limited by chemical hydrolysis at physiological temperature and may not be suitable for long term

release kinetics. This is a rate limiting step for applying mRNA in medical devices such as micro-needle technology. Hence improving solution stability of naked mRNA at physiological temperature will be a significant advancement in this area

1.2.3 Barriers to Non-Viral mRNA Nanoparticle Tumor Vaccination

mRNA nanoparticle tumour vaccination is a multifaceted process. The first stage implicates the gene delivery process (Gene Delivery, Figure 2) where nanoparticles encapsulating the mRNA need to overcome extracellular barriers to enter antigen presenting cells, and then intracellular barriers to release the mRNA so that it can be expressed in the cytoplasm. In second stage, the protein translated from mRNA has to be optimally presented on major histocompatibility complexes (MHC) molecules (MHC presentation, Figure 2) so that T cells can be activated through the recognition of MHC-peptide complexes. In the third stage, antigen presenting cells needs to be immunologically primed (Immune Activation, Figure 2) so that it can provide the necessary co-stimulatory signals and pro-survival cytokines to ensure the robust development and proliferation of antigen-specific T cells to perform its therapeutic function. These three stages form a framework of barriers through which mRNA nanoparticles have to overcome in order to achieve success, and will be the subject of the following section.

1.2.3.1 Extracellular Gene Delivery of Nanoparticles to Target Organs

The gene delivery process is the first hurdle to mRNA nanoparticle vaccination (Figure 2). When mRNA nanoparticles are administered, they need to translocate to the target organ and be efficiently taken up and expressed by antigen presenting cells. To achieve the former, nanoparticles have to overcome extracellular barriers defined as the

impediments to efficient transport of nanoparticles from the point of administration to the antigen presenting cells. To achieve the latter, nanoparticles have to overcome intracellular barriers defined as the ability to escape the endosomes and efficiently released from the gene carrier (discussed in the next section). The route of administration, no doubt, determines the magnitude of extracellular barrier. As this is a diverse yet well reviewed topic,[56-58] we will focus our discussion on extracellular barriers of systemic, subcutaneous and intranasal route of administration, highlighting delivery barriers and ideal nanoparticle properties.

1.2.3.2 Systemic Administration

In systemic delivery, colloidal stability of mRNA nanoparticles is critical to ensure efficient transport through the blood stream to the target organs, preferably the spleen. Colloidal instability can be caused by particle aggregation when cationic gene carrier itself bridges anionic phosphate groups of the nucleic acids. When injected into the systemic circulation, positively charged nucleic-acid nanoparticles will further aggregate through interaction with erythrocytes and other negatively charged serum proteins such as albumin, IgM, IgG, complement C3. Ho *et al.* showed that DNA-polyplexes formulated with Turbofect© (poly*(*2-hydroxypropyleneimine)) aggregates rapidly via the first mechanism unless its formulation is confined within picoliter volume droplets generated by a microfluidic chip.[59] Li *et al.* also showed that the particle size of non-pegylated liposome-protamine-DNA complexes (LPD) increases from 135nm to 647nm after they were mixed with serum.[23] Particle aggregation creates a problem because upon reaching the target organ, they become too large to extravasate out of the blood capillaries through the endothelial fenestrations to get to the underlying cells (Figure 2).

Blood vessels in the liver and spleen are organized into sinusoids, where endothelial fenestrations are wider and blood flows slower. This allows nanoparticles that remained stable (or did not appreciably aggregated) to extravasate into the tissues reaching the inner hepatocytes in the liver or white pulp cells in the spleen (predominantly T cells, DCs and macrophages). Aggregated particles that are too large to pass through the endothelial fenestrations they will be cleared from the blood stream by Kupffer cells found in between hepatocytes in the liver lobules (Figure 4a) and marginal zone macrophages (MZϕ) in the spleen (Figure 4b) via scavenging receptor-mediated endocytosis. The particles distributed via intravenous administration are unevenly distributed. For example, 60% and 55% of intravenously injected non-pegylated LPD lipopolyplexes[56] and PEI-25K-DNA polyplexes [60] accumulated in the liver. Similarly, 80% and 10% of mRNA lipopolyplexes administered intravenously via the tail vein accumulated in the liver and spleen respectively.[40]

As lipid-based nanoparticles are the most frequently evaluated formulation for mRNA immunization, we will further elaborate on its *in vivo* distribution. Lipid-based nanoparticles that are distributed to the spleen after IV administrations are sequestered in the splenic marginal zone after 12 hours and gradually move out into the white pulp (T cell region) after 24 hours (Figure 4c). At the 24th hour time point, an increased infiltration of CD11b^{+} and CD11c^{+} cells in the spleen is detected.[61] At this time, about 25% of splenic CD11b+ cells and 15% of splenic CD11c^{+} cells are reported to have taken up lipopolyplexes (e.g. LPDs) distributed to the spleen after intravenous administration,[61] but only about 4% of CD11c^{+} cells express the encapsulated GFP mRNA.[40] The transfection efficiency of CD11c^{+} cells is increased (from 4% to 13% based on GFP+ cells) when mRNA lipopolyplexes are functionalized with mannose.[40] As macrophages

can also present antigens to T cells after being activated via a ROS mediated pathway[62] directly by themselves or indirectly through DCs, the total number of antigen presenting cells targeted by intravenous administration is actually quite reasonable. Still, this may not be an efficient strategy because a significant amount of nucleic acid is actually taken up by the liver and not the spleen. These nucleic acids that are distributed to the liver are also very poorly expressed,[23, 60] presumably degraded by Kupffer cells. Similarly, splenic MZϕ and immature DCs both engender highly degradative endocytic pathways[27] that break down intracellular cargoes destined for MHC class II processing through the endosome-lysosome pathways (Figure 2).[63] Hence, it is important that nanoparticles must be able to escape from the early/late endosome efficiently, otherwise a large proportion of the mRNA nanoparticles taken up by the DCs and macrophages in the spleen will be degraded. In addition, due to a lobe-sided biodistribution, large nanoparticle doses will be required to achieve adequate splenic transfection, which may lead to gene carrier mediated toxicities. Nevertheless, there have been numerous reported CTL assay that proved intravenous administered mRNA nanoparticle formulations can activate antigen specific CTLs.[37, 39-41, 64, 65] These studies will be reviewed in later sections. Whether such CTL levels are robust enough to achieve therapeutic responses comparable to mRNA-DC vaccine remain to be seen. To summarize, for systemic administration of mRNA nanoparticles, it certain that the nanoparticles will be taken up by antigen presenting cells in the liver and spleen. However, a large dose is necessary because the particles are distributed poorly to the spleen and DCs are not efficiently transfected. Hence for IV administered mRNA nanoparticle vaccine formulations, improving splenic distribution, transfection efficiency

of splenic DCs and evaluating these parameters against therapeutic outcome are issues that should be addressed to advance the field.

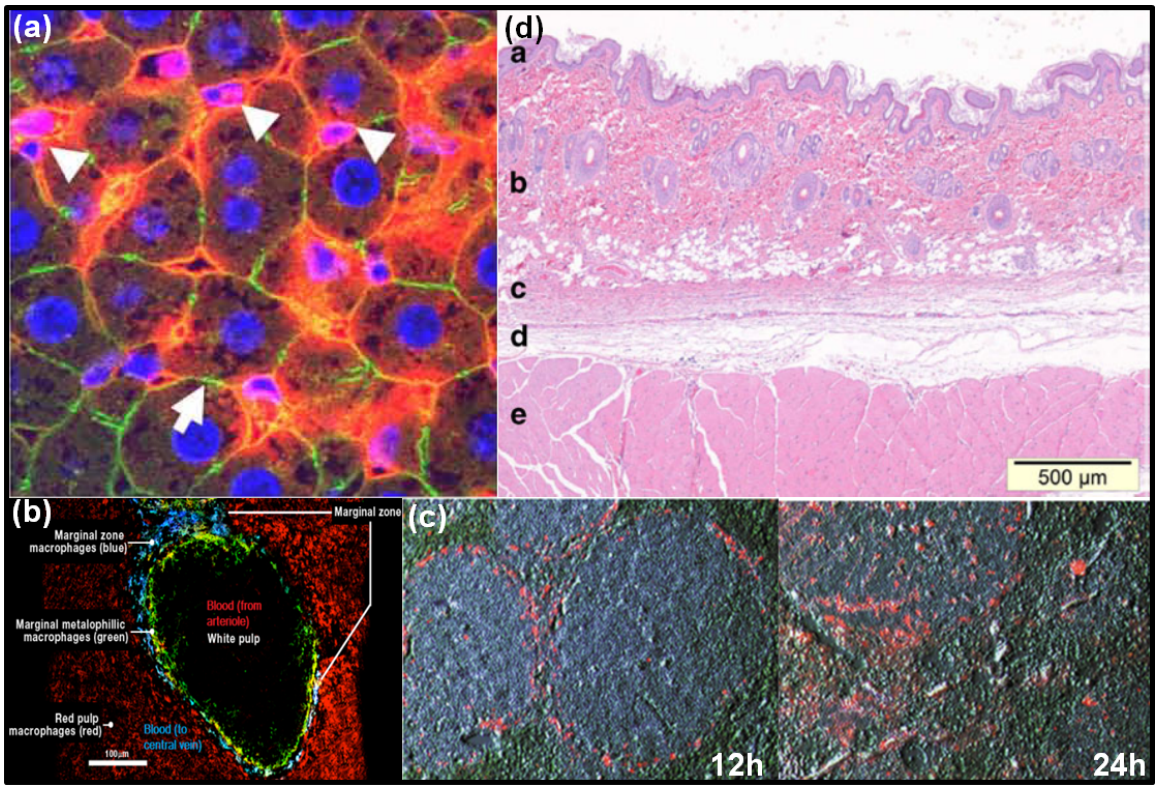

Figure 4. Histology of murine liver, skin and spleen

(a) Cross section of murine liver sinusoids. Systemically administered non-pegylated fluorescently labeled LPD lipoplexes trapped within the sinusoids of liver lobules and taken up by Kupffer cells (white arrows).[66] Red: LPD, Blue: DAPI, Green: Phalloidin.

(b) Immunostain of mouse spleen's cross-section showing locations of white pulp (DCs & T cells) and marginal zone. Blood flow direction from white to red pulp. (Blue: marginal zone macrophages; green: marginal metalophillic macrophages; red: red pulp macrophages).

(c) Localization of non pegylated LPD in mouse spleen 12 and 24 hours after intravenous administration.[67]

(d) Anatomy of the skin. (a epidermis, b dermis, c skin (panniculus) muscle, d subcutaneous connective tissue, and e skeletal muscle of trunk).[68] Reproduced with permission.[68,66,67.]

1.2.3.3 Subcutaneous Administration

In subcutaneous administration, the objective is to deliver mRNA encapsulated nanoparticles to lymph node DCs through the lymphatic system (and transfecting them), or alternatively transfect dermal dendritic cells already present in the skin. Although intradermal injection may be more favourable due to the prevalence of dermal DCs, administering a single dose precisely within the thin layer of dermis ('b' in Figure 4d) may be a challenging procedure in mice models, where most experimental vaccination studies are conducted. The subcutaneous space is a non-cellular region ('d' in Figure 4d) found between the skin and skeletal muscles ('c' and 'e' in Figure 4b) that can be easily accessed through skin folding. Consequently, extracellular barriers associated with this subcutaneous vaccination are related to poor targeting of dermal dendritic cells and trafficking efficiency of particles to the lymph nodes.

Studies conducted to investigate the determinants of lymphatic trafficking reveal that that particle size, charge and colloidal stability are factors influencing the rate of transport through the subcutaneous space. Although particles in these studies were made with a wide range of materials, there is a consensus that ultra-small particles (<50nm) are the most efficiently transported[69, 70], while those ranging from 100nm to 300nm can also reach the lymph nodes[64, 69-75]. Proteins (~7% by mass, predominantly albumins and globulins) are also present in interstitial fluids[76] but their concentrations are significantly lower compared to blood and as a result particle aggregation may not be a significant impediment in subcutaneous vaccination.

Another observation made by Moghini *et al.* [72] using neutral DOPC liposomes is that increased particle hydrophilicity (via pegylation) enhanced trafficking efficiencies through

reduced non-specific interactions with interstitial proteins. In a similar study, Zhuang *et al.* [71] showed that a high cationic charge on DOTAP liposomes (ζ-potential: +43mV) significantly reduce its trafficking capacity (Figure 5a) compared to pegylated DOTAP liposomes (ζ-potential: +15mV). Pegylated liposomes appeared in the lymph node as soon as 30 minutes after administration compared to 4 hours (non pegylated), confirming a passive lymphatic transport mechanism (note: transport of Evans Blue subcutaneously through the tail base labels the inguinal lymph node within 30 minutes[77]). Notably in both studies, increasing PEG length accelerated particle transport, but they could not be efficiently retained in the lymph node (Figure 5b). Beside liposomes, polymeric particles composed of chitosan/heparin (size: 200nm to 1μm, ζ-potential +25mV) can be found in popliteal lymph nodes 45 minutes after footpad injection (Figure 5c).[73]

Although nodal transfection mediated by subcutaneously administered mRNA nanoparticles have not been well studied, transfection efficiency and transgene expression kinetics mediated by mRNA nanoparticles at the subcutaneous site has been reported. mRNA subcutaneously administered in nanoparticle form is not only more poorly expressed, but is also expressed over a shorter period of time compared to naked mRNA at the site of injection.[78] The poor local transfection performance may be caused by entrapment within the extracellular matrix, while naked mRNA can diffuse through the ECM to reach muscle and dermal cells on each side. Although particle properties were characterized (250nm in 50% serum, ζ-potential -15mV), their transport to the lymph node has not been determined. On the other hand, the fact naked mRNA can mediate high transfection efficiencies via subcutaneous administration shows that it can remain

relatively stable in the subcutaneous space. However, it could not remain stable enough to be transported through the lymphatics to the lymph node.[36]

Despite of a lack of direct evidence of nodal DC transfection from subcutaneously administered mRNA nanoparticles, antigen specific CTL cell responses are efficiently induced[37, 38, 41] and anti-tumour therapeutic responses have been reported.[37] These studies indicate that dermal DCs may play a significant role in the induction of immunity for subcutaneously injected mRNA nanoparticles.

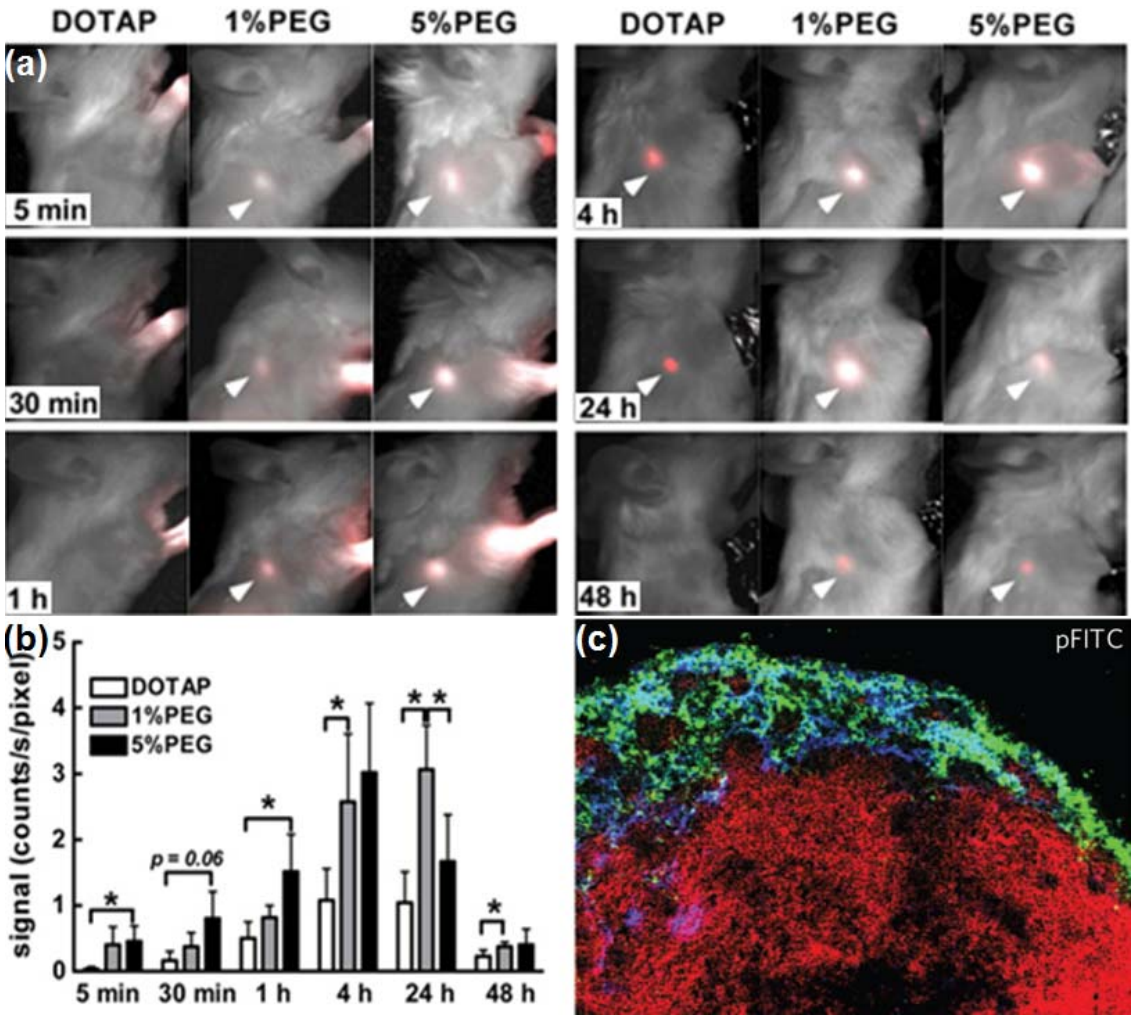

Figure 5. Nanoparticle trafficking after subcutaneous administration

(a) Lymph node trafficking of DOTAP liposomes (0%/1%/5% PEG) over six time periods.[71]

(b) Distribution of DOTAP Liposomes (0%/1%/5% PEG) in the lymph node over time measured based on radioactivity.[71]

(c) Popliteal lymph nodes isolated 45 minutes after injection of heparin-polylysine particles. Green: polylysine, Blue:Lyve-1 (lymphatic endothelial cells), RED: B220(B cell marker).[73]

(d) Anatomy of the skin. (a epidermis, b dermis, c skin (panniculus) muscle, d subcutaneous connective tissue, and e skeletal muscle of trunk).[68]

Reproduced with permission.[68,71,73]

1.2.3.4 Intranasal Administration

In intranasal administration, particles are directly delivered to lymphoid tissues located in the nasal cavity (Figure 6a) avoiding barriers posed by systemic or lymphatic transport discussed earlier. Immune cells within these lymphoid tissues are arranged in an organized follicular tissue structure (nasal associated lymphoid tissue, Figure 6b)[79] found directly under the nasal epithelium. The objective is to deliver particles through the thin nasal epithelium to the immune cells composed of not only B and T cells, but also dendritic cells (Figure 6c, 6d). The nasal epithelium above the NALT is a single layer of epithelial cells littered with microfold cells (M cells). M cells are of interest in nasal particle delivery because they translocate particles from the epithelium to the underlying NALT.[80] Particles translocated by M cells may be taken up by NALT cells, drained passively to the cervical lymph nodes through lymphatic vessels or transported actively through DCs that took up these particles. Particle size (and aggregation issues) may not be a significant barrier to transport across the nasal epithelium because M cells are known to translocate particles with sizes up to several microns.[81] Nevertheless, many studies show that particles at or below 1 micron tend yield better functional outcomes.[81-83] As the epithelial surface is negatively charged due to the presence of the glycocalyx, particles with net positive charges have been reported (and expectedly so) to mediate better immune responses. Ironically, particles with higher negative zeta potentials (at least -25mV) can also be efficiently transported by M cells.[82, 83] It appears that decreased ionic concentration of the buffer used to suspend the particles can increase M cell uptake, through potentiating particle charge density.[82]

The relatively permissive transport mechanism through the nasal epithelium is undermined by the fact that fluid instilled into the nasal cavity is rapidly clear from the

nose shortly after administration (80% by mass within the first hour).[84] Therefore increased particle adhesion onto the nasal walls, especially through the use of mucoadhesive materials such as chitosan can enhance immune responses albeit at a very high dose.[85, 86] Although mucoadhesion increases the residence time of particles on the nasal epithelium, it can also impede their movement through the mucus, making it a property that needs to be carefully applied to achieve optimal results.[87] We have reported nasal transfection with lipid based mRNA nanoparticles (180nm, +40mV in water).[78] Although these particles were cleared almost as quickly as naked mRNA, luciferase expression peaked at the 4th hour and remained detected for up to 24 hours compared to naked mRNA which was only detectable at 4th hour post administration.[78] Similar expression kinetics was observed in another study where luciferase mRNA surface adsorbed on pegylated core shell nanoparticle (280nm, +40mV in water) were intranasally administered.[88]

Unlike drug loaded particles, cellular uptake is a requirement for gene loaded particles to exert a biological effect. As mentioned earlier, the mucus barrier is one that should not be underestimated because a mucus layer as thin as 20nm can block particle access to M cells.[89] Hence particle properties that facilitate transport across the mucus will enhance nasal delivery of nanoparticle vaccine. It has been shown that pegylated (PEG length ~5kda) or medium sized particles (200nm and 500nm) diffuse through mucus more efficiently than non-pegylated or smaller particles (100nm).[87] Since the mucus barrier of NALT in a healthy subject is relatively thin, it is uncertain the pegylation approach will enhance delivery efficiencies.

In summary, nasal administration of mRNA nanoparticle vaccine is an attractive strategy for tumour vaccination due to its non-invasive nature. Recent studies have demonstrated that nasal transfection using mRNA encapsulated in nanoparticles is a feasible concept. Further studies are warranted to ascertain if this route of delivery can induce an anti-tumour response. M cell transport efficiencies may be enhanced by using highly negatively charged particles, increasing residence time of the particles on nasal epithelium as well as enhancing mucus penetrating power of the nanoparticles. The incorporation of such properties into mRNA nanoparticles will help overcome extracellular barriers associated with nasal nanoparticle vaccine delivery.

.

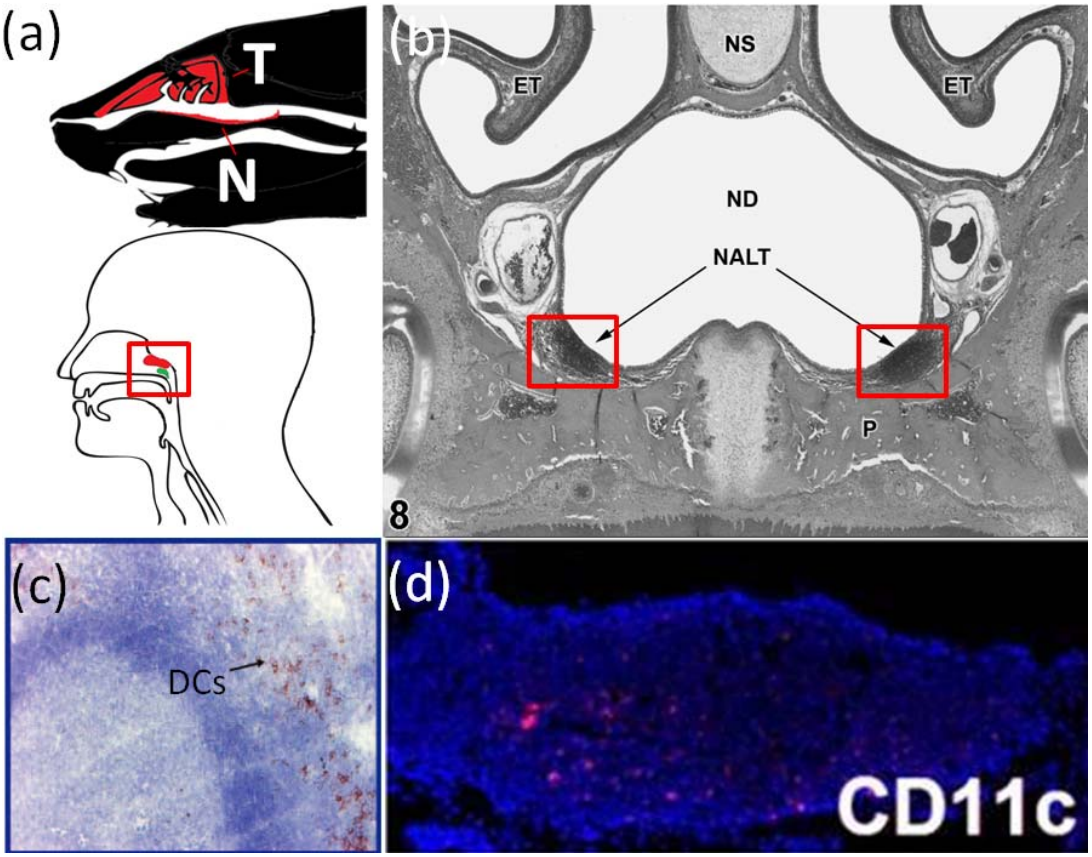

Figure 6. Nasal Associated Lymphoid Tissue (NALT)

(a) Location of NALT in mouse (top; T: turbinates, N: NALT) and human (bottom; Red: adenoids; Green: tubal tonsil). T: Turbinate; N: NALT. cross section of

(b) Cross section of nasal cavity showing location of NALT in mouse.[79] (NS: nasal septum; ND: nasal cavity; ET: turbinate)

(c) NALT stained for CD11c+ DCs (red).[90]

(d) Cross section of human adenoid tonsil stained for plasmacytoid DCs (brown).[91]

Reproduced with permission.[91,90,79]

1.2.3.5 Cytosolic Gene Delivery of mRNA in Dendritic Cells

Upon reaching the target organ, mRNA nanoparticles need to be efficiently taken up by antigen presenting cells, mediate endosome escape and single stranded mRNA has to be released from the gene carrier for protein translation. It was concluded at a very early stage that DCs can only be poorly transfected with lipoplexes.[8] Based on %GFP+ cells, transfected immature and mature human DCs using DMRIE-C were 7.5% and 4%, respectively. In the same study, transfection mediated by electroporation was 63% and 33%, respectively. Consequently, there was little interest in chemical mediated transfection of DCs. But significant advances in gene carrier development were made in the past decade through systematic investigations into the structure-to-function relationship of gene carriers. In this section we will review gene carriers that have been applied to mRNA transfection of DCs. *In vitro* transfection is commonly studied using DC2.4[92] and JAWS II (ATCC) cell lines, as well as primary murine bone marrow derived dendritic cells (BMDCs) and human monocyte derived DCs.

Perche *et al.*[40] developed a targeted lipopolyplexes prepared by addition of mannosylated and histidylated liposomes to mRNA pre-condensed with PEG and histidine modified polylysine based on the LPD concept.[93] Lipids and polylysine, the building blocks of LPD, are custom synthesized incorporating imidazole moieties to enhance endosome escape via the proton-sponge effect. A portion of the lipids are also conjugated with mannose to enhance targeting. Interestingly, the lipid tail is linked to it head group via a phosphoramide bond to improve biocompatibility. Transfection efficiencies based on GFP+ cells against DC2.4 in Opti-MEM using these targeted lipopolyplexes is significantly higher (60%) compared to the same lipopolyplexes without mannosylated lipids (40%).

Cheng *et al.*[94] developed a series of "DPE" triblock co-polymers composed of a DMAEMA (dimethylaminoethyl methacrylate) segment for cationic-mediated mRNA binding, a PEGMA (polyethylene glycol methacrylate) segment to impart colloidal stability and a DEAEMA-co-BMA (copolymer of diethylaminoethyl methacrylate and butyl methacrylate) segment to achieve pH sensitivity for endosome escape. Transfection efficiencies against DC2.4 cells in serum free media reached 50% (GFP+).

Su *et al.*[88] developed a formulation where mRNA is delivered via lipid-enveloped pH sensitive core-shell nanoparticles. Based on a similar concept reported for DNA vaccine[95], mRNA is electrostatically adsorbed onto the surface of pegylated cationic nanoparticles composed of pH-sensitive core and a PEG/DOTAP/DOPC lipid shell. These particles were efficiently taken up by 80% of DC2.4 in the presence of 10% serum and but only 30% were transfected. This discrepancy is likely attributed to degradation of mRNA, which may not be well protected via surface adsorption.

Surprisingly, commercially available mRNA transfection reagents are also relatively efficient in DC transfection. Mockey *et al.*[43] used lipofectamine to transfect JAWS II cells with luciferase mRNA to study the potentiation of mRNA translation by the length of the poly-A tail. Phua *et al.*[78] used Stemfect mRNA transfection reagent to study the transfection efficiency and transgene expression kinetics of mRNA in naked and nanoparticle format. Based on %GFP+ cells, the transfection efficiencies against immature BMDC and immature human monocyte derived DCs were 63% and 52% respectively, while that against DC2.4 and JAWS II cells were 98% and 80%, respectively. Kariko *et al.* [48] used Mirusbio Trans-IT mRNA transfection reagent to study enhancement in protein translation mediated by luciferase mRNA synthesized with

various modified nucleotides. Compared to its unmodified form, luciferase expression was increased by up to 4 fold in immature BMDCs. Weissman *et al.*[65] transfected human monocyte derived DCS with HIV gag encapsulated in lipofectin (DOTMA) to study the *in vitro* primary immune responses. DOTAP based liposomes have also been used for mRNA immunotherapy, although only *in vivo* immunotherapy data was reported.[37]

1.2.4 Major Histocompatibility Complex (MHC) presentation

Dendritic cells transfected and matured by the mRNA nanoparticle vaccine must at the same time be able to present the relevant antigen epitopes on MHC I molecules. Antigen protein translated from exogenously delivered mRNA is broken down into smaller peptides by proteasomes (Figure 2). These peptides enter the MHC class I pathway[96] and the end result is the presentation of MHC I-peptide complexes on DC' surface. It is these surface MHC I-peptide complexes that trigger the first T cell response through activation of $CD8^+$ cytotoxic T lymphocytes (CTLs).

In a classical infection model, pathogens endocytosed by DCs go through the endosome-lysosome pathway (synonymous to MHC II processing pathway in antigen presenting cells).[96] DCs present antigens to $CD4^+$ T cells through MHC class II molecules and also to the CTLs through MHC class I molecules (via cross presentation),[96] activating both $CD4^+$ T cells and CTLs. Activated $CD4^+$ T cells then stimulate CTLs through the production of IL-2 and license DCs through CD40/CD40L interactions (Figure 2). Licensed DCs up-regulate co-stimulatory molecules CD70, CD80 and CD86 needed to provide co-stimulation (i.e. second signal) to complete CTL activation and support their proliferation (Figure 2). CTL activated in this way are programmed for survival, while those that do not receive co-stimulation (i.e. activation by

unlicensed DCs that do not provide co-stimulation via CD70/80/86) are eventually deleted.[97] It is therefore evident that antigens have to be presented on both MHC I and II for proper DC and T cell activation to achieve a robust cellular immune response.

In contrast to a classical infection, antigen proteins are instead derived from within the cytoplasmic compartment. Although in this way antigen can be efficiently presented on MHC class I molecules, they tend to be poorly presented on MHC class II molecules, as only 10-30% of peptides bound to MHC II are derived from cytoplasmic and nuclear proteins.[96] It is now known that cytoplasmic antigens are presented on MHC II via various autophagy mechanisms, in particular, the chaperone-mediated autophagy is major pathway involved in MHC II presentation of translated antigen protein. In this pathway, cytoplasmic chaperones Hsc70 and Hsp90, together with lysosomal transmembrane protein (LAMP) selectively shuttles epitopes into lysosomes, effectively infiltrating into the MHC II pathway.[96] To enhance mRNA tumour vaccination, the chaperone-mediated autophagy pathway has been exploited to increase MHC II-peptide presentation. It has been shown that a single LAMP-1 or DC-LAMP[16] sequence can be cloned into the cDNA template so that the mRNA is eventually translated as a LAMP tagged protein (Figure 2). Co-delivering mRNA encoding both LAMP tagged and untagged protein has been shown to be effective in enhancing anti-tumour immunity in colorectal and melanoma immunotherapy models.[12, 39, 98]

In summary, the lack of MHC II presentation in mRNA vaccination is problem that has been overcome through co-delivery of LAMP-tagged mRNA to access the MHC II pathway. Besides LAMP-tagged mRNA, co-delivery of multiple mRNAs encoding additional adjuvants, such as the TriMix[19] or GM-CSF[37] is a proven concept that has

been shown to enhance anti-tumour immunity. This suggests that the future of mRNA nanoparticle vaccine will necessarily be a co-delivery system. It is a great challenge to ensure every single nanoparticle contains every type of mRNA required by design in a particular study. Significant heterogeneity may result because bulk handling methods employed in co-encapsulation/loading of mRNA into nanoparticles may not provide a consistent formulation process. While this may not be a deal breaker in proof-of-concept studies, issues related to throughput and batch-to-batch consistency may impact the translation of nanoparticle vaccines. Hence, operator-independent nanoparticle formulation methods will be necessary to ensure controlled and consistent synthesis of nanoparticles in the future.[99].

1.2.5 Immune activation

To achieve a robust T cell response, the mRNA nanoparticle formulation must not only ensure that dendritic cells translates and presents tumour antigens encoded by the mRNA, it must also concomitantly stimulate them to maturity, which is defined as the secretion and expression of immunological factors and co-stimulatory molecules necessary for complete T cell activation. If immune activation is inadequate, transfected dendritic cells will turn tolerogenic and create immunological acceptance of the tumour instead.

Major immune activation pathways associated with mRNA are shown in Figure 1. The signalling involved can be broadly classified into the TRIF and MyD88 pathways. The former leads to the secretion of type I interferon while the latter results in the secretion of pro-inflammatory cytokines (Interleukins and TNF family). mRNA itself activates toll-like receptors (TLR3, 7 and 8)[47] located in the endosomes of immune cells as well as

fibroblasts and epithelial cells. TLR3, which senses double stranded RNA (derived from internal hairpin structures of mRNA), trigger the secretion of both type I interferon via a TRIF dependent pathway as well as pro-inflammatory cytokines via the MyD88 pathways. TLR7, which senses single stranded RNA, triggers the secretion of inflammatory cytokines via MyD88 pathway. In addition to endosome associated immune receptors, cytosolic retinoic acid inducible gene-I (RIG-I) receptor [100] can be activated by triphosphates at the 5' end of uncapped mRNA leading to the secretion of type I interferon (Figure 2). Although it is a common practice to cap the 5' end of mRNA with an anti-reverse cap analogue during *in vitro* transcription, capping efficiency is usually about 80%, leaving exposed 5' triphosphates from uncapped fraction available for RIG-I activation. MDA5 is another cytosolic receptor sharing the RIG-I signalling pathway that can be activated by long-double stranded RNA (such as self-replicating RNA, which has re-emerged recently in the vaccine field). [101]

Pro-inflammatory cytokines induced from mRNA have been identified as TNF-α,[19,102] IL-1β,[36] IL-12,[36,103, 104] IL-6,[19,36, 102, 104, 105] IL-8.[105] Similarly Type 1 interferon induced from mRNA are IFN-α[100, 102, 103, 106] and IFN-β.[100, 102] Interestingly, chemokines such as GRO (Growth-Regulated Oncogene), MCP-1 (Monocyte Chemoattractant Protein-1), RANTES (Regulated on Activation, Normal T cell Expressed and Secreted) and MDC (Macrophage-Derived Chemokine) have also been reported when peripheral blood cells are pulsed with naked mRNA.[105] These secretions exert not only an immediate anti-viral response (innate immunity), but also adaptive immune responses by facilitating the maturation of professional antigen presenting cells (dendritic cells, B cells, activated macrophages) through up-regulation of MHC II and co-stimulatory molecules (CD80, 86)

as well as a change in chemokine receptors. The secretion of Type-1 interferon induced by innate immune response to mRNA has recently been shown to be counterproductive in the induction of antigen specific T cells when mRNA is delivered via DOTAP/DOPE lipoplexes.[41] This study confirms the idea that not all "self-adjuvant" effects derived from mRNA facilitate the development of cellular immunity.

The immunogenicity of mRNA has been highlighted in recent years due to increasing interest in their therapeutic application outside immunotherapy. A better understanding on the structural[103, 108] and molecular basis[33, 48] for mRNA's biological stability and mechanism of immune activation have led to increased translational capacity mRNA and boosted its potential for gene therapy applications. However, as reports describing non-modified mRNA as "non-immunogenic" exist,[12,45] the impression that mRNA is highly immunogenic has to be put into perspective. It has been shown that mRNA delivered by electroporation is not efficient in mediating DC maturation. DC maturation marker CD83 (<30%) and costimulatory molecule CD80(<40%)[8, 14] are both poorly upregulated in human monocyte derived DCs *in vitro*, even though the transfection efficiency based on GFP expression is 76%. However, the other co-stimulatory molecule CD86 is relatively well up-regulated (>70%), indicating that transfected DCs can be partially matured with mRNA. CD86 up-regulation of a similar magnitude is also observed in nodal DCs, when mRNA is directly injected into inguinal lymph nodes. However this study did not report the transfection efficiency based on GFP+ cells, staining of CD83 and CD80, making it difficult to conclude extent of DC maturation. Overall, these data suggest that partial maturation may only occur in mRNA-loaded DCs *in vitro*, compared to >90% maturation (for CD 80,83,86) yield in cytokine treated DCs.

An inherent advantage of mRNA nanoparticle vaccine is that its overall immunogenicity can be modified by the gene carrier. When delivered in nanoparticle format, CD80 and CD86 of human monocyte derived DCs (pulsed with mRNA-lipofectin) were both more efficiently up-regulated (>90%) compared to cytokine treatment (>80%). CD83 expression, however, remained relatively muted.[65] Interestingly, CD80 and CD86 are both up-regulated (>50%) by lipofectin liposomes alone while CD83 expression remained low (4%). As the transfection efficiency mediated by lipofectin against human monocyte derived DCs is unlikely to be >90%, this response is more consistent with immunostimulating effects of cationic liposomes via ROS mechanism, a topic that has been comprehensively reviewed.[75,109] In another study, Rettig *et al.* compared the cytokine secretion profile when human peripheral blood mononuclear cells (PBMCs) are treated with β-Gal RNA either in naked form or encapsulated by protamine. Using a cytokine array, it was observed that β-Gal RNA nanoparticles mediated significantly higher levels of IL-6, IL-8 and MCP-1 compared to naked mRNA,[105] suggesting that cytokine secretion can also be affected by the addition of protamine. Protamine condensed mRNA also induced CD86 on dendritic cells, but the transfection efficiency of the mRNA is abrogated. Similarly, Oliwia *et al.* also showed that mRNA lipoplexes induced high levels of IL-6 and IL-12 and TNF-α in murine lungs following intranasal instillation.[110] Unfortunately in this study, cytokine secretion from liposome alone or naked mRNA was not available. Nevertheless in another study, subcutaneously injected mRNA-DOTAP/DOPE liposomes but not the liposomes alone, induce high levels of IL-6, IL-1β and type I interferon in DCs.[41] This lack of cytokine induction by empty liposomes is consistent with the adjuvant effects of DOTAP-based vaccines,[109] and an interesting contrast between lipid and polymeric gene carriers.

In an effort to evaluate the use of modified RNA for immunotherapy, Pollard *et al.* investigated the effects of IFN-α on T cell response.[41] Surprisingly, IFNα knockout mice immunized subcutaneously with DOTAP/DOPE mRNA lipoplexes develop more robust antigen specific T cell responses compared to wild type mice. Although results coming from knock out models are encouraging, a direct confirmation is needed from wild type models immunized with modified mRNA to confirm its utility in immunotherapy.

Gene carriers may also decrease the overall immunogenicity of the mRNA formulations. Uchida *et al.* show mRNA encapsulated in nanomicelles (PEG-polyamino acid block co-polymer) administered into the central nervous system induces lower levels of IL-6, TNF-α, IFN-α4 and IFN-β1 from neural tissues compared to naked mRNA.[102]

To summarize, immunotherapies that apply mRNA encapsulated in nanoparticles may benefit from immunogenicity or lack thereof of gene carriers. Immune stimulating properties of mRNA in terms of the mechanism of activation and the extent to which it can modify DC phenotype are well characterized. But there is still a knowledge gap on how molecular structure of the gene carrier modifies mRNA's basic immunogenicity. Lipid-based formulations are highly capable of upregulating costimulatory molecules such as CD80/86, but are poor in inducing DC maturation and cytokine secretions necessary for a complete T cell activation. Protamine can upregulate CD86 expression and also induce high levels of proinflammatory cytokines. PEG-poly amino acid nanomicelles, on the other hand, attenuate immune response

1.3 mRNA nanoparticle vaccine delivery systems for tumor immunotherapy.

In the previous sections, we discussed a framework for mRNA nanoparticle delivery: namely (1) gene delivery, (2) immune activation and (3) MHC processing. Despite numerous reports on mRNA nanoparticle (mRNA-NP) delivery, only a handful studied its therapeutic efficacy in terms of either immune responses (CTL assay/IFN-γ secretion) or overall survival. In this section, we review these studies (listed in Table 1) highlighting current progress in mRNA-NP mediated tumour vaccination and provide a perspective on the bottleneck in this niche but exciting area of research.

The first attempt in mRNA-NP vaccine was reported in 1993 by Martinon *et al.*[111] using anionic liposomes composed of phosphatidylcholine(PC)/ phosphatidylserine(PS)/ cholesterol. mRNA encoding influenza nucleoprotein was encapsulated into liposomes by the hydration method. This formulation method was inefficient and yielded about 10% encapsulation efficiency.[111] Even so, antigen specific CTL response was induced if the particles were administered via IV or SC but not IP.[111] IP vaccination route also failed to induce CTL response in another study where mRNA was encapsulated in Unifectin-based lipoplexes and lipopolyplexes.[38] The authors speculated the reason for ineffective IP route was due to either particle aggregation or an insufficient number of peritoneal antigen presenting cells.[111] This study is interesting because these pH insensitive anionic liposomes not only do not interact well with negatively charged cell membranes, they are also inefficient in endosome escape (Figure 2). Yet they mediate antigen specific CTL responses indicating that mRNA had been translated by antigen presenting cells. This PS containing mRNA formulation may have been taken up by antigen presenting cells of the monocyte-phagocyte system via PS receptors. In addition, the anionic nature of the

lipoplexes can resist opsinin-mediated aggregation in the blood when administered IV, and since these liposomes were previously extruded with a 200nm membrane, they can also efficiently drain to the lymph nodes. This formulation will be promising if the encapsulation efficiency is increased and if pH sensitive molecules are incorporated..

Hoerr *et al.* demonstrated that the use of liposomes (Unifectin) protected mRNA from nuclease-mediated degradation in vivo and significantly increases CTL response via IV route, but failed to induce any CTL response via the IM and IP routes.[38] In addition, despite evidence showing small amounts of protamine can protect naked mRNA from nuclease degradation (for about 30 minutes), mice subcutaneously immunized with mRNA formulated with protamine alone (without Unifectin) did not enhance CTL response compared to unprotected naked mRNA.

Hess *et al.* first reported survival data from mRNA nanoparticle tumour vaccination.[37] In this detailed study, OVA mRNA encapsulated in DOTAP liposomes was intradermally administered into mice ear pinnae twice (14 days apart) in a prophylactic immunotherapy model, followed by subcutaneous tumour challenge with E.G7-OVA cells. Splenic $CD8^+$ T cells from immunized mice demonstrated lytic activities both *in vitro* (CTL assay) and *in vivo* (adoptively transfer of CFSE labelled OVA pulsed splenocytes). These mice also experienced significant delay in tumour onset and progression against E.G7-OVA tumour challenge through Day 16. The formulation applied in this study was DOTAP lipoplexes prepared by mixing mRNA with DOTAP liposomes in PBS. These lipoplexes were not characterized for size and zeta potential in this study. Nevertheless, the use of PBS would have caused aggregation because it has been reported that DOTAP lipoplexes aggregate when they are formulated in the presence of salt.[112].

Particle aggregation, as mentioned earlier, reduces extracellular and intracellular gene delivery efficiencies. And this was likely reason for a higher CTL response from IV route compared to ID route and an absence thereof from SC route (tail base). Also, aggregated particles administered IV can still be taken up by macrophages in the liver and spleen, develop into antigen presenting cells through ROS mediated activation (by DOTAP) and transfer the antigen to endogenous DCs or activate T cells directly. Intradermal administration induced a dose dependent CTL response because a small fraction of mRNA lipoplexes were still bioactive and could transfect dermal DCs, which eventually induces the CTL response. As this is a small fraction of the given dose, a larger dose may lead to higher DC transfection and presumably higher CTL response. In this review, we are able to correlate observed CTL responses to particle properties of lipoplexes because they have been characterized in other studies under similar conditions. As shown in Table 1, mRNA nanoparticle tumour vaccination studies are often reported without much information about particle properties. To optimize therapeutic outcome, particle characterization such as size, zeta potential measured under the applied physiological conditions should be an important aspect of future immunotherapy experiments.

In the same study (Hess *et al.*), it was observed that CTL response from mRNA encapsulated in DOTAP/DOPE is also 4 times higher than in DOTAP liposomes. This shows that the inclusion of DOPE, a helper lipid with fusogenic property, facilitated intracellular gene transfer to antigen presenting cells.[113] This shows, at least in the DOTAP-based mRNA liposomes, that endosome escape is a rate limiting step for immune modulation. In addition, co-delivery of OVA mRNA with either GM-CSF (to attract DCs), CD80 (co-stimulatory molecule) and IL-2 (T cell proliferation) was

evaluated. It was found that CTL response was enhanced with GM-CSF mRNA, but not CD80 or IL-2 mRNA. These results demonstrate the threshold levels of GMCSF needed to enhance immune response is much lower than CD80 and IL-2. It also re-affirms that a co-delivery system is the optimal mRNA nanoparticle tumour vaccine.

Mockey *et al.* also reported anti-tumour efficacy of mRNA nanoparticle vaccination using histidylated lipids optimized for mRNA delivery.[39] These phosphoramide lipids were synthesized with single histidine head groups to facilitate endosome escape via proton sponge effect. Mannosylated lipids (11% molar ratio) were later incorporated in the formulation (Man_{11}-LPR) to enhance uptake.[114] The colloidal stability of mRNA nanoparticles formulated with these lipids in physiological salt concentration and in serum is unknown although particles were about 150nm in size (ζ-potential +14-18mV) in 10mM Hepes. But given its almost identical *in vivo* biodistribution with LPD, their colloidal stability may be the similar to unpegylated LPDs. In Mockey *et al.*, MART-1 (Melanoma antigen recognized by T-cells 1) mRNA encapsulated in these histidylated lipopolyplexes is intravenously administered into mice via tail vein twice (7 days apart) in a prophylactic model, followed by a subcutaneous tumour challenge with B16 F10 cells. Developed tumours progressed more slowly in immunized mice compared to control mice vaccinated with luciferase mRNA nanoparticles. In a subsequent study by Perche *et al.,*[40] MART-1 mRNA encapsulated in Man_{11}-LPR or non-mannosylated LPR formulations were re-evaluated in the prophylactic B16 F10 melanoma immunotherapy model. The median survival of mice immunized with MART-1 mRNA nanoparticles formulated with Man_{11}-LPR was 5 and 10 days longer than mice immunized with non-mannosylated LPR and NaCl controls, respectively. Although the effectiveness of Man_{11}-LPR in a therapeutic immunotherapy model remains to be determined, this study

demonstrated that the presence of a targeting ligand improved overall therapeutic efficacy through enhanced uptake of nanoparticles by antigen presenting cells.

In this section, we reviewed studies that evaluated mRNA nanoparticle formulations for tumour vaccination. Although nanoparticle properties are not well characterized in these immunotherapy studies, it can be concluded that the use of mRNA nanoparticles can induce consistent CTL responses. Evidence shows that nanoparticle delivery of mRNA tumour vaccination is a feasible research direction and much work has yet to be done.

Ref	Antigen/μg x number of doses/delivery system	Cytotoxic T Lymphocyte Response					Splenic IFN-γ	Survival Data	Size/ Zeta Potential
		IV	SC	ID	IM	IP			
Martinon et al (1993)[95]	Influenza nucleoprotein/12μg x 2/ Anionic Lipoplex: DPPC/DPPS/Chol (Encapsulation efficiency 5-10%)	+	+			-			Not reported
Zhou et al (1999)[13]	GP100/ 8μg x 2/ HVJ-liposomes: Egg PC/Chol/DC-Chol	Works only if injected directly into spleen. CTL levels comparable with positive control							Extruded through 200nm membranes
Hoerr et al (2000)[9]	LacZ/30μg x1/Lipopolyplex: Unifectin+protamine	++	+		-	-			Not reported
	LacZ/30μg x1/ Lipoplex: Unifectin only				-	-			
	LacZ/30μg x1/Protamine only	-	-	+	-				
	mLacZ/30μg x1/Naked format			+					
Hess et al (2006)[8]	OVA/5μg x 2/Lipoplex: DOTAP			+				+	
	OVA/3μg x2/Lipoplex: DOTAP/DOPE	+	-	+					
	OVA+GMCSF/3+1μg x1/Lipoplex:DOTAP-DOPE	++							
Mockey et al (2007)[10]	MART-1/25μg x2/Lipopolyplex: PEG-HpK,HDHE,Chol	+					+	+	100nm/ +13mV (10mM Hepes)
Perche et al (2011)[11]	MART-1/25μg x 2(IV)/ Targeted lipopolyplex: PEG-HpK, HDHE/HDHE-mannose,Chol)							+	150nm/ +17mV (10mM Hepes)
Pollard et al (2013)[12]	GAG/20μg x2 (IV,SC, wild type mice)/ Lipoplex: DOTAP-DOPE(IV/SC)						+		Not reported
	GAG/20μg x2 (IV, IFNα -/- mice)/ Lipoplex: DOTAP/DOPE(IV)						++		

Table 2. mRNA nanoparticle tumor vaccination studies evaluated for T cell response or survival

IV: intravenous (tail vein); SC: subcutaneous (base of tail); ID: intradermal (ear pinnae); IM: intramuscular; IP: intraperitoneal. "+" and "-"respectively indicate statistically significant and insignificant result compared to controls. "++" indicates results are significantly higher than "+" samples reported in the same study.

1.4 Conclusions

Advances in the past decade have deepened our understanding of mRNA's biological stability, immunological properties and provided extensive evidence to support the need for engineering innovations to deliver mRNA for genetic vaccination. In this review we discussed the physical stability of mRNA in aqueous buffers and clarified the technical possibility of subjecting mRNA to engineering manipulations. Presently, mRNA administered directly in vivo benefits from being encapsulated with gene carriers in nanoparticle format and a growing number of published studies have looked at the feasibility of applying nanomedicine concepts to mRNA tumour vaccination. Although a few deliberate attempts were made on the rational design of mRNA gene carrier,[40, 88, 94] most have not been functionally evaluated in vivo for immune or therapeutic response.[40, 94] Instead, off-the-shelves gene carriers are the most frequently used to encapsulate mRNA and evaluated for their ability to stimulate antigen specific T cell responses, often without adequate particle characterization. Clearly, the optimal mRNA gene carrier for tumour vaccination application has yet to be determined. But given the sustained interests in this field, the discovery of better mRNA formulations will no doubt accelerate in the near future. Based on our knowledge on gene delivery and mRNA immunotherapy, we discussed a model frame work that highlights the barriers to the development of a robust anti-tumour immunity mediated by mRNA encapsulated in nanoparticles, and reviewed studies that evaluated therapeutic outcome of mRNA nanoparticle vaccination. mRNA nanoparticle tumour vaccination can be advanced if we bring nanomedicine closer to mRNA immunotherapy.

2 Specific Aims

2.1 Significance

A major reason for the failure of direct *in vivo* injection of naked mRNA is due instability caused by extracellular nucleases. Consequently, direct mRNA vaccination via administration of naked mRNA is found to be effective only when it is directly injected into the lymph nodes [42, 46]. These studies demonstrate that when naked mRNA is delivered directly to lymphoid tissues (e.g. lymph nodes) where antigen presenting cells (DCs, macrophages), T and B cells reside in an organized way, anti-tumor immune responses can be effectively generated. However, intranodal vaccination is highly invasive in mice and technically challenging in humans. Moreover, repeated administration (DC vaccine is administered 3 to 4 times biweekly in humans) and hence multiple surgeries, are required to acquire immunity making it relatively unattractive for clinical translation.

Although this limitation can be addressed by formulating mRNA into nanoparticles with gene carriers, *in vitro* transfection efficiency (based on %GFP population) on primary dendritic cells mediated by mRNA encapsulated in nanoparticles has been poor and as a result, only a few studies applied mRNA nanoparticles as a proof-of-concept for tumor vaccination. Hence there is a need to identify better mRNA formulations that have the ability to transfect primary dendritic cells efficiently.

Although the use of mRNA nanoparticles renders a shift away from cell based vaccination (mRNA transfected DCs), the latter is already a more matured technology that widely reproduced in the clinics worldwide. mRNA transfected DC vaccine is an effective, but also a laborious, time consuming and costly method to induce anti-tumor

immunity. The average time required to generate DCs from human peripheral blood monocytic cells (PBMCs) is 6 days. This is in addition to 4-6 hours of cell isolation and overnight culture with specially formulated media to mature antigen loaded DCs. It is only recently known that DCs are known to be capable of “cross-dressing” i.e. Balb/c DCs (mice that are incapable of presenting SIINFEKL (OVA) peptide on MHC I molecules) pulsed with OVA peptide, mediate the expression of MHCI-OVA complex in naïve C57Bl/6 derived DCs (mice capable of presenting OVA peptide on MHC I molecules).[115] In addition, Yewdall *et al.* provided direct *in vivo* evidence that demonstrates that *ex-vivo* transferred DCs do not significantly activate $CD8^+$ T cells, but instead act as vehicles that transfer the antigens to endogenous DCs.[116] This raises the possibility of using alternative cell types for mRNA cell based vaccination, which may obviate extensive manipulation and culture required for mRNA-DC vaccination.

In conclusion, the direct in vivo mRNA vaccination using nanoparticles as well as the use of alternative cells types that obviates logistical requirements of mRNA-DC vaccine are both viable approaches that may facilitate broad translation of mRNA based vaccination.

2.2 Thesis Objective

A significant bottle neck to broad translation of mRNA cell based vaccination is the need for extensive cell manipulation and culture to derive matured mRNA transfected DCs from autologous blood monocytes. The objective of this thesis is to address this bottleneck to facilitate broad translation of mRNA vaccination. As shown on Figure 7, a two-prong approach is adopted.

The first approach is to use of mRNA nanoparticles for tumor vaccination. The limiting factor in this approach has been poor transfection efficiencies of nanoparticle formulations. Nevertheless more efficient gene carriers have been developed in the past decade with some even made commercially available. In Chapter 3 (Specific Aim 1), a selected number of gene carriers that have been shown to be effective for other applications are evaluated for their ability to transfect primary DCs, and the best performing formulation is further evaluated in vivo for its transfection efficiency and expression kinetics.

In Chapter 4 (Specific Aim 2), therapeutic efficacy of intranasal mRNA tumor vaccination is evaluated. The intranasal route of delivery is non-invasive and is amenable for repeated administrations. However, intranasal mRNA vaccination (with naked mRNA) has not been shown to induce anti-tumor immunity. Chapter 4 shows, for the first time, that intranasally administered mRNA can induce anti-tumor immunity in nanoparticle but not naked format.

In Chapter 5, whole blood cells are evaluated as alternative cell based mRNA carriers. The rationale for choosing whole blood cells as the alternative cell source will be elaborated in later sections. In this Chapter, whole blood cells is evaluated for their ability

to encapsulate intact and functional mRNA, and for the induction of therapeutic anti-tumor immunity against tyrosinase related 2 (TRP-2) in a melanoma immunotherapy model.

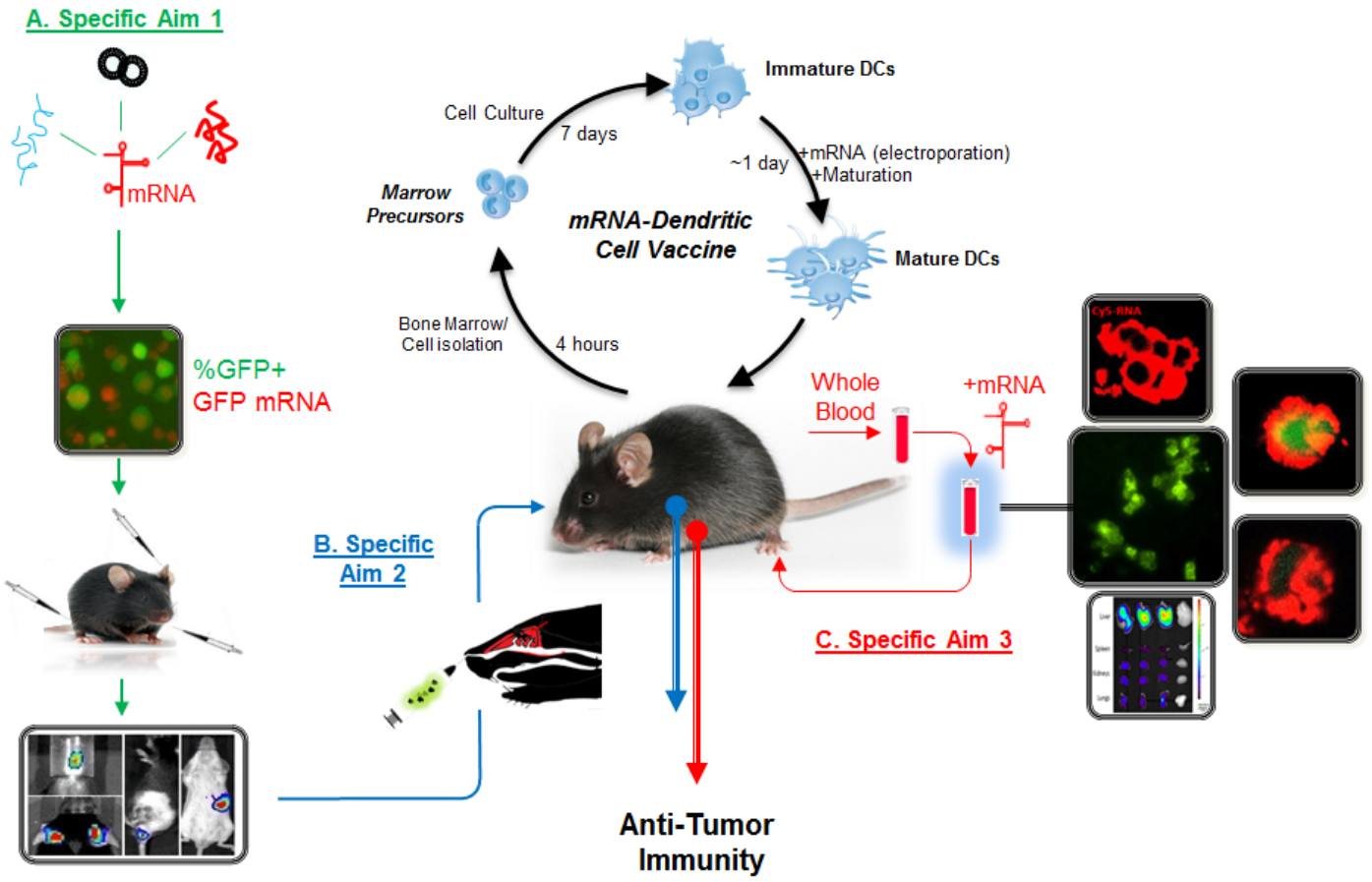

Figure 7. Overview of thesis objectives

This thesis presents two mRNA delivery strategies that obviate extensive cell culture and manipulation needed for mRNA tumor vaccination.

A. Compare transfection efficiency and kinetics of mRNA delivered in naked and nanoparticle formats.
B. Intranasal mRNA nanoparticle vaccination induces prophylactic and therapeutic anti-tumor immunity.
C. Whole blood cells loaded with mRNA as an anti-tumor vaccine.

2.2.1 Specific Aim 1: Compare transfection efficiency and kinetics of mRNA delivered in naked and nanoparticle formats

In this aim, I screen for the optimal gene carrier that is capable of transfecting primary dendritic cells in vitro. A list of gene carriers is preliminary screened for their ability to transfect DC cell line (JAWS II, ATCC) based on %GFP+ population. The best formulation is then further evaluated on in vitro transfection efficiency and expression kinetics in primary mouse and human DCs. Using this formulation, I compare the transfection efficiency and transgene expression kinetics of luciferase mRNA delivered in naked and nanoparticle format. Naked mRNA and mRNA encapsulated in nanoparticles (formulated using the optimal gene carrier) are administered via intravenous, intranasal and subcutaneous (ear pinna and base of tail) routes. Transfection efficiency is evaluated based on relative lights units measured using IVIS while the expression kinetics is tracked over the necessary duration until luminescence matches negative controls (OVA mRNA encapsulated in nanoparticles). The effects of RNAse inhibitors and pH on naked mRNA mediated subcutaneous transfection are also investigated.

2.2.2 Specific Aim 2: Demonstrate preclinical efficacy of intranasal mRNA nanoparticle tumor vaccination

In this aim, I test the hypothesis that intranasally administered mRNA can induce an anti-tumor response only if it is encapsulated in nanoparticle format. Using OVA as a model antigen, C57Bl/6 mice are immunized intranasally with OVA mRNA with cholera toxin as an adjuvant. Mice are immunized with OVA encapsulated in nanoparticles, naked OVA mRNA delivered in Ringer's lactate as well as GFP mRNA encapsulated in nanoparticles (negative control). Cellular immunity is evaluated by measuring OVA specific CD8+ T cells via tetramer staining. Therapeutic efficacy is then evaluated in an E.G7-OVA immunotherapy model, where time-to-tumor onset, overall survival as well as tumor

progression are monitored. Intranasal vaccination is evaluated in both prophylactic and therapeutic models.

2.2.3 Specific Aim 3: Evaluate whole blood (WB) vaccine as a viable approach to cell-based tumor vaccination

In this aim, I test the hypothesis that whole blood cells loaded with mRNA can induce an anti-tumor response in mice. First, whole blood cells are evaluated for their capacity to be loaded with intact and functional mRNA via electroporation. Electroporation parameters are optimized based on flow cytometry and mRNA loading is visualized using fluorescence and confocal microscopes. The integrity of the loaded mRNA is confirmed by RT-PCR and the functionality of loaded mRNA is confirmed by gene expression from nucleated cells within the whole blood cell population. The biological properties of mRNA-loaded whole blood cells are characterized to determine it's suitability as a vaccine formulation. C57Bl/6 mice are then immunized with mRNA-loaded whole blood cells and evaluated for antigen specific immune responses. Finally, the therapeutic efficacy of mRNA-loaded whole blood cell vaccine is evaluated in a B16-F10 melanoma immunotherapy model using tyrosinase-2 related protein (TRP-2) as an antigen.

3 Transfection efficiency and transgene expression kinetics of mRNA delivered in naked and nanoparticle formats.

3.1 Introduction

The development of mRNA therapeutics received a significant boost following studies that demonstrated dendritic cells (DCs) pulsed with mRNA *in vitro* could become potent antigen-presenting cells *in vivo*[1]. Various delivery methods were explored to ascertain the most efficient method to transfect DCs with mRNA [8] and electroporation emerged as the preferred method. *Ex vivo* approaches to vaccination using autologous blood-derived DCs electroporated with tumor mRNA were developed and translated into clinical studies in patients with cancer [117]. Nevertheless, nanoparticle-mediated delivery of mRNA to DCs warrants attention because of its potential advantages, the most important of which is the possibility of direct *in vivo* administration of mRNA vaccines without *ex vivo* manipulation of DCs. Encapsulation of mRNA in nanoparticles can also protect the mRNA from nuclease degradation, facilitate uptake, promote endosome escape, and provide conjugation sites to attach DC-specific receptor ligands for targeted delivery. An alternative that has been extensively investigated is *in vivo* administration of naked mRNA, which has been shown feasible to engender immune responses. Structural modifications such as length of poly-A tail [118], modified cap analogues [119], and pseudouridine substitution [48] as well as the use of Ringer's Lactate (RL) [120] have enhanced naked mRNA transfection efficiency *in vivo*.

As a rapidly emerging class of nucleic acid therapeutics, there are key benefits in using mRNA over plasmid DNA for vaccine or therapeutic applications. First, mRNA contains no viral promoters (e.g. CMV) and bacterial sequences that can cause toxicity. Second,

mRNA does not integrate into host genome, which may lead to deleterious mutation [121]. Third, gene expression via mRNA is relatively transient and therefore safer to use compared to DNA. Last but not least, as mRNA does not need to cross the nuclear envelop, it increase the chances of successfully transfecting quiescent cells such as DCs. Indeed, mRNA can mediate a higher level of protein expression *in vivo* compared to DNA over shorter durations [120]. Most recently, encouraging *in vivo* transfection mediated by naked mRNA has been reported where calcium-containing buffers such as Hank's Balanced Salt Solution or Ringer's Lactate are used in the injection [19].

mRNA delivery to DCs using nanoparticles has also been recently explored. Su *et al.* [88] adsorbed GFP-encoding mRNA to a pegylated and lipid-coated cationic core to obtain a 30% transfection efficiency on DC2.4 cells *in vitro,* and achieved *in vivo* gene expression via intranasal administration. Perche *et al.* [40] encapsulated GFP mRNA into mannosylated lipopolyplexes and achieved approximately 60% transfection efficiency on DC2.4 cells *in vitro*. They also observed anti-tumor effects when mice were vaccinated intravenously with lipopolyplexes encapsulating the antigen mRNA. Intuitively, mRNA encapsulated in nanoparticles should mediate higher transfection efficiencies *in vivo*, but given the encouraging data reported on naked mRNA transfections, it becomes necessary to evaluate and compare transfection efficiency of gene carrier-mediated mRNA with naked mRNA delivery *in vivo*. In this paper, we hypothesize that mRNA delivered in nanoparticle format can be, in some ways, more efficient than naked mRNA. Using a commercially available mRNA transfection reagent, we show that it is possible to formulate stable mRNA nanoparticles in small volumes compatible with *in vivo* administration. We then evaluate and compare transfection efficiencies and transgene expression kinetics of these mRNA formulations (p/mRNA) with naked mRNA (n/mRNA)

on primary human and mouse DCs *in vitro*. This comparative evaluation is then performed *in vivo* at four potential vaccination sites: subcutaneous (ear pinnae 'SubQ-EP' and base of tail 'SubQ-BOT'), intranasal and intravenous administration.

3.2 Materials and methods

3.2.1 Ethics statement

Human: Primary human cells used in these experiments were isolated from blood obtained from healthy human volunteers following informed written consent using a protocol approved by the Duke University Institutional Review Board.

Murine: In conducting the research described in this paper, the investigators adhered to the "Guide for the Care and Use of Laboratory Animals" as proposed by the committee on care of Laboratory Animal Resources Commission on Life Sciences, National Research Council. The facilities at the Duke vivarium are fully accredited by the American Association for Accreditation of Laboratory Animal Care (AAALAC), and all studies were conducted using a protocol approved by the Duke University IACUC.

3.2.2 Cell lines and mice

Jaws II cells were obtained from ATCC and DC2.4 cells was a kind gift from Dr. Kenneth Rock. 5-6 weeks old C57BL/6 or Balb/c mice from Jackson Lab were used for transfection experiments. Balb/c mice were used for intravenous (IV) administrations while C57BL/6 mice were used all other routes of injection. Human DCs and murine DCs were derived using previously reported protocols [122] from adherent monocyte obtained peripheral blood mononuclear cells (PBMCs) and bone marrow precursor cells from C57Bl/6 mice, respectively.

3.2.3 In vitro transcription, nanoparticle formulation and characterization

In vitro Transcription (IVT) kit and ARCA cap were purchased from New England Biolabs and Trilink Biotech respectively. Luciferin was obtained from Biosynth International. IVT was performed according to manufacturer's protocol. An initial GTP/ARCA cap ratio of 1:3 was used and slightly adjusted to ensure mRNA yield was 40-50 μg/reaction. Adjustment is necessary to ensure a consistent capping efficiency of ~80%. Stemfect mRNA transfection reagent was purchased from Stemgent. RNAse free sodium acetate (Ambion) was adjusted with hydrochloric acid to pH 5 and subsequently diluted with RNAse-free glucose to 100 mM/5% glucose (NaAc buffer). mRNA nanoparticles were formulated by adding 8 μl ethanolic reagent to 10 μl of mRNA (0.2 μg/μl) suspended in NaAc buffer under gentle vortexing. Vortex speed was optimized to prevent mRNA degradation from excessive shear stress. The mixture was adjusted to appropriate volumes/pH and incubated at room temperature (RT) under vacuum to completely remove ethanol. Size and zeta potential measurements were obtained using the NanoZS (Malvern) by diluting the 10 μl nanoparticles (0.2 μg/μl) into 100 μl of DI water or mouse serum (diluted with sterile water to obtain respective concentrations). Mouse serum was obtained from whole blood of C57BL/6 mice. Whole blood was obtained by cardiac puncture and allowed to clot for 10 min at room temperature. Cells were removed via centrifugation (4000rpm) at 4°C. Supernatant (without buffy coat) was removed and centrifuged again at 4°C to completely remove suspended particles.

3.2.4 *In vitro* transfection and kinetics

For analysis of GFP expression, cell lines were seeded at a density of $8x10^4$ cells/well while primary DCs were seeded at a density of $1.5x10^5$ cells/well on 24-well plates. Cells

were transfected with nanoparticles at 0.5 μg/well (cell lines) and 1.3 μg/well (primary cells). Transfections were done in the presence of serum. For human DCs, heat inactivated FBS was added to AIM V media to a final concentration of 10%. GFP expression was assayed by flow cytometry 8 hours post-coculture of cells with mRNA.

For analysis of luciferase expression, cells were seeded at a density of $3x10^4$ cells/well on 96-well white opaque plates (Nunc). Cells were transfected with nanoparticles at 0.4 μg/well and analyzed at various time points. Before assay, microplates were centrifuged (1000 rpm, 5 min), media aspirated and cells were lysed with 75 μl Glo-Lysis buffer. Luciferase expression was assayed by adding an equal volume of Steady-Glo Luciferase substrate (Promega). Bioluminescence was measured by plate reader (Optima) with 15-second exposure time for human DCs and a 10-second exposure time for mouse DCs.

3.2.5 *In vivo* transfection and kinetics

Nanoparticles were prepared at 0.2 μg/μl as described above, combined and adjusted with 5% glucose to appropriate volumes. Naked mRNA controls were diluted in NaAc buffer (5% glucose/100 mM NaAc, pH5) and Ringer's Lactate (Baxter) respectively. Where indicated, 1M Hepes was added to adjust the pH to 7.4 (monitored using pH paper). Anesthesia was achieved using isofluorane, if required.

Subcutaneous injection: Mice were injected with 4 μg mLuc in 40 μl subcutaneously at the base of each ear pinnae under anesthesia or with 8 μg mLuc in 60 μl at the base of tail. RNAse inhibitor (New England Biolabs), where applicable, is added to a final concentration of 1unit/μl.

Intranasal injection: 4 μg in 20 μl was gently pipetted into the nostrils of anesthetized mice. Intravenous injection: 26 μg of mLuc nanoparticles in 200 μl was injected intravenously via tail vein.

A new syringe was used for each injection. There was no incidence where 2 or more doses were drawn into the same syringe and injected sequentially into 2 or more mice. Luciferase expression was monitored non-invasively at 4, 8, 12, 24 and 36-144 hours (SubQ only) post-injection with IVIS Caliper 100 Imaging System. Each mouse was administered with 200 μl of luciferin (28.5 mg/ml dissolved in PBS) intraperitoneally at all indicated time points. To prevent false positive readings, non-transfected controls were always included on the same platform and imaged at the same time.

3.2.6 Statistics and regression analysis

Statistical analysis was performed using correlation functions for two-tailed Student's t-Test or One-way Anova (followed by Bonferroni Multiple Comparison Test) with the software Graph Pad Prism. Transgene expression kinetics data were fitted into a first order exponential decay model: $y=A*exp(-\lambda t)$, where y = bioluminescence in photons/sec/cm^2/sr, t = time in hours, A is the bioluminescence at t=0 and λ is the decay constant. Apparent half-lives were derived using the formula $t_{1/2}= \ln(2)/\lambda$.

3.3 Results

3.3.1 Primary DCs can be efficiently transfected with mRNA nanoparticles.

mRNA nanoparticles formulated with Stemfect mRNA transfection reagent, even when formulated at a concentration as high as 0.2 μg/μl, were colloidally stable in NaAc buffer with an average diameter of 150 nm (PDI=0.2). They aggregated gradually in various

dilutions of mouse serum but remained stable for at least 80 min with an average diameter below 350 nm, a size that remained conducive for endocytosis (Figure 8A). GFP mRNA nanoparticles were highly efficient *in vitro*. DC2.4 cells were transfected with a transfection efficiency >97%. JAWS II cells, which were morphologically more consistent with primary mouse DCs, were transfected reproducibly with at least 80% GFP+ efficiency. The transfection efficiencies of primary mouse and human DCs were >60% and >50% respectively (Figure 8B). These transfection efficiencies, to the best of our knowledge, were the highest in literature for mRNA nanoparticle delivery to DCs *in vitro*. Naked mRNA, however, failed to transfect any of the DC lines (Figure 8B).

In vitro transgene expression kinetics on DC cell lines with mRNA nanoparticles were consistent with other cell types reported in literature [44]. We also observed similar kinetics in primary mouse and human DCs (Figure 8C and 8D). Mouse DCs expressed luciferase within the first hour of transfection, much earlier than the typical 2-4 hour incubation time used for *in vitro* transfection. Transgene expression peaked rapidly at 5-hour post-transfection and interestingly tapered off in a bi-phasic manner: a rapid and almost symmetrical drop in expression at the 9-hour time-point followed by a more gradual decrease that extended beyond 15-hr post-transfection. The trend in primary human DCs was similar although expression rose more gradually to peak at 7-hour post-transfection.

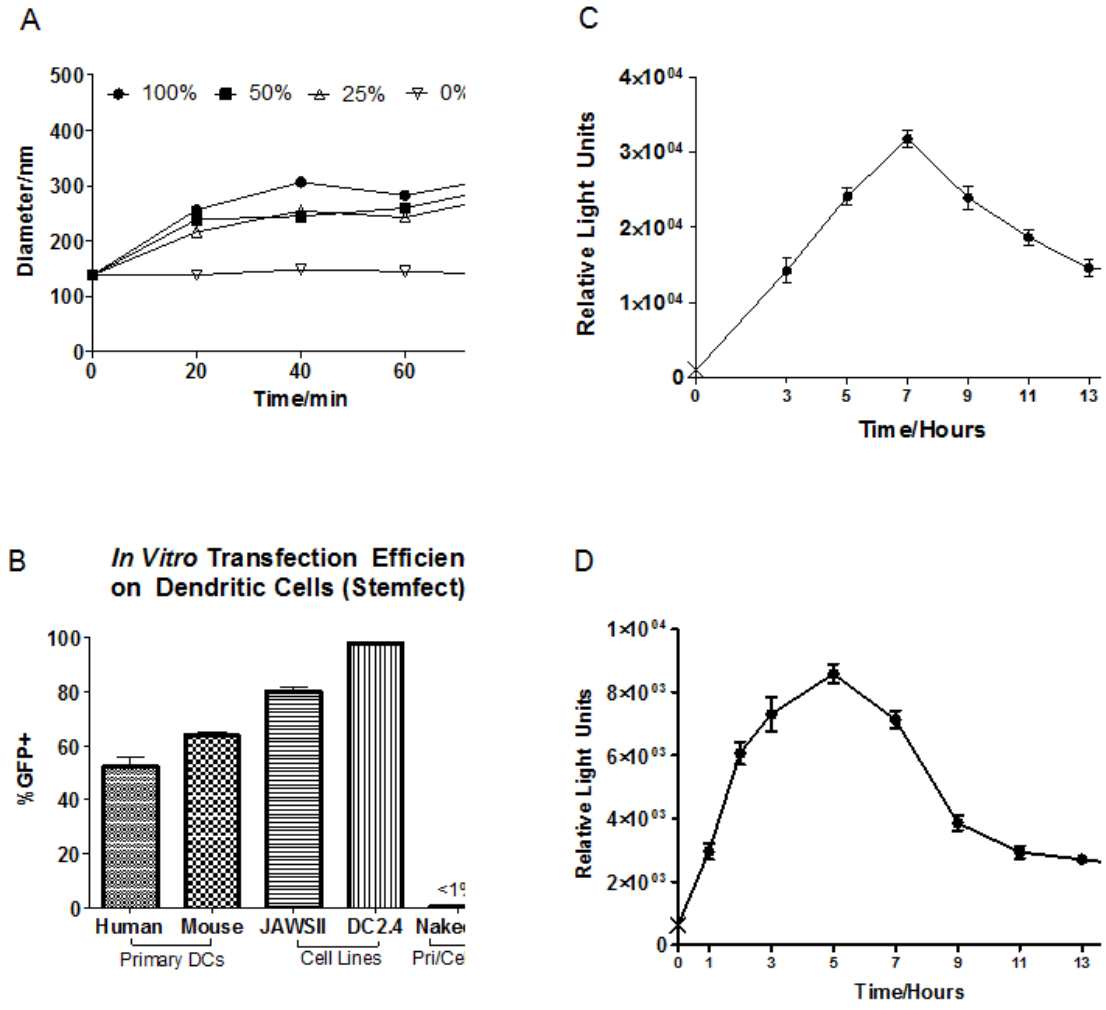

Figure 8. Transfection efficiency of nanoparticle mRNA and naked mRNA in vitro.

(A) Aggregation kinetics of p/mLuc in 0-100% mouse serum.

(B) In vitro p/mGFP and n/mGFP transfection of primary DCs and DC cell lines.

(C) and (D) In vitro p/mLuc transgene expression kinetics of primary human peripheral blood monocyte-derived DCs and primary mouse bone marrow precursor-derived DCs respectively ('X' represents background luminescence). Cells seeded on the same 96-well plate were transfected at various time points with 0.4 μg mLuc (n=5) and assayed after 15 hours. Results were averages of 3 independent experiments.

3.3.2 Nasal cavity can be consistently transfected with p/mRNA but not n/mRNA. When administered intranasally, only mLuc delivered in nanoparticle form (p/mLuc) resulted in consistent and statistically significant bioluminescence (Figure 9A) over negative controls (non-transfected mice and mice transfected with mOVA nanoparticle). Luciferase expression peaked at about 4 hours and decayed exponentially to near background at 24 hours post-mRNA delivery. Expression levels mediated by p/mLuc were consistently detected in 5 independent experiments (n>15) and were not confounded by false positives. Bioluminescence signal with mLuc delivered in naked form (n/mLuc) were similar to negative controls. However, we were able to observe weak signals (but statistically significant ($p < 0.05$) bioluminescence in mice transfected with n/mLuc-RL. This signal was only evident at 4-hour post-mRNA delivery (Figure 9). It should be noted that negative controls when injected with luciferin also showed detectable bioluminescence at the nasal site (creating false positives) as shown in Figure 9A.

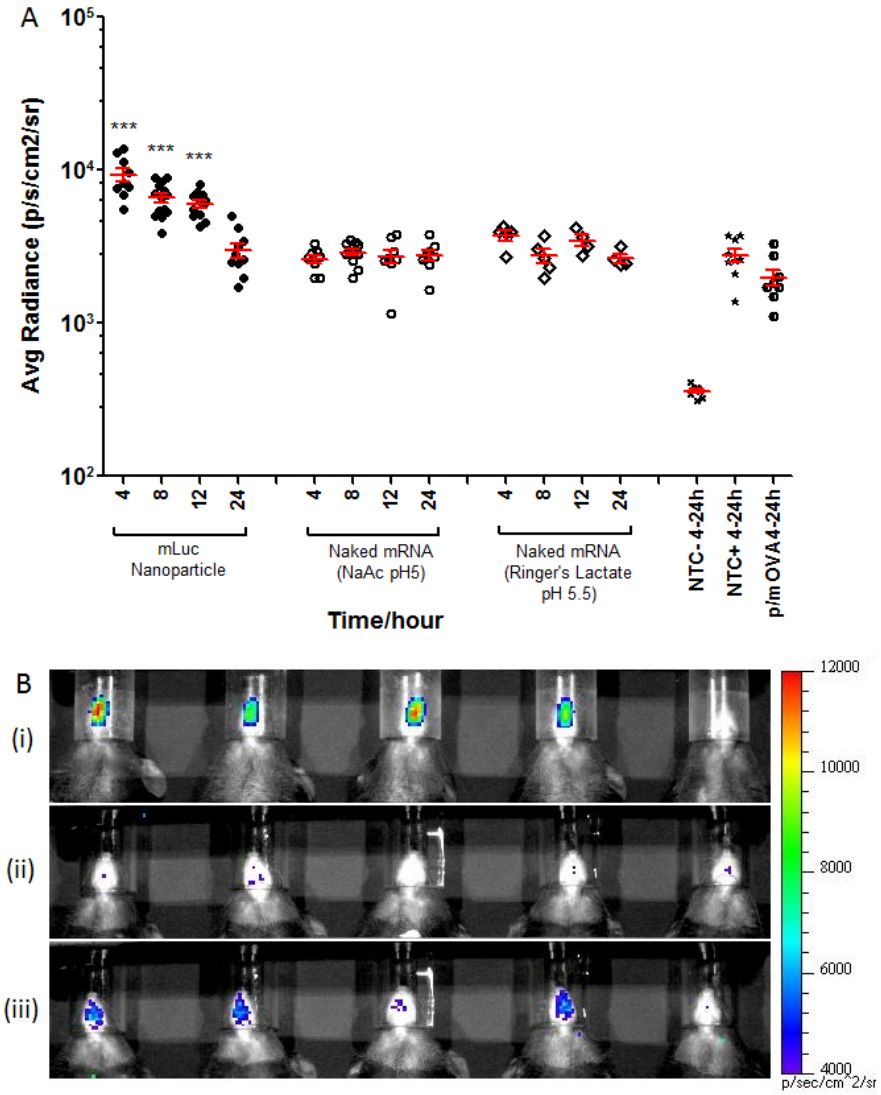

Figure 9. ***In vivo*** **transfection efficiency of nanoparticle mRNA and naked mRNA administered intranasally.**

(A) Bioluminescence in C57BL/6 mice transfected intranasally with 4 μg of p/mLuc and n/mLuc over a 24 hour time period. NTC-: Non Transfected Control, no luciferin injected; NTC+: Non Transfected Control, luciferin injected; p/mOVA: mOVA nanoparticle

(B) Representative set of IVIS images of nasally transfected mice 4 h post-intranasal delivery: (i) p/mLuc (ii) n/mLuc in NaAc Buffer (iii) n/mLuc in Ringer's Lactate. Fifth mouse in panels (i) to (iii) is NTC+. *** $p<0.0001$ compared to p/mOVA, NTC- and NTC+ based on one-way anova (all 15 groups) followed by bonferroni multiple comparison test. * $p<0.05$ based on two tailed student's t-test.

3.3.3 Luciferase expression of nanoparticle mRNA in the RES is short lived after intravenous administration

As shown in Figure 10A, the only time we could detect any bioluminescence using the intravenous mode of delivery was following p/mLuc administration. Bioluminescence following n/mLuc delivery was observed only around the site of injection in the tail skin, presumably caused by leakage into the subcutaneous space during IV injection (Figure 10B). As expected, serum nucleases were efficient in degrading naked mRNA even when dissolved in Ringer's Lactate, reinforcing the notion that any enhancement mediated by Ringer's Lactate was not due to mRNA protection. Interestingly, transfection was observed predominantly at the spleen instead of liver and may be attributed to gene carrier property. However, the luciferase expression was short lived. While expression could be detected in some mice at other sites after 24 hours, splenic luciferase expression was undetectable after 24 hours in all mice. Tissue barriers (super fascia, skin and fur) might have scattered weaker signals that would otherwise be detected. In some mice, injected particles leaked into the subcutaneous space transfecting skin of tail (Figure 10B, mouse #1 and #5). This provided a convenient internal control that further confirmed rapid clearance of luciferase from the spleen. As initial luciferase expression levels were reasonably high (average radiance between 10^5- 10^6), its short-lived kinetics might not be attributed to poor transfection but likely indicated rapid breakdown of luciferase protein and/or mRNA in splenic cells.

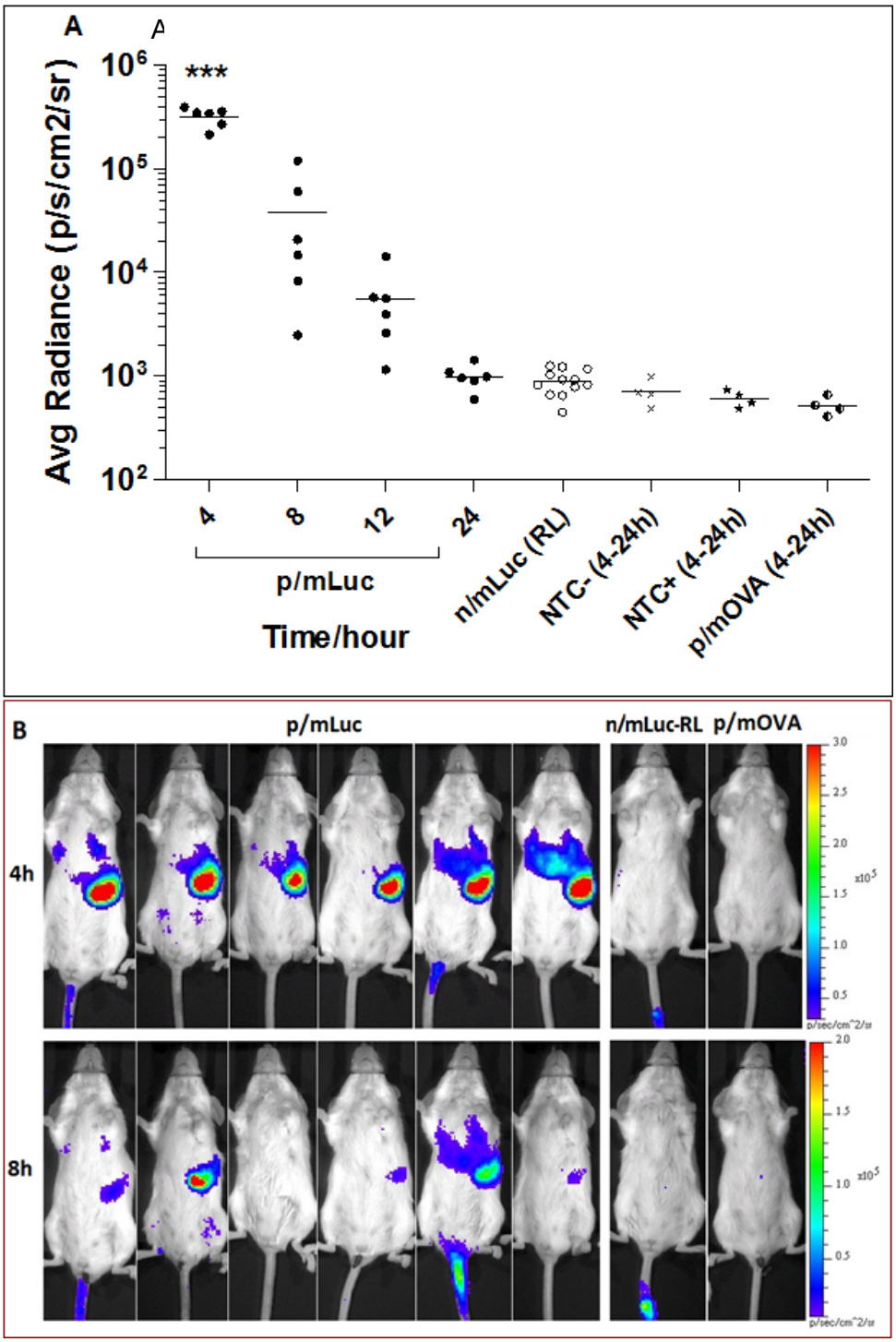

Figure 10. Evaluating in vivo transfection efficiency of nanoparticle mRNA and naked mRNA administered intravenously.

(A) Bioluminescence signal in BALB/c mice intravenously administered with 26 ·g of p/mLuc and m/Luc.

(B) IVIS images of mice transfected in (A) at 4 and 8 h time points with respective color scales. p/mOVA: mOVA nanoparticle NTC-: Non Transfected Control, luciferin not injected; NTC+: Non Transfected Control, luciferin injected. *** $p<0.0001$ compared to n/mLuc, p/mOVA, NTC- and NTC+ based one-way anova (all 8 groups) followed by bonferroni multiple comparison test.

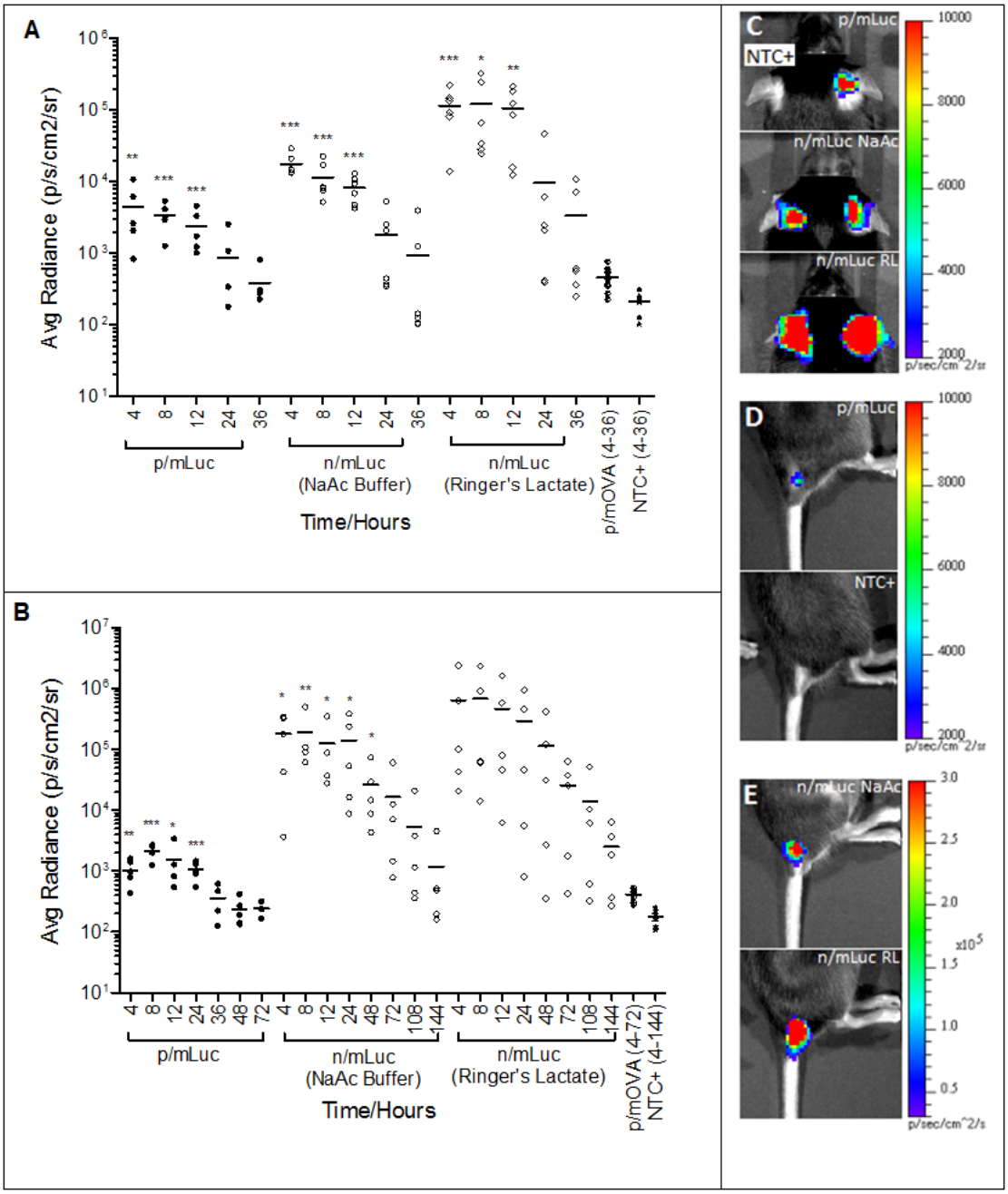

Figure 11. Evaluation of in vivo bioluminescence after subcutaneous injection of mRNA

(A) *In vivo* bioluminescence in C57BL/6 mice transfected subcutaneously at the base of the ear pinna (SubQ-EP) with p/mLuc and n/Luc (in NaAc and RL) from 4-36 hours.

(B) *In vivo* bioluminescence in C57BL/6 mice transfected subcutaneously at the base of tail (SubQ-BOT) with p/mLuc and n/Luc (in NaAc and RL) from 4-144 hours. pH of p/mLuc and NaAc buffer was adjusted to 7.4 with 1M Hepes, while pH of Ringer's Lactate was kept at its native value of 5.5. (C, D, E)

Representative IVIS images of transfected mice ear-pinnae (C) and base of tail (D) and (E) base of tail 4h post injection. *, **, ***: $p<0.05$, 0.005, 0.001 respectively based on two-tailed Student's t-test (p/mLuc vs p/mOVA, n/mLuc vs NTC+). Detailed statistical analysis of (A) reported in Supplementary Figure 2.

3.3.4 Naked mRNA mediates higher and more sustained transfection than nanoparticle mRNA when delivered subcutaneously.

When we compared naked versus the nanoparticle format for mRNA delivery at subcutaneous sites, n/mRNA was significantly more efficient than p/mRNA with higher transfection efficiencies. As shown in Figure 11A, both p/mLuc and n/mLuc were capable of transfecting subcutaneous tissue at ear pinnae with statistically significant levels for at least 12 hours. In particular, when n/mLuc was dissolved in Ringer's Lactate, luciferase expression was more than one order of magnitude above p/mLuc at the ear-pinnae site. This was unexpected because we previously showed that p/mRNA possessed good colloidal stability (Figure 8) and has been shown by the manufacturer to transfect primary fibroblasts efficiently. The contrast between both delivery formats was more striking at the base-of-tail subcutaneous site (Figure 11B). This particular site was chosen because of enhanced lymphatic drainage to the inguinal lymph node in mice. At SubQ base-of-tail site, statistically significant levels of luciferase could be detected in all groups for at least 24 hours. It should be noted that a higher mLuc dose (8 μg) was applied because we could not detect consistent luciferase expression with 4 μg of mRNA. Interestingly, expression at base-of-tail lasted for more than 6 days, with luciferase expression still detectable in 3 out of 5 n/mLuc-RL transfected mice at the end of day 6. Within the n/mLuc groups, greater transfection enhancement by Ringer's Lactate was observed at ear pinnae site compared to base-of-tail site of injection. Overall, gene expression by n/mLuc at both SubQ sites was sustained and at 1-2.5 orders of magnitude higher compared to p/mLuc.

3.3.5 Subcutaneous transfection is pH dependent, but independent of RNAse inhibitor.

When n/mLuc was injected SubQ-EP, we observed as others did, an enhancement in naked mRNA transfection with calcium-containing Ringer's Lactate. As shown in Figure 12A, the transfection efficiency of naked mRNA was not further enhanced, nor deteriorated when injected together with RNase inhibitor. Hence, RNAse did not appear to pose a problem to n/mRNA at SubQ sites. In addition, as RNase inhibitor used was a protein, our data further suggested that the addition of proteins in mRNA did not affect n/mRNA transfection. We also observed that acidic pH reduced transfection efficiency of n/mRNA (Figure 12B). When neutralized with Hepes, statistically significant enhancement in transfection was observed. As the native pH of Ringer's lactate was 5.5, we investigated whether physiological pH might further increase the transfection efficiency. However, we did not detect any enhancement in transfection efficiency (Figure 12B), indicating that the use of Ringers' Lactate rendered transfection insensitive to pH.

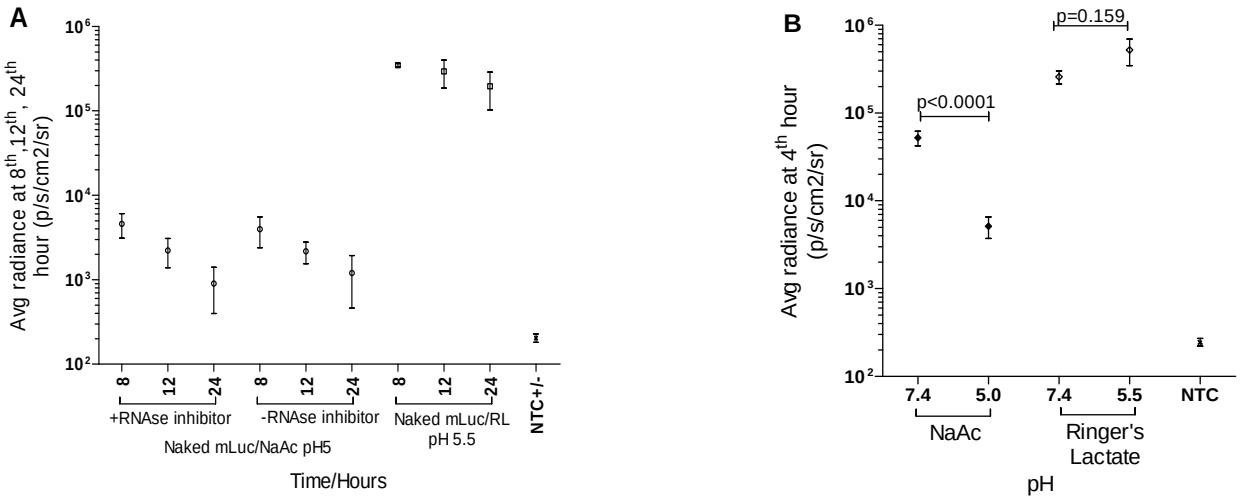

Figure 12. Effect of RNase inhibitor and pH on mRNA transfection.

(A) Effect of RNAse inhibitor on n/mLuc transfection at SubQ-EP. C57BL/6 mice were transfected with n/Luc +/- RNAse inhibitor (1unit/μl) at SubQ-EP. Bioluminescence was assayed at 8, 12, and 24 h.

(B) Effect of pH on n/mLuc transfection. C57BL/6 mice were transfected with n/Luc dissolved in NaAc (pH 5 or 7.4) and Ringer's Lactate (pH 5.5 or 7.4). pH was adjusted with 1M Hepes. Bioluminescence was assayed at 4 h post injection. p values were calculated using two-tailed student's t-test.

3.3.6 Exponential decrease of transgene level with time at all sites of administration. The luciferase expression kinetics were characterized by an exponential decrease in gene expression that could be fitted into exponential curves based on first order decay kinetics $y=Ae^{-\lambda t}$ (Figure 13 and Supplementary Figure 1). The trend was unexpectedly consistent and did not depend on the site of injection (R^2= 0.97-0.99) or delivery format. Hence, *apparent* half-lives of luciferase protein expressed by mLuc *in vivo* could be computed and were tabulated in Table 3. Apparent luciferase half-lives determined for p/mLuc were relatively consistent across all sites (except IV). While the trend was consistent at subcutaneous sites, apparent half-lives of n/mLuc at SubQ-BOT were higher compared to SubQ-EP. We also observed an inverse relationship between transfection efficiency and apparent half-lives in the n/mLuc group. The use of Ringer's Lactate in n/mLuc transfections increased the transfection efficiencies, but also slightly decreased apparent half-lives at both base-of-tail and ear-pinna sites.

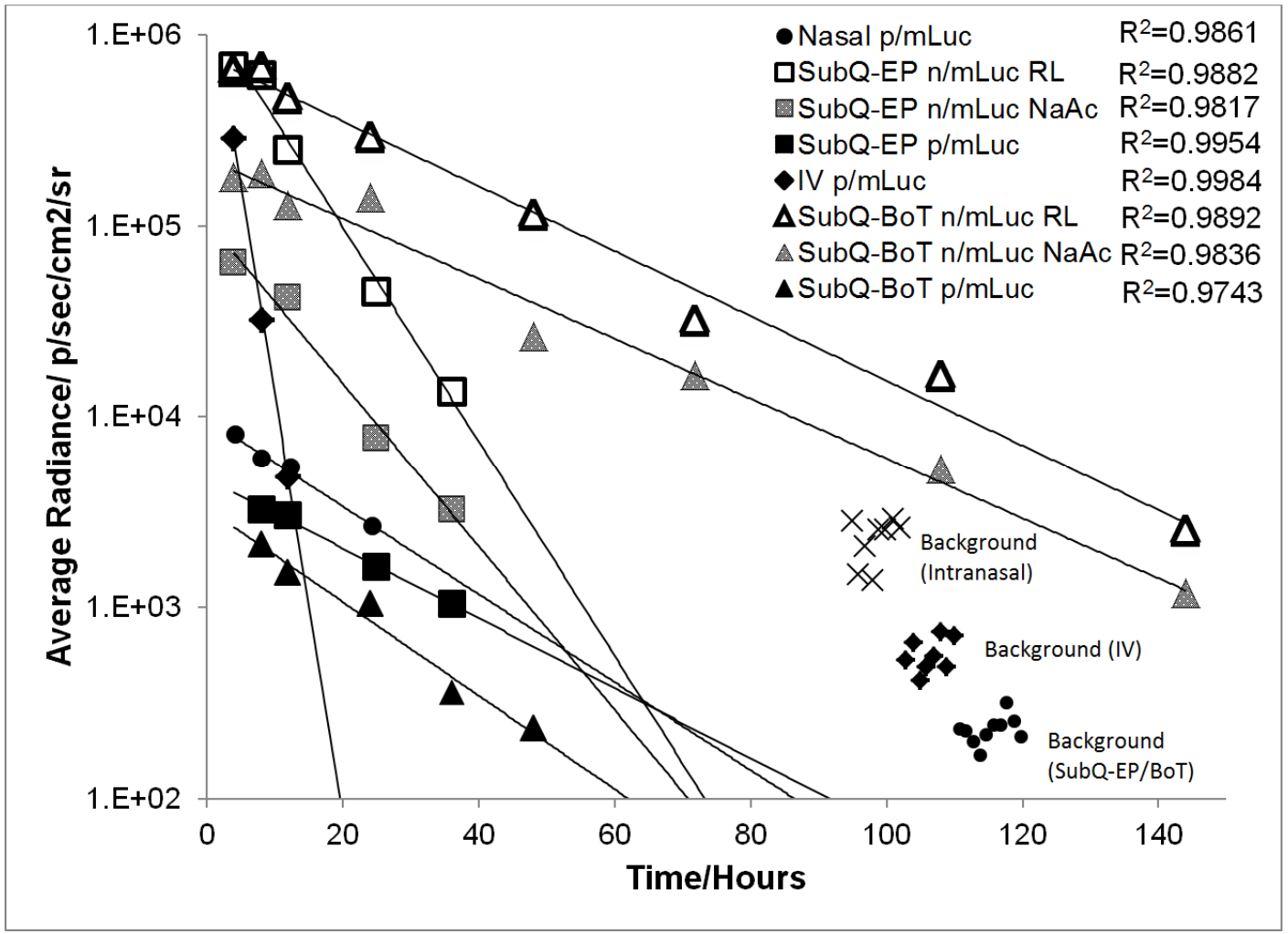

Figure 13. Regression analysis of luciferase expression kinetics in vivo.
Representative curves from each site/format were shown above. Additional regression curves were shown in Supplementary Figure 1.

Table 3. Apparent in vivo half-life of luciferase protein expressed from mRNA

Apparent Luciferase Half-Lives Expressed From mRNA			
Administration Site	Delivery Format/Buffer	Decay Constant	Apparent Half-life/h
Intranasal	p/mLuc Exp 1	0.044	15.8
Intranasal	p/mLuc Exp 2	0.054	12.8
Intranasal	p/mLuc Exp 3	0.053	13.1
SubQ-Base of tail	p/mLuc NaAc	0.056	12.4
SubQ-Ear Pinnae	p/mLuc NaAc Exp 1	0.051	13.6
SubQ-Ear Pinnae	p/mLuc NaAc Exp 2	0.042	16.5
Intravenous	p/mLuc NaAc	0.510	1.4
SubQ-Base of tail	n/mLuc NaAc	0.036	19.3
SubQ-Base of tail	n/mLuc RL	0.039	17.8
SubQ-Ear Pinnae	n/mLuc NaAc Exp 1	0.098	7.1
SubQ-Ear Pinnae	n/mLuc NaAc Exp 2	0.092	7.5
SubQ-Ear Pinnae	n/mLuc RL Exp 1	0.129	5.4
SubQ-Ear Pinnae	n/mLuc RL Exp 2	0.138	5.0

3.4 Discussion

Reports on nanoparticle-mediated delivery of mRNA, particularly in vivo, are relatively scarce compared to DNA delivery despite the advantages of obviating nuclear entry, avoiding insertional mutagenesis and more rapid gene expression. The transient and non-integrating nature of mRNA transfection is well suited for genetic vaccination. In this study, we first evaluated a number of mRNA nanoparticle formulations against dendritic cells with respect to their transfection efficiency, cytotoxicity, and colloidal stability at high concentration. The last parameter is important because it will allow us to vaccinate at a high dose in small injection volume. Of all gene carriers screened (Supplementary Figure 3), which include lipofectamine, chitosan, PEI (25kda), polyamidoamine (CBA-ABOL) [123] and lipopolyplexes of DOTAP/Chol and DOTAP/DOPE/Chol, Stemfect® produced the best results. In DC2.4 cell line, Stemfect attained a transfection efficiency of 97% (GFP+ population) compared to 60% by Perche *et al.* [40], 30% by Su *et al.*[88] and 50% by Cheng *et al.* [94]. There has not been any report on mRNA nanoparticle transfection of primary DCs, and we find that mRNA nanoparticles formulated using Stemfect transfect primary human and mouse DCs at transfection efficiencies of 52% and 64% (GFP+ cells) respectively. Our study provides encouraging direct evidence to proof the concept that it is possible to transfect primary DCs efficiently using mRNA nanoparticles. With the exception of one study reported by Perche *et al.* [40], mRNA vaccination has relied on the application of naked mRNA. In this study, we systematically compare the performance of mRNA nanoparticles formulated using Stemfect (p/mLuc) versus naked mRNA (n/mLuc) in intranasal, intravenous, or subcutaneous administrations. While p/mLuc outperforms n/mLuc in both intranasal and intravenous delivery, n/mLuc produces higher and more sustained transgene expression in subcutaneous injection. Since the intranasal and

intravenous routes target directly the Nasal Associated Lymphoid Tissues (NALT) and the spleen respectively, this study indicates the utility of nanoparticle-mediated mRNA for vaccination.

Aside from targeting NALT, nasal administration of vaccine is popular due to its non-invasive nature. We show that p/mLuc (4μg dose) consistently achieves gene expression in the nasal cavity with an average radiance of $9x10^3$ p/sec/cm2/sr at 4-hr post-delivery, whereas n/mLuc only produces background level at all time-points. Compared to the only other study that reported intranasal mRNA nanoparticle transfection (4μg dose) [88] , this is the highest *in vivo* transfection efficiency we have observed. Within the n/mLuc groups, we are only able to detect bioluminescence from n/Luc (RL group) at 4^{th} hour time point. Despite being transient, our finding highlights a significant contrast with naked pDNA, which does not transfect the nasal mucosa[124]. As the residence time of n/mLuc and p/mLuc in the nasal cavity is similar (Supplementary Figure 4), higher transfection efficiency of p/mLuc is unlikely due to better mucoadhesion. Furthermore, since RL is known to improve naked mRNA transfections via enhanced cellular uptake [120], we can reasonably infer that n/mLuc transfects poorly due to RNAse present in the nasal tissues. In our study, we also consistently detect bioluminescence from nasal cavities of non-transfected mice that are injected with luciferin (NTC+, Figure 9A) compared to those without luciferin (NTC-, Figure 9A). The difference, in photons/sec/cm^2/sr, between NTC+ and NTC- is about one order of magnitude (Figure 9A). This appears to be unique to intranasal site as no such differences are observed in the spleen, ear pinna and base-of-tail.

In contrast with other transfected sites, luciferase expression is most short-lived when delivered via intravenous route, which coincidentally targets the spleen. The near spleen-specific transfection is likely due to the unique properties of the gene carrier, which is closely related to a class of lipidoid previous reported for siRNA delivery [125]. We also speculate that the colloidal stability of the nanoparticles in mouse serum promotes biodistribution to the spleen. In a preliminary experiment where we formulated p/mLuc with an un-optimized protocol that led to aggregation, transfection in the liver is also observed (Supplementary Figure 5). In Figure 10, where p/mLuc are formulated with an optimized protocol, moderate levels of transfection in the liver can still be observed in 2/6 mice. Bulk mixing, the method used to formulate p/mLuc nanoparticles for this study, produces mRNA nanoparticles that are heterogeneous in size, surface charge, and likely composition. Recent literature has shown that a more controlled self-assembly of lipoplexes and polyplexes may lead to better performance with respect to colloidal stability, transfection efficiency, and even cytotoxicity[59, 126, 127]. These observations suggest that a more controlled formulation of the mRNA nanoparticles may improve and better predict in vivo performance.

The significantly shorter half-life of luciferase at the spleen may be attributed to transfection of antigen presenting cells, which are very efficient in breaking down endogenous protein and presenting them on MHC complexes. In our hands, intravenously administered p/mRNA has an apparent half-life of 1.4 hours (R^2=0.9984, N=6) and becomes undetectable at 24 hours. Unlike the subcutaneous or intranasal sites, the spleen is found under several layers of tissues and would have a higher threshold of detection, which may have contributed to a shorter apparent half-life as weaker luminescence at later time-points may not be detected.

Subcutaneous transfection with naked mRNA is well studied, but direct comparison with mRNA polyplexes or lipoplexes has not been reported. In this study, we reproduced published data where n/mLuc transfection is enhanced by RL at SubQ-EP by an order of magnitude [120]. We also observe n/mLuc outperforming p/mLuc, not unlike pDNA transfection where naked DNA is often superior, if not equal, to polyplexes in intramuscular or subcutaneous transfection [128, 129]. Since the predominant cell types transfected by naked m/Luc at the ear-pinnae would be MHC-II negative such as muscle cells, fibroblasts and keratinocytes [120], we speculate several reasons for this observation: First, the majority of cells that take up and express mRNA could have been muscle cells, which are well known to be more efficiently transfected by naked nucleic acid. Second, uptake mechanisms for n/RNA and p/mRNA are different with the former significantly more efficient than the latter. Indeed naked mRNA uptake is facilitated by nucleic acid specific receptors [120], while nanoparticles uptake may have to depend on other non-specific endocytic mechanisms, which may be directed into various degradative pathways. In this study we include an additional SubQ site at the base-of-tail, which not only is a favorable site for lymphatic drainage (5% Evans Blue injected subcutaneously at base-of-tail labels the inguinal lymph node within 30min [77]), but also serves as an additional control to ear pinna site. We find consistent trends of higher transfection efficiency by n/mLuc over p/mLuc at both ear pinna and base-of-tail sites, indicating that SubQ may not be an ideal vaccination site for p/mLuc.

An interesting finding from our study is that in vivo luciferase levels decay exponentially in a consistent manner regardless of format or site of administration. Hence apparent in vivo half-lives of luciferase protein expressed from mRNA, at given doses used in this study, can be computed. We noted earlier that apparent half-lives found between BOT

and EP sites are different for subcutaneous n/mLuc transfection. This can be attributed to the difference in cell type subdistribution at both sites as the BOT site is significantly more muscular than ear pinnae. Our reasoning is also supported by Figure4, where transfection enhancement by RL is much smaller at BOT (Figure 11B) compared to that at EP (Figure 11A). Cells found in the former respond more favorably to naked mRNA, reducing the need of RL for enhancement. Due to a different cellular makeup, intracellular stability of mLuc and/or luciferase protein consequently varies between both sites.

Luciferase expression can be further extrapolated towards background levels to predict duration of gene expression. For SubQ-EP, detectable expression of both n/mLuc and p/mLuc can be extrapolated to 2-3 days, which is consistent with n/mLuc data from Probst *et al.* (3 days) [120]. As one of the attractions of mRNA delivery is its transient nature, our data further support the idea that mRNA gene expression can be predictable and potentially controllable. This will help accelerate the translation of mRNA therapeutics into clinics.

3.5 Conclusion

In vitro and *in vivo* transfection efficiency and transgene expression kinetics of mRNA in naked and nanoparticle format are evaluated. We show that primary DCs can be efficiently transfected with mRNA nanoparticles with gene expression decaying in a biphasic manner. mRNA nanoparticles are also efficient *in vivo* when administered intranasally and intravenously, while naked mRNA dissolved in Ringer's Lactate is the most efficient at subcutaneous sites (ear pinna and base-of-tail). Gene expression at all sites decays in consistent exponential trends, which may render mRNA gene therapy not

only safe but also predictable. This study shows that mRNA therapeutics adds to the armamentarium of biologics that can impact genetic medicine and warrants further research.

4 Intranasal vaccination with mRNA nanoparticles induces prophylactic and therapeutic anti-tumor immunity

4.1 Introduction

Tumor vaccination employing mRNA transfected dendritic cells (DCs) has been shown to be an effective strategy for treatment of cancer[130-135]. Promising results emerging from recent clinical trials[3, 15, 136] supports the notion that this is a strategy that can be translated to humans and is amenable to commercialization. However, this process involves harvesting cells from patients via leukapheresis, generating DCs *in vitro* from adherent monocytes, loading them with mRNA, maturing them *in vitro* and re-injecting these mRNA-loaded DCs back into the patient. This is a cost, labor and resource intensive procedure. Because of these reasons, researchers have explored alternative cell-based approaches[34, 35], as well as direct *in vivo* injection of mRNA in naked[19, 36] and nanoparticle formats[37-42]. However, due to rapid degradation of naked mRNA *in vivo*, direct injection of mRNA is effective only when it is injected directly into lymph nodes[19, 36]. Intranodal injection is a highly invasive procedure in mice and hence not amenable for repeated administrations. Moreover, although intranodal injection is performed using ultrasound-guidance in humans, it remains a technically challenging procedure that requires surgical expertise. While this approach is an improvement over the existing *ex vivo* DC-based approach, scale-up remains a significant challenge thus hindering its broad application.

A strategy that overcomes this problem is encapsulating mRNA in nanoparticles, which not only protects mRNA from nuclease degradation, but also facilitates its uptake by cells and endosome escape within cells leading to enhanced delivery efficiencies. This approach may obviate the need for intranodal administration, while still permitting direct

in vivo application of an off-the-shelf mRNA vaccine formulation via conventional routes of administration. Indeed, mRNA nanoparticle delivery has attracted interest from many research groups in recent years[40, 44, 107, 137, 138]. In addition, therapeutic efficacy of mRNA encapsulated in nanoparticles for tumor vaccination has also been recently demonstrated[39, 40]. Notably, tail vein and subcutaneous injections are the only routes evaluated in all of these studies. We have previously reported that primary DCs can be efficiently transfected by mRNA encapsulated in nanoparticles *in vitro*. These particles are about 180nm and 300nm in hydrodynamic diameter and have zeta potentials of +40mV/-12mV in water and 10% FBS supplemented media, respectively[139]. In the same study, we determined that luciferase expression mediated by nasally administered mRNA nanoparticles last for about 24 hours compared to naked mRNA, which is detectable only up to 4 hours post-administration[139]. The bioavailability of transgene product is clearly superior to nasally instilled soluble protein antigens, where >85% of the soluble antigen is cleared from the nasal site within 6 hours[140].

In this study, we hypothesize that nasal vaccination could be an effective strategy for mRNA tumor vaccination. Intranasal route of immunization is desirable because of its non-invasive nature, amenability for repeated administration and is associated with high patient compliance. It has been previously reported that intranasal immunization with naked mRNA can induce a moderate level of protection against tuberculosis in mice[141]. We reason that significantly higher nasal transfection efficiencies mediated by mRNA nanoparticles could translate to the induction of anti-tumor immunity. In addition, a previous study has reported that intranasal tumor vaccination with soluble OVA peptides can induce robust anti-tumor immunity[142]. Therefore we reason that the prolonged presence of antigen at the nasal site where the Nasal-Associated Lymphoid Tissues

(NALT) are located[79] could translate to enhanced immune responses. Last but not least, we observe that nasally administered nanoparticles are taken up by $CD11c^{high}$ cells isolated from NALT (Supplementary Figure 8), indicating that this route of administration could be used to directly target DCs.

Based on above rationale, we set up an immunization scheme to investigate the therapeutic efficacy (Figure 14) of chicken ovalbumin (OVA) encoding mRNA nanoparticle vaccination in prophylactic and therapeutic immunotherapy models with E.G7-OVA tumor cells. The immunization schemes are based on published prime-boost protocol that entails weekly nasal administration for three weeks[143] (prophylactic) and four injections every other day[36] (therapeutic). Because we use cholera toxin (CT) as an adjuvant, there is a possibility that tumor immunity is induced by CT and not the OVA mRNA nanoparticle. To rule out this possibility, we immunize mice with green fluorescent protein (GFP) mRNA nanoparticles as controls.

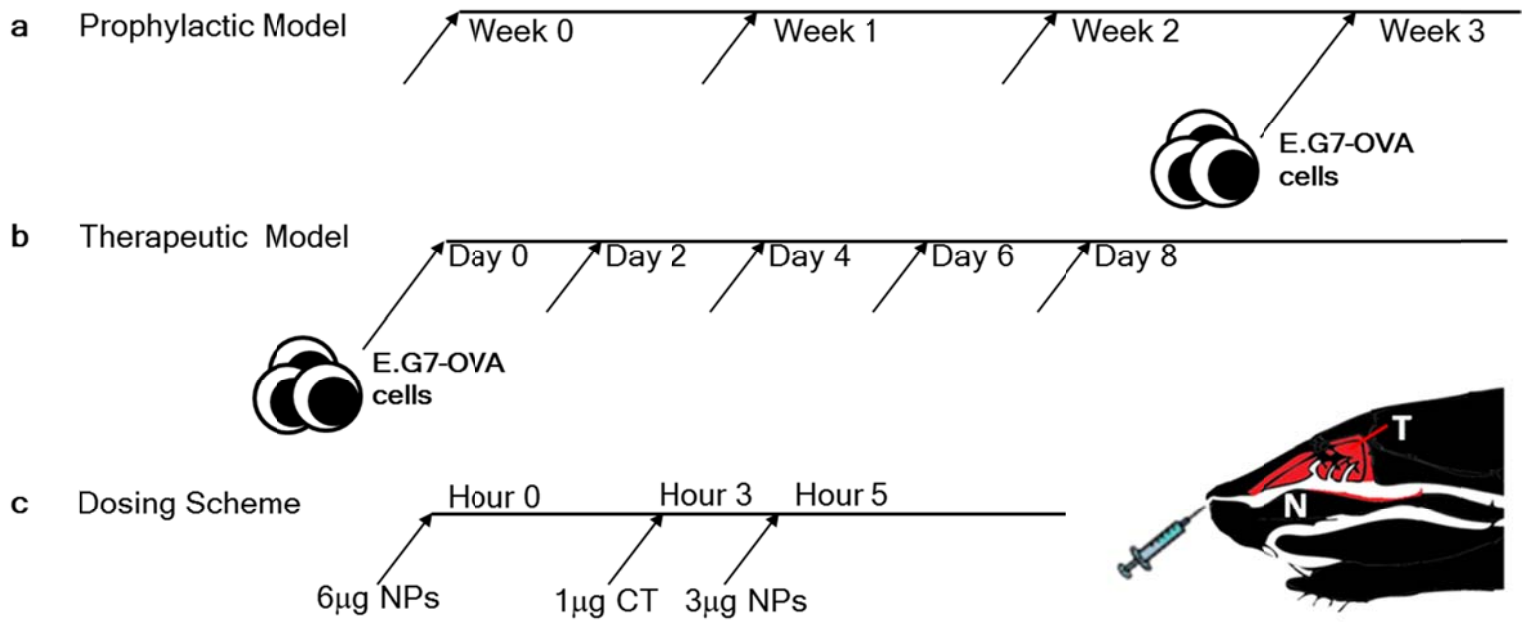

Figure 14. Immunization scheme for intranasal mRNA tumor vaccine.
Immunization scheme for intranasal mRNA tumor vaccine. **a**) Prophylactic immunization. **b**) Therapeutic immunization. **c**) Dosing Scheme. (NP: mRNA nanoparticles, CT: Cholera Toxin, N: NALT, T: Turbinates). Additional details are provided in materials and methods.

4.2 Materials and methods

4.2.1 Cloning of pGEM4Z/GFP/A64 and pGEM4Z/OVA/A64

The cDNA for green fluorescent protein (GFP) was derived from pEGFP-N1 (Clontech, Palo Alto, California) and inserted into pGEM4Z/A64[122]. Chicken ovalbumin cDNA in pUC18 was kindly provided by Dr. Barry T. Rouse, University of Tennessee, Knoxville. The 1.9 kb EcoR1 fragment containing the coding region and 3' untranslated region was cloned into the EcoR1 site of pGEM4Z/A64 to generate plasmid pGEM4Z/OVA/A64[144].

4.2.2 *In vitro* transcription of mRNA

Each plasmid of interest was digested with the restriction enzyme SpeI to linearize the DNA. After purification, DNA was used as template for *in vitro* transcription using T7 High Yield RNA Synthesis Kit (New England Biolabs, NEB) in the presence of anti-reverse cap analogue (ARCA, NEB). *In vitro* transcribed (IVT) mRNA was purified with RNEasykit (Qiagen), quantified by spectrophotometry, and analyzed by MOPS formaldehyde gel electrophoresis to confirm the synthesis of full-length mRNA. GFP mRNA was labeled with Cy5 labeling kit (Mirusbio) according to manufacturer's protocol.

4.2.3 Nanoparticle formulation

mRNA nanoparticles were formulated (as previously described[34]) by adding 8μl ethanol reagent (mRNA Transfection Reagent, Stemgent) to 10μl of mRNA (0.2μg/μl) suspended in Stemfect buffer under gentle vortexing for 10 seconds. The mixture was incubated at room temperature (RT) for 12 min under vacuum to completely remove ethanol. Size and zeta potential of nanoparticles were confirmed using NanoZS (Malvern) in both DI water (180nm/+40mV) and serum (300nm, -12mV), consistent with what was previously reported[34].

4.2.4 Ethics statement

In conducting the research described in this paper, the investigators adhered to the Guide for the Care and Use of Laboratory Animals" as proposed by the committee on care of Laboratory Animal Resources Commission on Life Sciences, National Research Council. The facilities at the Duke vivarium are fully accredited by the American Association for Accreditation of Laboratory Animal Care (AAALAC), and all studies were conducted using a protocol approved by the Duke University IACUC.

4.2.5 Intranasal vaccination

6 to 7-week old female C57Bl/6 mice were obtained from Jackson Labs. Intranasal immunization with mRNA encoding ovalbumin (mOVA) or green fluorescent protein (mGFP) encapsulated in nanoparticles was performed according to Figure 14. Each nasal administration was done in 3 steps as detailed in Figure 14C. Mice were anesthesized with isofluorane in a gas chamber and queued for nasal administration. Each time a single mouse was taken out of the chamber, held in supine position, nasally administered with 15μl of mRNA nanoparticles (3μg) using a P20 pipette (fitted with a gel loading tip) and laid back inside the gas chamber in supine position. This procedure was repeated for the next animal in sequence. Consequently, each mouse was handled twice at an interval of approximately 5 minutes between each 15μl dose for a total of 30μl (6μg) of mRNA nanoparticles. Mice were rested for 4 hours to allow gene expression to peak and subsequently administered with 1μg cholera toxin (CT) in 10μl (List Biologicals). Mice were rested for another 2 hours to allow early immune response at the nasal site and subsequently administered with an additional 15μl (3μg) of mOVA

nanoparticles. In summary, each mouse received a total of 9μg of OVA mRNA nanoparticles and 1μg of CT per vaccination.

4.2.6 Tumor immunotherapy models

For prophylactic immunization, $4x10^5$ E.G7-OVA cells (in 100μl PBS) were injected subcutaneously into the left flanks of immunized mice 7 days after the last immunization (Figure 1). For therapeutic immunization, $2x10^5$ E.G7-OVA (in 100μl PBS) were injected subcutaneously into the left flanks of naïve mice 2 days before the first vaccine dose. Tumors were monitored every other day for signs of onset and measured with vernier calipers. Mice with tumors greater or equal to 500mm^3 were sacked. Tumor volume was calculated using Equation 1, where length is the longer of the 2 measurements. Specific Growth Rates were calculated using Equation 2[145].

$$Tumor \quad Size \quad = \frac{Length \times Width^2}{2} \qquad \text{Equation 1}$$

$$Specific \quad Growth \quad Rate \quad = \frac{\ln\left(V_2/V_1\right)}{D_2 - D_1} \qquad \text{Equation 2}$$

Where V_2/V_1 is the numerical ratio of tumor size measured from the same animal on respective days (D_2 and D_1).

4.2.7 Tetramer staining

Female C57Bl/6 mice were immunized under prophylactic or therapeutic setting as detailed above. 7 days after the last immunization, spleens were isolated and crushed through a 70 micron filter. Splenocytes were depleted of erythrocytes with ammonium chloride/Tris and re-suspended with PBS/10%FBS at a concentration of 10^7 cells/ml. Cells were blocked on ice with CD16/32 (Fc block, Bio legend) for 15 minutes and

subsequently stained on ice with CD8-APC, isotype-PE antibodies (Bio legend) and PE-iTag-MHCI-OVA tetramer (Beckman Coulter) for 30 minutes. Antibody staining was carried out per manufacturer's protocol. For tetramer staining, 2μl of CD8-APC antibody and 5μl of MHC class I H-2Kb-OVA tetramers were added to 10^6 cells (in 100μl) and incubated for 30 minutes at room temperature. Cells were washed, fixed with PBS/1% paraformaldehyde and analyzed by flow cytometry (FACs Caliber).

4.2.8 Statistical analysis

For tumor studies, comparison between two groups was performed using the log-rank test (Mantel-Cox test). Additional comparisons between groups was done by determining the median survival for each group. Tumor growth curves over time were compared using two-way ANOVA with Bonferroni multiple comparison post-test. Statistical significance in tetramer staining comparing two groups was done using paired two-tailed Student's *t* test. A probability of less than 0.05 ($P<0.05$) was considered statistically significant. Calculations were performed using GraphPad Prism.

4.3 Results

4.3.1 Prophylactic immunization with nasally administered mRNA vaccine

We tested intranasal immunization using a prophylactic tumor model, where mice were challenged with $4x10^5$ E.G7-OVA cells injected into the left flank 7 days after the last immunization (Figure 14a). Mice intranasally immunized with OVA mRNA nanoparticles (mOVA-NP) demonstrated tumor inhibition ($p<0.01$) and overall survival efficacy ($p<0.01$) compared to mice immunized with GFP mRNA nanoparticles (mGFP-NP) or naked OVA mRNA (mOVA-N) (Figures 15a and 15b). The median tumor free and overall survival duration for the mOVA-NP group were 14.5 and 23 days, which were significantly longer compared to control groups (6 and 14 days for mGFP-NP group; 7 and 13 days for mOVA-N group, respectively). 2 out of 10 mice in the mOVA-NP group remained tumor free for the duration of the study (40 days). Notably, the tumor growth kinetics of mOVA-N group overlapped completely with negative control (mGFP-NP group, Figure 15c), indicating that intranasal administration of naked mRNA did not induce prophylactic tumor immunity. Hence, we concluded that intranasal vaccination with mRNA encapsulated in nanoparticle has an anti-tumor effect in the murine prophylactic E.G7-OVA tumor model.

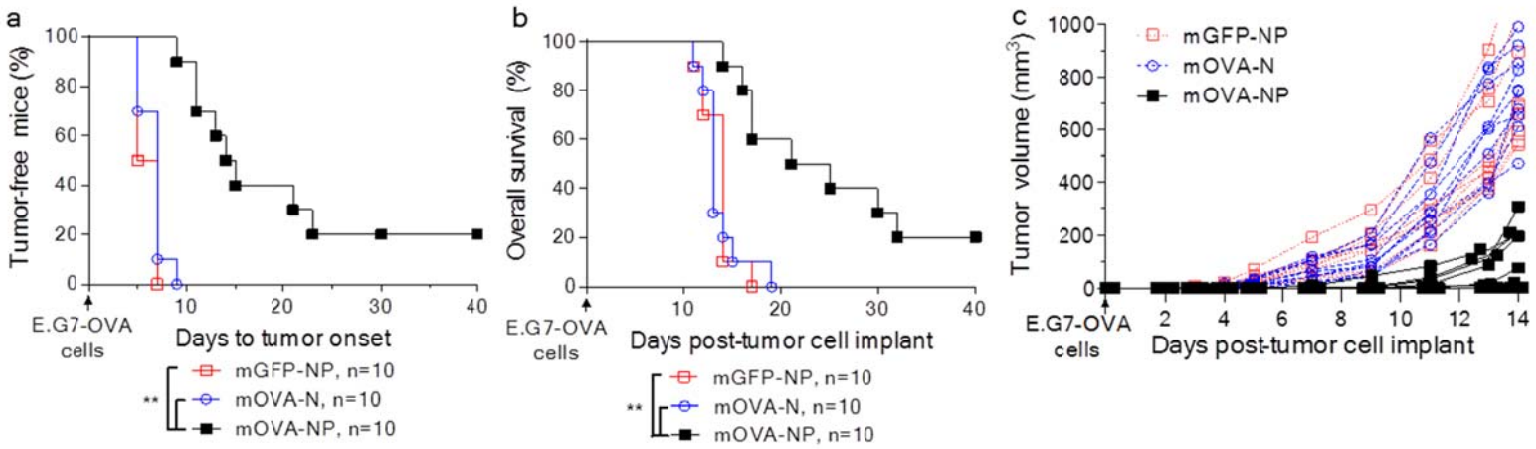

Figure 15. Intranasal mRNA Nanoparticle Vaccination Induces Prophylactic Tumor Immunity.

Prophylactic immunization with OVA mRNA nanoparticles, but not GFP mRNA nanoparticles or naked OVA mRNA induces anti-tumor immunity. Female C57Bl/6 mice were immunized as shown in Figure 14. 4x105 E.G7-OVA tumor cells were subcutaneously injected 7 days later. Mice were sacrificed once tumor volume reached 500mm3. This experiment was conducted twice with similar results. Results from the second experiment were shown. **a**) Onset of palpable tumors. **b**) Overall survival. **c**) Tumor growth over 14 days. For tumor studies, comparison between two groups was performed using the log-rank test (Mantel-Cox test). ** $p<0.01$.

4.3.2 Therapeutic immunization with nasally administered mRNA vaccine.

We further evaluated the potential of intranasal mRNA tumor vaccination using a therapeutic tumor model, where mice were injected with $2x10^5$ E.G7-OVA cells into left flank 2 days before the first vaccine dose (Figure 14b). The number of tumor cells used in the therapeutic tumor model is half that used in the prophylactic model because of the increased stringency of a therapeutic protocol wherein tumor cells are implanted prior to start of immunizations. This provided a treatment window of 7-10 days to determine if the test vaccination regimen could have a potential therapeutic effect. The therapeutic immunization scheme (Figure 14b) was based on a similar protocol used for intranodal naked mRNA vaccination that entailed four immunizations performed every other day[36]. The median tumor free duration for mOVA-NP group (15 days) was statistically significant compared to the control mGFP-NP group (9 days, $p<0.01$) but not mOVA-N group (11 days, $p=0.067$) (Figure 16a). However, the median overall survival for mOVA-NP group (23.5 days) was significant when compared to both mGFP-NP group (15 days, $p<0.001$) and mOVA-N group (17.5 days, $p<0.05$). Two out of eight mice in the mOVA-NP group remained tumor free (Figure 16b) for the duration of the study (40 days).

We observed that following tumor onset, it took a relatively long time for tumors to grow in the mOVA-NP group. The effect of immunization in controlling tumor growth rate was consistently observed in every animal in the mOVA-NP group (Figure 16c). To gain further insight, we analyzed specific tumor growth rates[145] (Equation 1) of each tumor bearing animal every 48 hours for 16 days (Figure 16d). In the mGFP-NP and mOVA-N immunized mice, tumor volumes increased aggressively as soon as nascent tumors appeared. Specific growth rates were arrested rapidly from 0.9 day^{-1} (on day 2) to about 0.3 day^{-1} (day 6 and onwards) for reasons we speculated were related to tumor size (inefficient nutritional transport and onset of necrosis at later time points). In mOVA-NP

immunized mice, specific growth rates did not progress at early time points, and this translated into the observed growth delay (Figure 16c). Amongst the six tumor-bearing mice within the mOVA-NP group (two were tumor free), three showed negligible growth during the first 48 hours. Hence, we concluded that intranasal vaccination with mRNA encapsulated in nanoparticle format could also be effective for therapeutic tumor vaccination.

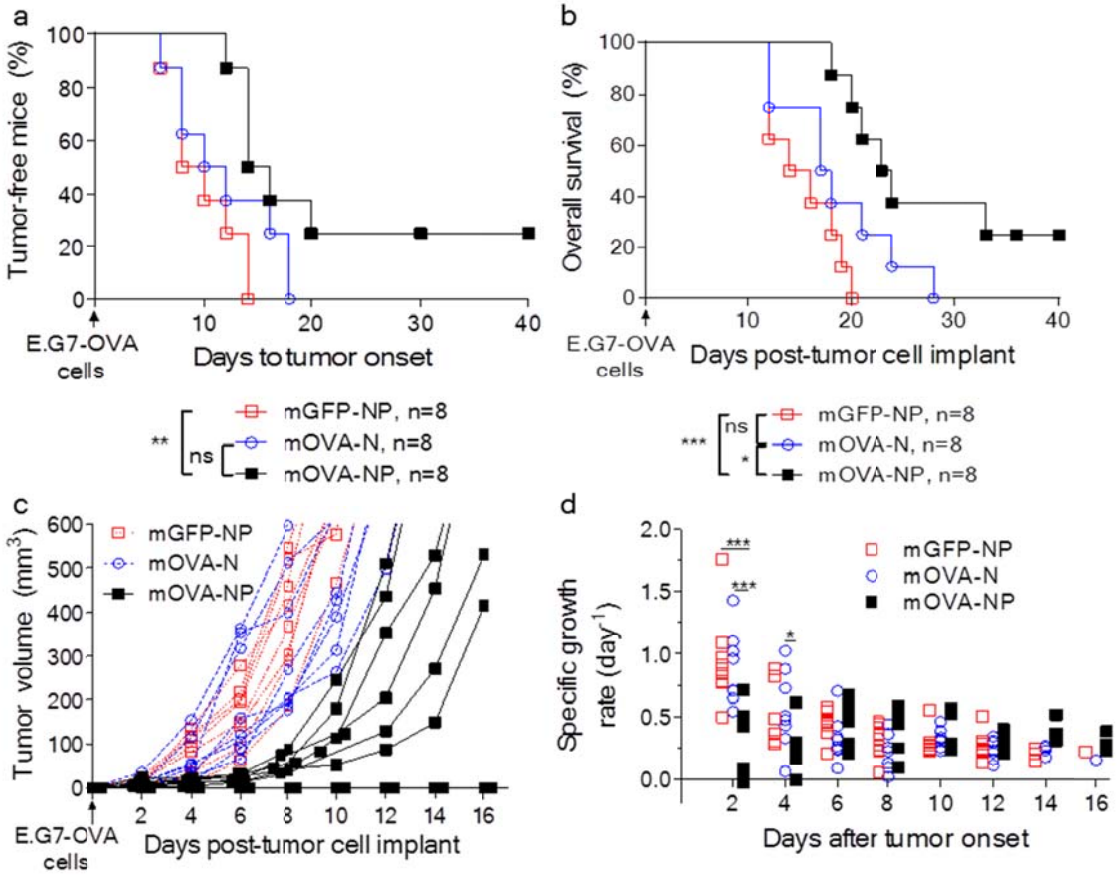

Figure 16. Intranasal mRNA Nanoparticle Vaccination Induces Therapeutic Tumor Immunity.
Therapeutic immunization with OVA mRNA nanoparticles, but not GFP mRNA nanoparticles or naked OVA mRNA induces anti-tumor immunity. Female C57Bl/6 mice were injected subcutaneously with $2x10^5$ E.G7-OVA tumor cells. 2 days later mice were immunized as shown in Figure 14. Mice were sacrificed once tumor volume reached $500mm^3$. This experiment was conducted twice with similar results. Results from the second experiment were shown. **a**) Onset of palpable tumors. **b**) Overall survival. **c**) Tumor growth over 16 days. **d**) Specific growth rate of tumors over time. For tumor studies, comparison between two groups was performed using the log-rank test (Mantel-Cox test). Specific growth rates were compared using two-way ANOVA with Bonferroni multiple comparison post-test. **p<0.05; **p<0.01; ***p<0.001.*

4.3.3 Tumor immunity requires mRNA to be delivered in nanoparticle but not in naked format.

Because T cells are the major cell type involved in tumor clearance, we hypothesized that anti-tumor immunity observed in mOVA-NP treated mice (Figures 15 and 16) would correlate with the presence of OVA-specific T cells. Indeed, consistent with this hypothesis, we observed the presence of H2Kb-OVA tetramer^{+} CD8^{+} T cells in splenocytes isolated from mice immunized with mOVA-NP but not mGFP-NP or mOVA-N (Figure 17). Anti-tumor immunity was only observed in mice immunized with OVA mRNA delivered in nanoparticle format in both the prophylactic and therapeutic tumor model. These data suggests that the use of mRNA for intranasal vaccination applications will require delivery in nanoparticle format.

Table 4. Summary of anti-tumor effect of intranasal vaccination in prophylactic and therapeutic E.G7-OVA tumor model

Groups	Prophylactic Model		Therapeutic Model	
	Median Tumor Onset (days)	Median Survival (days ± SD*)	Median Tumor Onset (days)	Median Survival (days ± SD)
OVA mRNA nanoparticle (mOVA-NP)	14.5	23 ± 1.4	15	23.5 ± 0.4
Naked OVA mRNA (mOVA-N)	7	13 ± 2.1	11	17.5 ± 0.4
GFP mRNA nanoparticle (mGFP-NP)	6	14 ± 0.7	9	15 ± 0.7

*SD: standard deviation

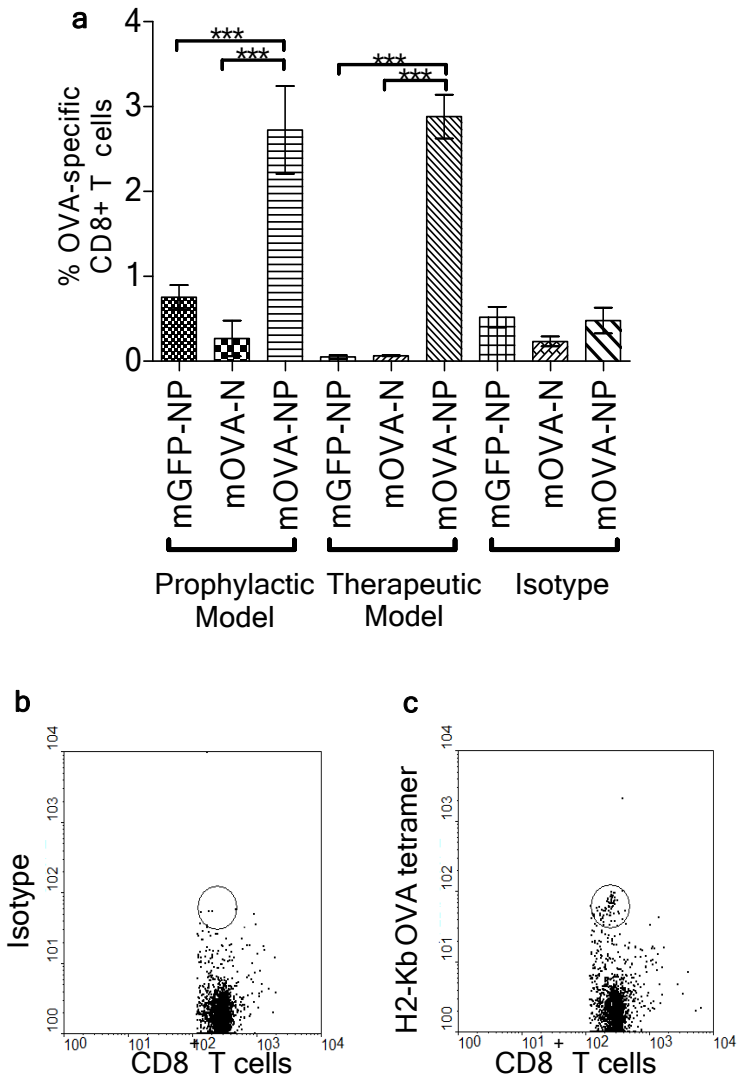

Figure 17. Induction of antigen-specific T cells following intranasal immunization with OVA mRNA nanoparticles.

a) OVA-specific splenic $CD8^+$ T cells stained with H2-Kb OVA tetramers. Groups were mOVA-NP: mice immunized with OVA mRNA nanoparticles, mGFP-NP: mice immunized with GFP mRNA nanoparticles, mOVA-N: mice immunized with naked OVA mRNA. Results were averaged from 2 independent experiments. Statistical significance comparing two groups was done using paired two-tailed Student's t test. ****p<0.001*. Representative flow plots of **b**) isotype and **c**) H2-Kb OVA tetramers, both from mOVA-NP group (prophylactic model).

4.4 Discussion

In this proof-of-concept study, we demonstrate for the first time that intranasally administered mRNA encoding a tumor antigen can induce tumor immunity for the treatment of cancer. Our hypothesis is based on higher nasal transfection efficiencies and longer transgene expression kinetics achieved by mRNA nanoparticles as compared to mRNA delivered in the naked format. Mice treated with OVA mRNA encapsulated in nanoparticle, demonstrated delay in both tumor onset and overall survival compared to controls in prophylactic and therapeutic E.G7-OVA tumor model.

The overall survival and tumor onset of mOVA-NP group in the prophylactic model are clearly superior to mOVA-N group (Figure 15, Table 4). However, in therapeutic model the improvement is less distinct. When tumor growth kinetics between mOVA-N and mGFP-NP groups are compared, we observe that growth curves in the mOVA-N group completely overlapped with mGFP-NP group in the prophylactic model (Figure 16c), but a minor difference is seen in the therapeutic model (Figure 16c). This suggests that naked mRNA immunization had a slight effect in the latter. However, the difference in the latter is not statistically significant. The reason for this could be that the robust innate immune response mediated by cholera toxin facilitated the induction of an adaptive immune response following naked mRNA immunization in the nasal cavity. This corroborates data from another study demonstrating that nasally administered naked mRNA induces immune responses for the treatment of tuberculosis[141].

In the therapeutic setting, we also observe that nascent tumors in every tumor bearing mouse treated with OVA mRNA nanoparticles do not proliferate aggressively. This may

be attributed to immune response generated from intranasal immunization. Since tumor cells can escape immune surveillance[146-149] through immune suppression[150, 151], altered expression of MHC class I[152, 153], as well as generation of immune escape tumor variants[154], specific growth rates eventually caught up with that of control groups (Figure 16c and 16d). Lastly, through tetramer staining analysis we demonstrate that to induce anti-tumor immunity via intranasal route, it is necessary that mRNA is delivered in a nanoparticle.

Because intranasal delivery is a desirable route for vaccination, it has been extensively studied in the past decade. In particular, micro- and nano-particle delivery systems that encapsulate protein antigens or DNA that encode for antigens have been evaluated. However, the focus of intranasal vaccination has often been on the treatment of infectious diseases[124, 143, 155-160]. Nonetheless, a recent study has demonstrated that nanoparticles composed of modified γ-polyglutamic acid (γ-PGA) encapsulating full length OVA protein instilled intranasally induced anti-tumor immunity against melanoma[83]. In addition, a recent study also investigated the use of mannosylated chitosan-DNA (CS-DNA) nanoparticle vaccine for the prophylactic treatment of prostate carcinoma via the intranasal route. Anti-tumor response was only observed in the group that received targeted CS-DNA nanoparticles, but not in the group that received non-targeted nanoparticles. However, the therapeutic efficacy of the targeted CS-DNA nanoparticles was relatively similar to intramuscular vaccination using soluble antigen[161].

Our results contribute to a relatively small number of studies published on mRNA nanoparticle mediated tumor vaccination where overall survival is one of the endpoints[37, 39, 40, 42]. In addition, results from our current study also support the concept of nasal

vaccination as an option for mRNA cancer immunotherapy. However, the therapeutic efficacy achieved in our current study is relatively moderate and we are uncertain how it compares with other administration routes or other established methods of mRNA vaccination. Therefore, future studies will focus on comparing this approach with other RNA-based methods and optimization of the current protocol to improve therapeutic efficacy.

For mRNA tumor vaccination to be clinically useful and broadly applicable, it is important that it is an off-the-shelf therapy that can be administered directly *in vivo*. In this report, we show that a convenient, non-invasive method can be used for direct *in vivo* administration of mRNA encoding tumor antigen, however it has to be delivered in nanoparticle format. This is an attractive prospect for the broad application of mRNA vaccines and reveals a major gap in the development of mRNA gene carriers for cancer immunotherapy.

5 Whole blood cells loaded with messenger RNA as an anti-tumor vaccine

5.1 Introduction

In vitro transcribed mRNA is an immunogenic and programmable molecule[1] that embodies key advantages as an antigen-encoding gene for cell-based immunotherapy. For example, the use of mRNA obviates prior knowledge of patient's Human Leukocyte Antigen (HLA) type, a pre-requisite for class I peptide epitope-based approaches. mRNA is also expressed more efficiently than DNA because it does not need to cross the nuclear envelope. To date a number of methods aimed at using mRNA to stimulate immune responses have been studied. They include transfection of antigen-presenting cells (APCs) *ex vivo* with mRNAs encoding defined antigens [1, 13] or with total mRNA repertoire from tumor cells, [162] as well as direct injection of mRNA *in vivo.* [19, 36, 163] Dendritic cells (DCs) are the most common APCs that have been loaded with antigen-encoding mRNA, as well as antigens in a variety of formats. A major disadvantage of using transfected DCs as a vaccine is that the process of harvesting, culturing and loading DCs is time- and resource-intensive. It requires that patients undergo at least one 4-hour leukapheresis procedure, followed by separation of the peripheral blood mononuclear cells (PBMCs), from which the monocytes are isolated and cultured for a week in a defined medium with cytokines. The resulting DCs are typically matured before or after being loaded with mRNA and frozen for storage. Aliquots are subsequently thawed prior to administration to patients. In efforts to circumvent these somewhat cumbersome procedures, many groups have investigated direct injection of antigen-encoding mRNA. [19, 36, 163] While this has the advantage of simplicity, there are still manufacturing steps that require time, specialized resources and often proprietary

formulations. This is particularly true in the case of mRNA, which has distinct advantages as a source of antigen but must be protected *in vivo* from nucleases. Recently, a study demonstrated that DC vaccination is significantly less effective in antigen-presenting cell (APC)-deficient mice [116] compared to wild-type mice. The authors concluded that *ex vivo* transferred DCs function primarily as vehicles for transferring antigens to endogenous APCs, which are responsible for the subsequent activation of T cells.[116] This raises the possibility of using alternative cell types for mRNA cell based vaccination. In the search of such an alternative, we find that the blood is an attractive cell source because it is biocompatible, quickly available in large quantities and contains a variety of immune cells. Notably, erythrocytes loaded with protein tumor antigens have been extensively studied as vaccine carriers.[164-169] In addition, peripheral blood monocytic cells loaded with tumor antigens also proved to be an effective tumor vaccine, e.g. Provenge [4] which is FDA approved in 2011. In both approaches, however, it is necessary to subject blood cells freshly derived from the body to manipulation[164-169] and cell culture[170] before arriving at the final vaccine preparation. This increases complexity and cost of treatment, dampening the prospect of broad application of cell-based vaccines.[5, 6] We hypothesize that cell-based vaccination can be achieved with a more simplified and direct approach by loading mRNA directly into whole blood cells immediately after isolation from the body. We take advantage of the fact that blood is made up of a heterogeneous cell mixture that includes not only erythrocytes, but also leukocytes and reticulocytes. Notably, reticulocytes still retain the ability to translate mRNA into proteins.[171] Hence, by loading mRNA into autologous whole blood cells, mRNA may be delivered to endogenous host APCs via erythrocytes (naturally enriched in RNase-inhibitor[172]) in form of untranslated mRNA. Additionally, leukocytes and reticulocytes may deliver both

untranslated mRNA as well as protein resulting from translation of the loaded mRNA. In this report we show that blood harvested from mice can be immediately loaded with mRNA and used as a vaccine to induce B and T cell responses, as well as anti-tumor immune responses. This is a relatively simple protocol that does not involve cell culture and can generate the cellular therapy product in about an hour.

5.2 Materials and Methods

5.2.1 Mice and cell lines

4-6 week old mice (C57Bl/6) were obtained from the Jackson Laboratory, Bar Harbor, ME. In conducting the research described in this study, the investigators adhered to the "Guide for the Care and Use of Laboratory Animals" as proposed by the committee on care of Laboratory Animal Resources Commission on Life Sciences, National Research Council. The facilities at the Duke vivarium are fully accredited by the American Association for Accreditation of Laboratory Animal Care, and all studies were conducted using protocols approved by the Duke University IACUC.

F10.9 clone of the B16 melanoma of C57Bl/6 origin is a highly metastatic, poorly immunogenic and a low class I expressing cell line.[173] EL4 thymoma cells and B16-F10.9 cells were maintained in DMEM with 10% FCS, 100 IU/ml penicillin and 100 µg/ml streptomycin.

5.2.2 *In vitro* transcribed (IVT) mRNA

Each plasmid of interest was digested with the restriction enzyme SpeI to linearize the DNA. After purification, this cut plasmid DNA was template for *in vitro* transcription using T7 High Yield mRNA Synthesis kit (NEB). Anti-Reverse Cap Analogue (ARCA, NEB) was applied at a ARCA:GTP ratio of 1:3 during transcription. IVT mRNA was purified

using a commercial kit (RNeasy, Qiagen, Valencia, CA), quantified by spectrophotometry, and analyzed by MOPS formaldehyde gel electrophoresis to confirm the synthesis of full-length mRNA. mRNA encoding TRP-2 (melanoma-associated tyrosinase-related protein 2),[144, 174] chicken ovalbumin (OVA),[144, 174] green fluorescent protein (GFP) [122] and murine actin (negative control) [144, 174] has been described in previous studies.[7] GFP mRNA was labeled with Cy5 labeling kit (Mirusbio) according to manufacturer's protocol.

5.2.3 Harvesting whole blood using cardiac puncture

Mice were anesthetized to a surgical plane of anesthesia (500µl of 1.25% tribromoethanol, intraperitoneally). Each mouse was placed in a supine position. A 1 cc syringe with a 26-gauge needle was inserted at a shallow angle just under the xiphoid process, the tip of the sternum. Peripheral blood (approximately 0.5ml per mouse) was drawn via cardiac puncture from the mouse into the 1 cc syringe containing 100µl of anticoagulant (100mM sodium citrate and 130mM glucose, pH 6.5). Mice were euthanized following blood collection. We routinely isolated 1 x 10^9 blood cells from one C57Bl/6 mouse.

5.2.4 Generation of murine bone marrow precursor-derived dendritic cells (DCs)

Marrow from tibias and femurs of mice were harvested followed by treatment of the precursors with ammonium chloride Tris buffer for 3 minutes at 37°C to deplete the red blood cells.[144, 174] The precursors were plated in RPMI-5% FCS with GM-CSF (15 ng/ml) and IL-4 (10 ng/ml) and supplemented with 20mM HEPES, 2mM L-glutamine, 1mM sodium-pyruvate, 100 IU/ml penicillin, 100 µg/ml streptomycin, 0.1mM non-essential amino acids and 5 x 10^{-5} M βME in 6-well plates. Cells were plated at 10^6/ml, 3 ml/well

and incubated at 37°C and 5% CO2. After 3 days the floating cells (mostly granulocytes) were removed and the adherent cells replenished with 3 ml of fresh GM-CSF and IL-4 containing medium. 4 days later the non-adherent DCs were harvested, washed and plated at 5 x 10^6 cells/ml. DCs were electroporated with mRNA, washed 3 times and then matured for 5 hours at 37°C in GM-CSF+IL4 medium supplemented with LPS (E.coli 026:B6, 100 ng/ml, Sigma). DCs were electroporated as described previously.[7]

5.2.5 Induction of T cell responses *in vivo* and restimulation *in vitro*

2.5x10^7 mRNA-loaded (murine TRP-2 or chicken ovalbumin [OVA] mRNA) blood cells were injected intravenously into mice. Splenocytes were harvested after 10 days and depleted of erythrocytes, washed and then filtered through a 70µm mesh filter to eliminate cell clumps. Splenocytes were allowed to adhere to tissue culture flasks for 1 hour at 37°C. Non-adherent splenic lymphocytes (10^7 cells) were cultured with irradiated stimulator cells at a responder: stimulator ratio of 10:1, in 5ml of RPMI with 10% FCS, 20mM HEPES, 2mM L-glutamine, 1mM sodium pyruvate, 100 IU/ml penicillin, 100 µg/ml streptomycin, 0.1mM non-essential amino acids and 5 x 10^{-5} M βME (complete RPMI-10% FCS) per well in a 6-well tissue culture plate. To generate stimulators cells, B16-F10.9 cells or B16-F10.9 cells expressing OVA (B16-F10.9-OVA) were incubated with IFN-γ (100U/ml) for 20 hours. The following day, cells were harvested, washed, irradiated at 7500 Rads and washed again prior to use as stimulators. Alternately, C57Bl/6 bone-marrow precursor-derived DCs transfected with either OVA or TRP-2 mRNA were used at stimulators at a R:S ratio of 50:1. Effector T cells were harvested on day 5 on Histopaque 1083 gradient (Sigma) for harvesting viable lymphocytes prior to

use in immune assays such as CTL assay or further separated into CD4 and CD8 T lymphocytes for analysis of IFN-γ production using ELISpot (described below).

Tumor cells expressing antigen were used as target cells (F10.9 or F10.9-OVA cells or EL4 thymoma cells transfected with TRP-2 or OVA-encoding mRNA). Electroporation of cells with mRNA was done as described earlier.[5] Cells were electroporated 10-15 hours prior to europium labeling of target cells.

5.2.6 Enzyme-linked immunospot (ELISpot) assay

CD8+ and CD4+ T cells were isolated by using the corresponding T cell negative isolation kit from EasySep. $1x10^5$ CD8+ or CD4+ T cells (responders) were incubated in the microwells of the ELISpot plate coated with the relevant mAb in the presence or absence of γ-irradiated antigen-expressing cells for 36 hours at 37°C. Subsequent steps in the protocol were exactly as described in the mouse IFN-γ ELISpot Kit from BD Biosciences. Spots were counted using an ELISpot reader (Carl Zeiss, Germany).

5.2.7 Europium (Eu)-release CTL assay

mRNA-electroporated target cells were harvested, washed to remove all traces of media and labeled with Eu. The europium-labeling buffer (1ml per target) contains 1ml HEPES buffer (50mM HEPES, 93mM NaCl, 5mM KCl, 2mM $MgCl_2$, pH 7.4), 10µl Eu (10mM $EuCl_3.6H_2O$ in 0.01N HCl), 5 µl DTPA (100mM diethylenetriamine pentaacetate in HEPES buffer) and 4µl DS (1% dextran-sulfate).[175] Cells were resuspended in 1 ml of the europium-labeling buffer very gently and incubated on ice for 20 minutes. 30µl of $CaCl_2$ solution (100mM) was then added to the labeled cells, mixed and the cells were incubated for another 5 minutes on ice. 30 ml of Repair buffer (HEPES buffer with 10mM glucose, 2mM $CaCl_2$) was added to the cells and the cells were centrifuged at 1000 rpm

for 10 minutes. Cells were counted and 5 x 10^6 cells were washed 4 times with Repair buffer. After the final wash the cells are resuspended in CTL stimulation RPMI-10% FCS medium with no penicillin-streptomycin at 10^5 cells/ml. 10^4 Eu-labeled targets (antigen-expressing cells versus antigen-negative cells) and serial dilutions of effector cells were cocultured in 200µl at 37°C for 4 hours. Eu-release in the supernatant (50µl) was measured by time-resolved fluorescence (Victor3, Perkin Elmer). % specific lysis = [(experimental release - spontaneous release)/(total release - spontaneous release)] x 100. Spontaneous release of the target cells was less than 25% of total release by detergent in all assays for the results of the assay to be valid. Spontaneous release of the target cells was determined by incubating the target cells in medium without T cells. All assays were done in triplicate.

5.2.8 B cell response

Mice were immunized with blood cells transfected with OVA mRNA two times over an eight-day interval. Seven days later, serum was harvested and anti-OVA IgG was measured using a commercially available anti-ovalbumin IgG1 (mouse) enzyme immunoassay (EIA) kit (Cayman Chemical). Serum collected from naïve mice served as a negative control.

5.2.9 mRNA encapsulation into whole blood cells

Whole blood was obtained from C57Bl/6 female mice by cardiac puncture using citrate as a stabilizer, diluted in PBS and filtered through a 70µm mesh. Whole blood cells were washed a second time with complete Opti-MEM by centrifugation at 1200 rpm for 5 min. Supernatant was discarded and the cell density of the pellet was determined using a hemocytometer.

Electroporation media (EP media) was composed of 5% sucrose, Hepes (5mM), NaCl (75mM), $MgCl_2$ (1mM) and $CaCl_2$ (2mM). Complete Opti-MEM is composed of Opti-MEM (Invitrogen) supplemented with reduced gluthathione (4mM), beta-mercaptoethanol (βME, 0.011mM) and $MgCl_2$ (2mM). For a typical preparation, blood cells were diluted into electroporation media (500µl) to obtain a final cell density of approximately 1 to 5 x 10^8/ml. Cell suspension (200µl) was transferred to a cuvette (0.2mm width, VWR) and mixed with mRNA (20µg). Cells were electroporated at room temperature using a BTX Square Wave electroporator at 300-325V for 2.0 millisecond and immediately transferred to pre-warmed complete Opti-MEM (2ml, 10x volume) and maintained at 37°C for at least 10 minutes. Recovered cells were analyzed using flow cytometry (BD FACSCaliber) for loading efficiency.

5.2.10 Characterization of mRNA-loaded whole blood cells

Prior to mRNA loading, cells were stained with thiazole orange (TO, Sigma) for endogenous mRNA and DNA to parse leukocytes, reticulocytes and erythrocytes. TO was added to cell suspension at a final concentration of 5µg/µl for 20 mins and washed 3 times with Opti-MEM to remove traces of TO before being diluted into electroporation media.

To quantify mass of loaded mRNA, cells were gently washed twice with complete Opti-MEM, re-suspended in 50µl of complete Opti-MEM and transferred to a black opaque microplate. A calibration curve was plotted to correlate fluorescence intensity and mRNA mass by adding varying amounts of Cy5 labeled mRNA into final volumes of 50µl respectively. Fluorescence was quantified using a microplate reader (FLUOstar Optima, BMG Labtech GmbH, Germany).

To quantify luciferase expression, cells were centrifuged, supernatant discarded, the cell pellet re-suspended in 50μl of Glo Lysis buffer and transferred to a white opaque microplate. 75μl of Steady-Glo luciferase reagent was added, mixed using an orbital shaker and luminescence read with a microplate reader (FLUOstar Optima) equipped with a luminescence optic.

5.2.10.1 RT-PCR

RNeasy Plus (Qiagen) was used to isolate total RNA from non-electroporated blood, as well as blood electroporated with actin or TRP-2 RNA. Total RNA was used in a reverse transcription reaction primed with oligo dT and carried out with SMARTScribe reverse transcriptase (Clontech). One-tenth of the RT reaction was used in PCR with actin primers:

5'-ATGGTGGGAATGGGTCAGAAGGAC-3' and 5'-CTCTTTGATGTCACGCACGATTTC-3', or TRP-2 primers: 5'-GCCATTGATTTCTCTCACCAAGG-3' and 5'-GTCCAGTGTTCCGTCTGCTTTATC-3'.

5.2.10.2 Fluorescence and confocal imaging

Cells were washed and fixed by retaining 50% of the supernatant, while replacing the other half with fixing media (Opti-MEM containing 4% paraformaldehyde prepared immediately before use). This was repeated 4 times and cells were transferred into 96-well microplates (BD), centrifuged (1000 rpm) and imaged at 40x magnification using a Nikon camera. For confocal microscopy, fixed cells were transferred to 96-well glass-bottom plates (Greiner) previously coated for 1 hour with 100μg/ml poly-L-lysine, centrifuged (1000 rpm) and imaged immediately using an inverted oil immersion confocal

microscope (Zeiss LSM 510) at 100x magnification. In some instances, images were digitally magnified to 200x.

5.2.10.3 *In vivo* biodistribution

To evaluate *in vivo* biodistribution, each mouse received 10^9 naïve or mRNA-loaded blood cells injected via tail vein. Lungs, spleen, liver and kidneys were isolated 2 hours post injection, weighed and imaged immediately using IVIS Kinetics (Calipers, Excitation 615-665nm; Emission 695-770nm).

5.2.10.4 Cell marker Staining

Cy5-labeled mRNA was loaded into whole blood cells as previously described. 10^9 mRNA loaded whole blood cells were prepared for 10 staining aliquots in 20ml pre-warmed complete Opti-MEM. Supernatant was discarded and erythrocytes were depleted by ammonium chloride lysis. Remaining cells were centrifuged and resuspended in 1ml PBS supplemented with 10% FBS. Cells were blocked with 25µl anti-mouse CD16/32 (Biolegend) for 15 minutes on ice. 100µl of cells were mixed with 2.5µl of FITC/PE-labeled antibodies (and corresponding isotypes) for 45min on ice. Cells were washed, fixed with PBS containing 1% paraformaldehyde and immediately analyzed by flow cytometry (BD FACSCaliber). Data was subsequently analyzed with WINMDI 2.9 freeware.

5.2.10.5 Biological states

Prior to the below mentioned assays, cell stock containing 200µl of electroporated cells recovered in 2ml of complete Opti-MEM were incubated at 37°C and 5% CO_2 for 2 hours. Live assay and reactive oxygen species (ROS) measurement were performed using calcein-AM (Molecular Probes). Calcein-AM was diluted into 0.5ml of complete Opti-

MEM to a final concentration of 1μM. 100μl from cell stock was then added, incubated at room temperature for 30 minutes and directly analyzed by flow cytometry. Live assay was quantified based on %FITC^{positive} cells while the ROS was quantified based on mean fluorescence intensity (MFI) of FITC.

To assay for caspase 3 activities, 500μl of mRNA-loaded cells (EP+RNA) or negative control (No EP, handled in exactly the same way except without electroporation) were diluted with 150μl of Opti-MEM to a final volume of 650μl. Alternately, tert-butylhydroperoxide (tBOOH, Sigma) was diluted into 100μl of Opti-MEM and immediately added to 500μl of naïve cells so that the final concentrations of tBOOH are 0, 1.3 and 2.6mM respectively. These positive controls were treated with tBOOH for exactly 8 minutes in Opti-MEM at room temperature. After 8 minutes, 50μl of βME (55mM, Gibco) was added to quench the reaction and 50μl from each tube was immediately mixed with 75μl of Caspase 3/7-GLO (Promega), transferred into 96-well white opaque plates, incubated for 30 minutes at room temperature and analyzed for luminescence using a microplate reader (FLUOstar Optima). Data were recorded after luminescence stabilized and normalized against cell number. Cell number in each tube was determined by counting using a hemocytometer.

To assay for phosphatidylserine exposure, 150μl from cell stock was aliquoted and supernatant was removed by centrifugation. 100μl of annexin V binding buffer was added followed by 5μl of PE (Biolegend) or Cy5 (Molecular Probes) labeled annexin V reagent. Cells were incubated for 15 minutes, diluted with 300μl of binding buffer and immediately analyzed by flow cytometry.

5.2.11 Immunotherapy model

$2.5x10^7$ mRNA-loaded (melanoma antigen murine tyrosinase-related protein2 [TRP-2] or chicken ovalbumin [OVA] mRNA) blood cells were prepared as described and injected intravenously into each mouse. To monitor the induction of antibody responses, mice were immunized with blood cells transfected with OVA mRNA two times with an eight-day interval. (A) Seven days later, serum levels of anti-OVA IgG were measured with a commercial kit. (B-C) To determine the induction of antigen-specific T cell responses, splenocytes were harvested 10 days post-immunization and depleted of red blood cells. Non-adherent splenic lymphocytes were cultured with irradiated stimulator cells (F10.9 melanoma cells or F10.9-OVA cells) at a responder: stimulator ratio of 10:1. T cells were harvested after a 5 day culture and used in a CTL (cytotoxic T lymphocyte) assay or separated into CD4 and CD8 T lymphocytes for an IFN-γ ELISpot (enzyme-linked immunosorbent spot). To evaluate the efficacy of mRNA-loaded whole blood cells in an immunotherapy model, $2.5x10^4$ B16-F10.9 cells were injected subcutaneously into the flanks of C57Bl/6 mice (N=10/group). 2 days later, $2.5x10^7$ mRNA-transfected blood cells were injected intravenously into mice. Alternately, mice were immunized with $2x10^5$ mRNA-transfected DCs intraperitoneally [176]. Time to tumor onset was recorded based on the detection of palpable tumors on a daily basis. For overall survival, mice were sacrificed once tumor diameter reached 20mm and date of sacrifice recorded. Tumor diameter was measured with vernier calipers based on the longest side of the tumor.

5.3 Results

We show that mRNA was loaded by electroporation (Figure 18A) into erythrocytes ($TO^{Low}FSC^{Low}$, TO: thiazole orange, FSC: forward scatter), reticulocytes ($TO^{Intermediate}FSC^{Low}$) and leukocytes ($TO^{High}FSC^{High}$). The finding was further confirmed

by both fluorescence and confocal microscopy (Figure 18B and Figure 18C). Using flow cytometry, we further determined, within the leukocyte population, that mRNA was loaded into MHC class II^+ antigen-presenting cells, $CD3^+$ T cells, $CD11b^+$ monocytes, $GR1^+$ granulocytes and $CD45R^+/B220^+$ murine plasmacytoid DCs (Figure 18D). Quantification of the fluorescently-labeled mRNA showed that about 300ng of RNA was loaded into $5x10^7$ blood cells (Figure 19A), and amplification by RT-PCR of full length mRNA from mRNA-loaded blood cells (Figure 19B) indicated that untranslated mRNA remained stable within the cytoplasm of whole blood cells. [172] Luciferase expression detected in luciferase mRNA-loaded blood cells (Figure 19A) confirmed the bioactivity of the mRNA. Thus, intact and functional mRNA could be loaded into whole blood cells by electroporation.

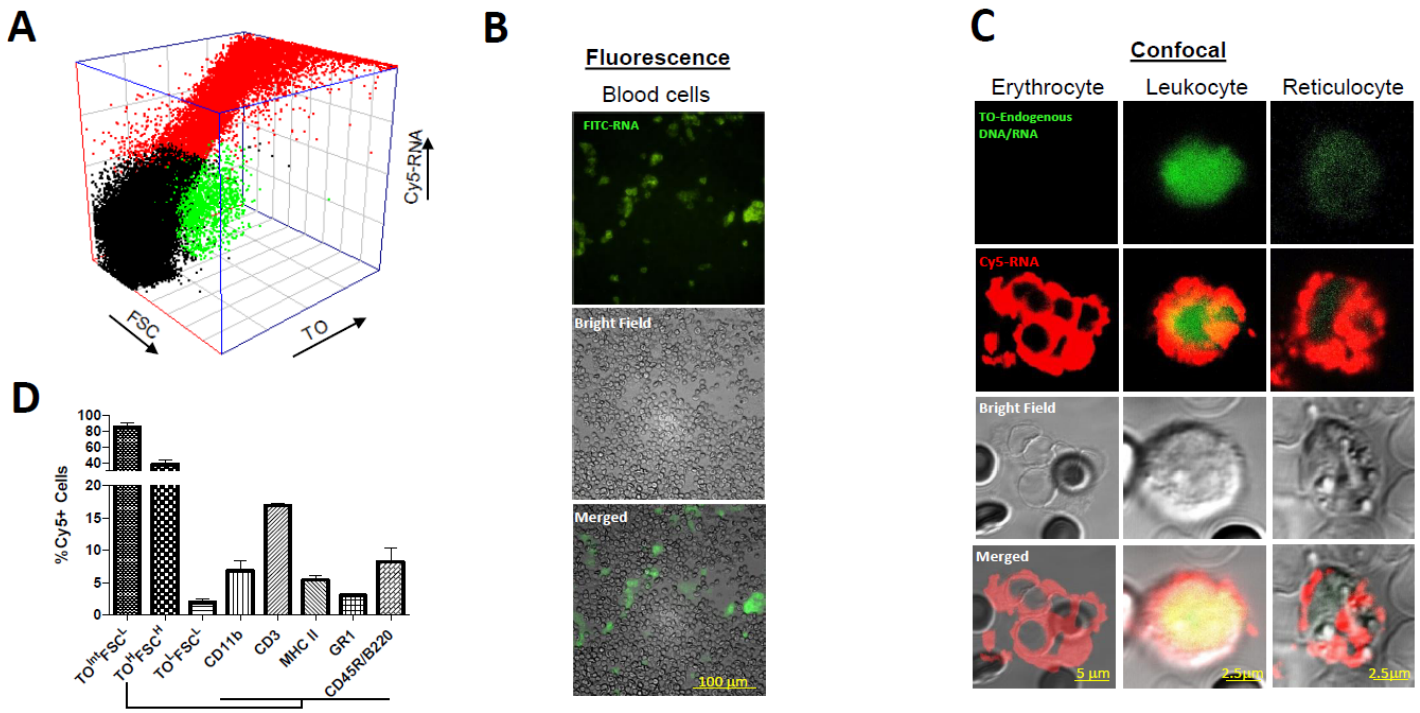

Figure 18. Whole blood cells can be loaded with mRNA.

A. Ungated 3D plot of Cy5-labeled GFP mRNA (Cy5-RNA) loaded into reticulocytes ($TO^{intermediate}FSC^{low}$), leukocytes ($TO^{high}FSC^{high}$), erythrocytes ($TO^{low}FSC^{low}$) based on size (FSC) and presence of endogenous DNA/RNA (Thiazole Orange, TO).

B. Fluorescence image of mRNA-loaded whole blood cells. GREEN: FITC-labeled GFP mRNA.

C. Confocal images of mRNA encapsulated in erythrocytes, leukocytes and reticulocytes. RED: Cy5-labeled GFP mRNA loaded by electroporation, GREEN: Thiazole stain of cellular DNA/RNA .

D. Loading efficiency of Cy5-labeled GFP mRNA into reticulocytes ($TO^{intermediate}FSC^{low}$), leukocytes ($TO^{high}FSC^{high}$), erythrocytes ($TO^{low}FSC^{low}$), monocytes (CD11b), T cells (CD3), antigen presenting cells (MHC II), granulocytes (GR1) and murine plasmacytoid DCs (CD45R/B220).

Next we characterized the biological properties of whole blood cells two hours post-electroporation. This time point was chosen because mRNA-loaded whole blood cells were typically administered into all mice by the second hour post-electroporation. We observed that mRNA-loaded blood cells remained viable (Figure 20A) based on the conversion of non-fluorescent calcein-AM to fluorescent calcein by intracellular esterases. We also found elevated levels of reactive oxygen species (ROS) in electroporated blood cells based on higher mean fluorescence intensity contributed by oxidized calcein-AM. Only those that were loaded with mRNA possessed higher levels of ROS (Figure 20B). ROS are pro-inflammatory and thereby a potentially favorable property for whole blood cell vaccines.[177] Using annexin V staining, we observed that cells loaded with mRNA externalized phosphatidylserine (PS) compared to unloaded blood cells (Figure 20C, Supplementary Figure 9). Surface presentation of PS could be caused by scrambling of cell membranes lipids facilitated by pore formation during electroporation, [178] or it could indicate that the blood cells were apoptotic. To ascertain whether PS externalization was physically mediated, we tracked PS externalization immediately after electroporation and found that cells were stained positive for annexin V immediately after electroporation (Supplementary Figure 10). Surface PS also appeared to be irreversible, increasing slightly during recovery but dropping back to levels seen immediately after electroporation by 24 h (Supplementary Figure 10). We then analyzed mRNA-loaded whole blood cells for apoptosis based on caspase-3 activities [179-181] and found that they were comparable to naïve cells (Supplementary Figure 11). This indicated that surface PS presentation was not caspase-mediated and suggested that PS presentation might not be biologically mediated. Surface PS commonly known as “eat-me” signals displayed selectively on live mRNA-loaded cells presumably target

them to the mononuclear-phagocyte system for uptake. To summarize, we show that electroporation of whole blood cells results in mRNA electroinsertion and priming for antigen uptake *in vivo*

Next we determined the biodistribution of mRNA-loaded whole blood cells following intravenous administration and found that RNA-loaded whole blood cells were distributed to multiple organs, including the APC-rich liver and spleen (Figure 20C). Additionally, mRNA-loaded blood cells, despite being relatively low in abundance (Figure 18A), efficiently co-localized with APCs *in vitro* (Supplementary Figure 12). This was consistent with prior reports on live erythrocytes that had phosphatidylserine artificially inserted in the cell membrane.[182] Hence we confirmed that mRNA-loaded whole blood cells were distributed to the liver and spleen, where they could be targeted to antigen presenting cells.

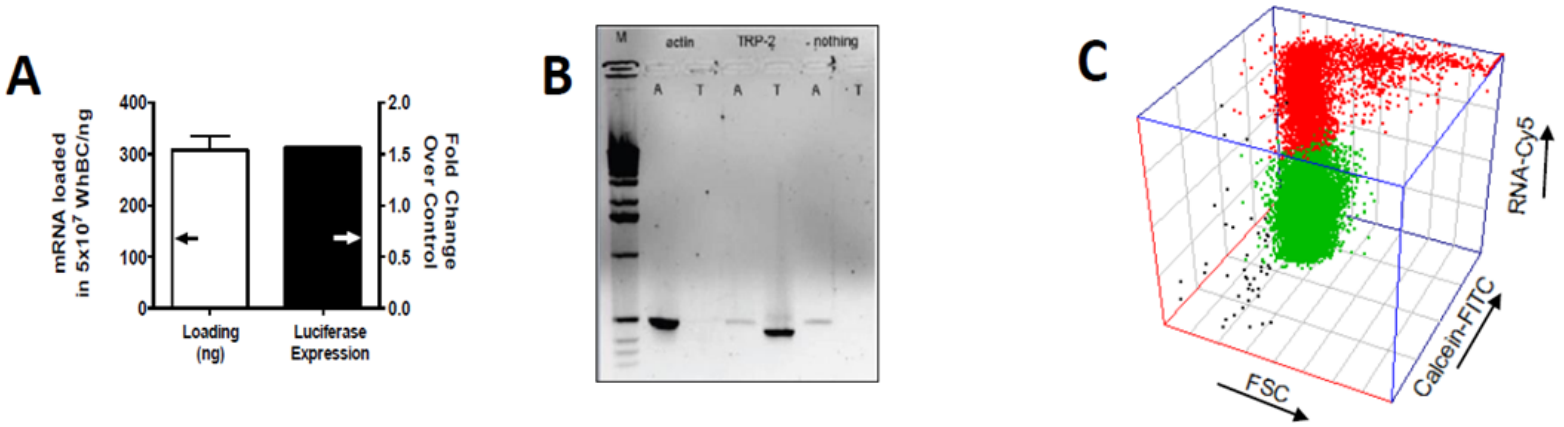

Figure 19. Characterization of electroinserted mRNA, biological properties and biodistribution of mRNA-loaded whole blood cells.

A. Mass of Cy5-labeled luciferase mRNA loaded in 10^7 whole blood cells (left axis) and luciferase expression per 10^7 whole blood cells normalized to 10^7 non-electroporated cells.
B. RT-PCR analysis of RNA recovered from whole blood cells loaded with actin mRNA ("A"), TRP-2 mRNA ("T") or nothing, respectively. Lane M is a 1 Kb DNA ladder (Invitrogen).
C. Ungated 3D plot of cell viability based on conversion of calcein-AM to calcein in whole blood cells loaded with Cy5-labeled GFP mRNA.

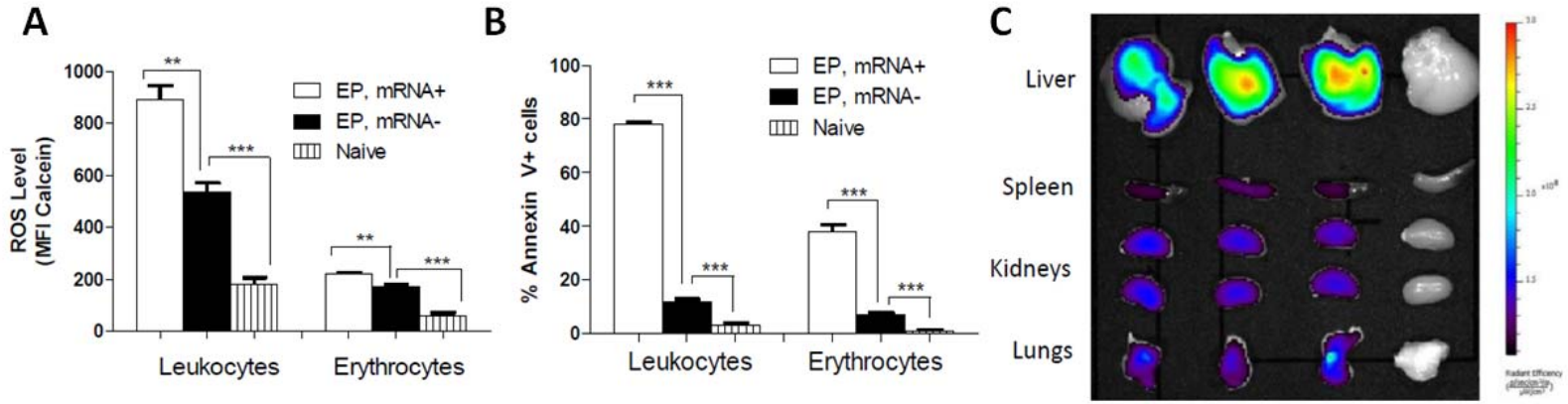

Figure 20. Characterization of biological properties and biodistribution of mRNA-loaded whole blood cells.

A. ROS levels in whole blood cells based on mean fluorescence intensity (MFI) of intracellular calcein[183].
B. Surface phosphatidylserine analysis by annexin V staining.
C. IVIS image of biodistribution of whole blood cells loaded with Cy5-labeled GFP mRNA administered intravenously via tail vein 2 hours post administration. This experiment was repeated 2 times with n=3 and one experiment is depicted. Cells were assayed 2 hours post-electroporation. $^{**}p<0.01$, $^{***}p<0.001$ (One-way anova/bonferroni multiple comparison test)

Based on the data presented in Figures 18-20, we hypothesized that whole blood cells loaded with mRNA encoding antigen protein could induce antigen-specific immune responses. We first monitored induction of B cell responses by measuring the presence of antigen-specific serum IgG in mice immunized twice with ovalbumin (OVA) mRNA-loaded blood cells. As shown in Figure 21A, OVA-specific serum IgG could be detected in immunized mice. To monitor induction of T cell responses, two groups of mice were immunized once with blood cells loaded with mRNA encoding either OVA or the murine melanoma antigen, tyrosinase-related protein 2 (TRP-2). Upon re-stimulation of splenic lymphocytes *in vitro*, we analyzed T cells for antigen-specific function by measuring IFN-γ secretion upon antigen re-encounter or lysis of target cells expressing antigen. Antigen-specific IFN-γ secretion by OVA- or TRP-2-specific CD8+ and CD4+ T cells is shown in Figure 21B. T cells also showed antigen-specific reactivity by selectively lysing target cells that expressed the corresponding antigen (Figure 21C). Hence, we conclude that mRNA-loaded blood cells injected immediately after electroinsertion and without further manipulation can induce both humoral and cellular immune response.

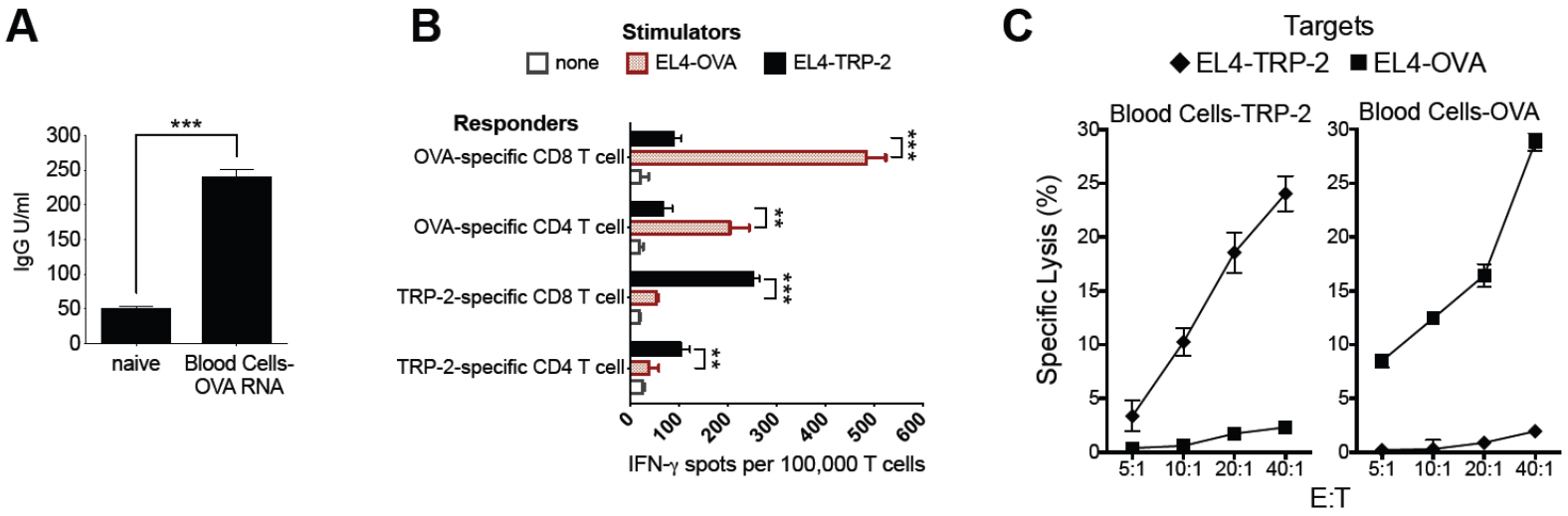

Figure 21. Immunization with mRNA-loaded whole blood cells induces immune responses *in vivo*.

A. Induction of OVA-specific antibody responses. Serum collected from naïve mice was used as the negative control. Statistical analysis was done using a student's t test. $^{**}p<0.01$, $^{***}p<0.001$

B. Induction of antigen-specific IFN-γ secreting T cells in mice immunized with mRNA-loaded whole blood cells. Isolated CD4+ and CD8+ T cells were stimulated with EL4 cells previously transfected with either TRP-2 or OVA mRNA. After overnight incubation an IFN-γ ELISpot was performed. Statistical analysis was done using a student's t test. $^{**}p<0.01$, $^{***}p<0.001$

C. Induction of antigen-specific cytotoxic T cells in mice immunized with mRNA-loaded whole blood cells. A europium-release CTL assay was performed 5-days post-stimulation. EL4 thymoma cells electroporated with antigen-encoding mRNA (TRP-2 or OVA) were used as targets to measure antigen-specific lysis.

We next evaluated the therapeutic efficacy of mRNA-loaded blood cells in the B16 melanoma immunotherapy model. Mice were immunized one time 2 days post-tumor implantation with mRNA-loaded whole blood cells and as a positive control, TRP-2 mRNA-loaded DCs (Figure 22A, 22B and 22C). Immunization with melanoma antigen TRP-2 mRNA-loaded whole blood cells delayed tumor onset (Figure 22A) and enhanced survival (Figure 22B) as compared to whole blood cells loaded with mouse actin mRNA. Moreover, there was no difference in tumor onset (p=0.57, Figure 22A), survival (p=0.33, Figure 22B) and average tumor diameter (p=0.97, Figure 22C) in mice immunized with TRP-2 mRNA-loaded whole blood cells and TRP-2 mRNA-loaded DCs. These results demonstrate that immunization with TRP-2 mRNA-loaded whole blood cells leads to an antitumor response that is comparable to TRP-2 mRNA-loaded DCs.

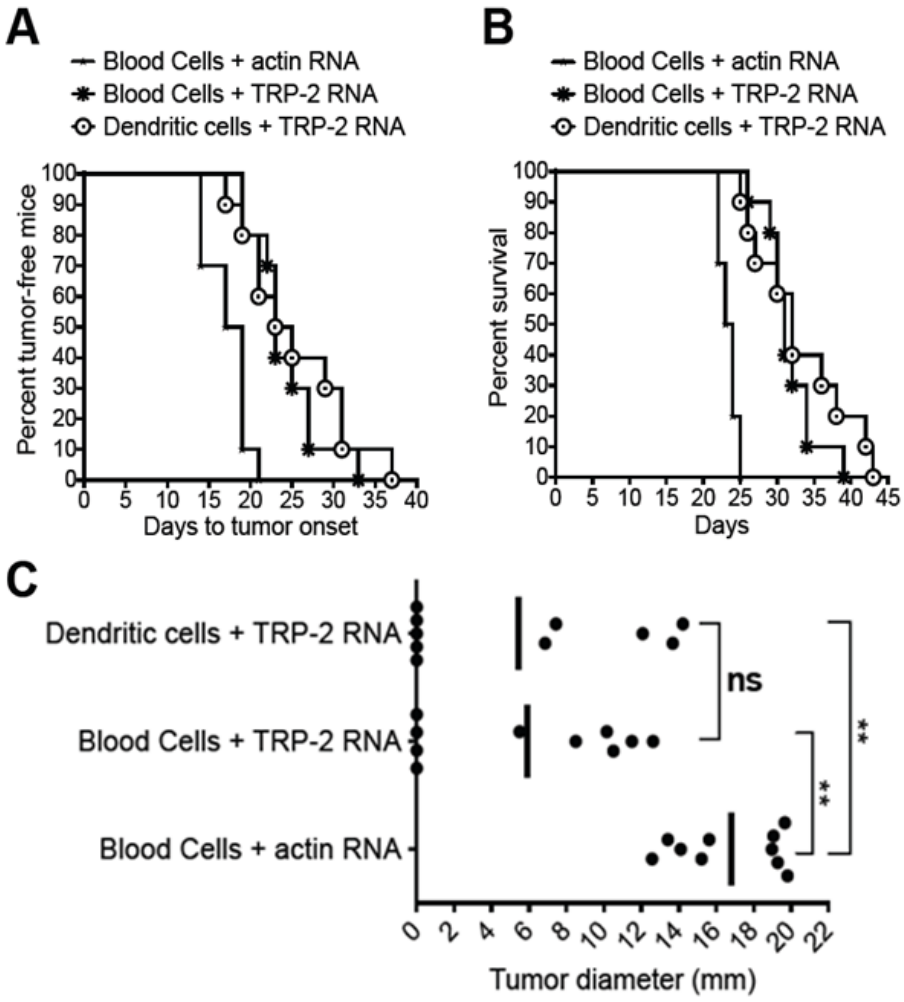

Figure 22. Immunization with mRNA-loaded whole blood cells is comparable to dendritic cell (DC) vaccination in the B16 melanoma immunotherapy model.

A. Delay in tumor onset in mice immunized with mRNA-loaded whole blood cells. Time to tumor onset was recorded based on the detection of palpable tumors (~4-5 mm diameter). Log-rank analysis (Mantel-Cox test) was used for statistical analysis: Blood cells+actin mRNA vs Blood cells+TRP-2 mRNA, p=0.0001; Blood cells+actin mRNA vs DCs+TRP-2 mRNA, p=0.0007; Blood cells+TRP-2 mRNA vs DCs+TRP-2 mRNA, p=0.52. Median time to tumor onset: Blood Cells+actin mRNA=18, Blood Cells+TRP-2 mRNA=23, DCs+TRP-2 mRNA=24.

B. Enhanced survival in mice immunized with mRNA-loaded whole blood cells. Survival was recorded based on tumor growth to 20 mm in diameter at which point mice were sacrificed. Log-rank analysis (Mantel-Cox test) was used for statistical analysis: Blood cells+actin mRNA vs Blood cells+TRP-2 mRNA, p=0.0001; Blood cells+actin mRNA vs DCs+TRP-2 mRNA, p=0.0001; Blood cells+TRP-2 mRNA vs DCs+TRP-2 mRNA, p=0.33. Median time to tumor onset: Blood Cells+actin mRNA=23.5, Blood Cells+TRP-2 mRNA=31, DCs+TRP-2 mRNA=32.

C. Induction of anti-tumor immunity is comparable in mice immunized with mRNA-loaded whole blood cells and DCs transfected with mRNA. Figure depicts tumor diameter in individual mice and average tumor diameter on day 22. The overall significance of the study as determined by Kruskal-Wallis (ANOVA) test is p=0.0002. The comparison between groups was done using the non-parametric Mann-Whitney test: Blood cells+actin mRNA vs Blood cells+TRP-2 mRNA, p<0.0001; Blood cells+actin mRNA vs DCs+TRP-2 mRNA, p=0.0002; Blood cells+TRP-2 mRNA vs DCs+TRP-2 mRNA, p=0.97.

5.4 Discussion

This report provides proof-of-concept of a rapid and affordable cellular immunotherapy. Our approach is based on the hypothesis that immunization with mRNA-loaded whole blood cells will lead to an anti-tumor immune response. As this vaccine is designed to be an autologous cell product, it is unlikely to be toxic or be affected by blood types of the individuals. We have also not observed other visible side effects from this vaccine formulation in all our animal experiments.

Our formulation is distinctly different from red blood cell vaccines. [164-169] Firstly, buffy coat cells (leukocytes) are not removed by Ficoll-Paque separation.[165] As a result, mRNA is also loaded into leukocytes, which leads to the translation of the mRNA into protein (Figure 19A). Secondly, mRNA is loaded into whole blood cells by electroporation instead of hypotonic loading. The latter is not suitable because it requires prolonged incubation of labile mRNA with cells, which requires a RNAse-free environment. Thirdly, our formulation is rapidly distributed to the liver and spleen compared to most red blood cell vaccine which requires additional pretreatment to achieve opsinization [184]. This rapid distribution could have been a consequence of cluster formation (Figure 18B and 18C) as well as the externalization of phosphatidylserine (PS) “eat-me” signals on the cell surface (Figure 20B).

As important, immunization with mRNA-loaded whole blood cells leads to induction of immune responses. Notably, the dose applied in this study contains only about 150 nanograms of mRNA (Figure 19A). Although nanogram quantities of mRNA encapsulated in nanoparticles using lipid-based gene carriers have been effective for erythropoietin delivery,[137] tumor vaccination may require microgram quantities as

previously reported for intravenously administered mRNA-nanoparticle vaccine.[114] It is also reasonable to assume that synthetic gene carriers will be more efficient than erythrocytes in transfecting APCs. As such, there is a very low chance for host APCs to be directly transfected by mRNA encapsulated inside erythrocytes. Our results suggest that transfected leukocytes may be involved in the induction of immune response, especially since a variety of them are loaded with tumor antigen encoding mRNA. This speculation is consistent with predominant role of cell-based vaccines for transfering antigens to host APCs.[116] Future studies will address the mechanism of immune response induction, which will allow us to further understand and optimize this vaccine formulation.

6 Conclusion

A significant bottle neck to broad translation of mRNA cell based vaccination is the extensive cell manipulation and culture required to derive matured mRNA transfected DCs from autologous blood monocytes. This thesis presents two viable strategies that eliminates or significantly reduce these time- and resource- consuming processes.

The first approach adopts a direct *in vivo* administration of mRNA. Due to a lack of a suitable mRNA carrier, therapeutic efficacy of directly injected mRNA has been shown only by intranodal injection of naked mRNA. Through screening of a selected number of gene carriers, an optimal formulation capable of transfecting primary dendritic cells efficiently is identified, demonstrating for the first time that primary dendritic cells can be efficiently transfected with mRNA encapsulated nanoparticles. The *in vivo* transfection efficiency and kinetics of mRNA nanoparticles are compared with naked mRNA, which is well characterized *in vivo*.

Results of the above study suggest a possibility for intranasal route of mRNA tumor vaccination, a delivery strategy that has not been studied. We further show, in a follow up study, that mice intranasally immunized with mRNA encapsulated in nanoparticles delivering OVA as a model antigen develop anti-tumor immunity under both prophylactic and therapeutic settings. Anti-tumor immunity correlates with the development of antigen specific CD8+ T cells, and is observed only when mRNA is delivered in nanoparticles but not in naked format. Intranasal administration is a highly attractive delivery route due to its non-invasive nature and amenability for repeated administrations. Results from this thesis show the potential for a broad clinical translation of a non-invasive mRNA tumor

vaccine. The development of safe and efficient gene carriers as well as further optimization of intranasal mRNA tumor vaccination are warranted.

The second approach explores the use of whole blood cells as alternative cell carriers of mRNA. The hypothesis is based on the fact that DC therapy relies heavily on endogenous DCs for anti-tumor immune response, suggesting alternative cell types may be equally effective. We show that intact and functional mRNA can be loaded into whole blood cells by electroporation. These cells engender properties such as high ROS and surface presentation of phosphatidylserine, which facilitates their uptake by endogenous antigen presenting cells. We show that mice immunized with mRNA-loaded whole blood develop both B and T cell antigen specific immune responses. And in a therapeutic melanoma immunotherapy model employing TRP-2 as the antigen, the overall survival of mice immunized with mRNA-loaded whole blood cells are comparable with intraperitoneally administered mRNA-transfect DCs.

In conclusion, we have demonstrated proof-of-concept methods of mRNA delivery that obviate the time- and resourcing- demanding procedures currently needed for mRNA tumor vaccination. Studies presented in this thesis opens additional significant areas of research for future work. For intranasal mRNA tumor vaccination, the optimal adjuvant and vaccination schedule still needs to be optimized. The therapeutic efficacy of an optimized intranasal mRNA tumor vaccination procedure should also be compared with other delivery routes as well as the mRNA-transfected DCs to ascertain its potential for clinical translation. For mRNA-loaded whole blood cell vaccination, a few attempts were made to optimize this formulation and results were mixed. These mixed outcomes are a result of a lack of true understanding on the mechanism of immune modulation mediated

by mRNA-loaded whole blood cells. A major complexity comes from the fact that a wide variety of cell types are loaded with mRNA. Future work in this area will focus on the elucidating the mechanism of action by this highly simplified tumor vaccination approach so that an appropriate study can be designed to optimize it. In addition, this method of vaccination may in its present form by extended to other disease models such as influenza or tolerogenic immunotherapy.

7 Future directions

An unexpected finding in Specific Aim 1 is that subcutaneous transfection with naked mRNA is more efficient and sustained compared to mRNA encapsulated in nanoparticles. Notably gene expression last for more than 3 to 7 days depending on specific subcutaneous locations. Protein expression from mRNA also decays with a first order kinetics regardless of route or format of delivery, rendering subcutaneous mRNA transfection a predictable event. These unique subcutaneous transfection properties of naked mRNA may be useful in wound healing and other skin injuries commonly encountered in plastic and reconstruction surgeries.

We have previously shown, as a proof-of-concept, that freshly obtained whole blood cells can be loaded with mRNA and immediately re-injected back into the body as an anti-tumor vaccine. The next logical step would be to optimize the vaccine formulation. To optimize mRNA-loaded whole blood cell vaccine, it is necessary to know the “relative contribution” of erythrocytes and leukocytes to antigen specific immune response. This is because unlike leukocytes, erythrocytes do not translate mRNA into protein. Consequently, immune modulation mediated by erythrocytes may be fundamentally different from leukocytes. This may lead to very different hypotheses on how tumor immunity was induced. The “relative contribution” approach may be used to first identify the cell type most implicated in the induction of antigen specific immune response. Based on this identified cell type, we will formulate testable hypotheses to probe a probable mechanism of action mRNA-loaded whole blood cells. The actual mechanism may be highly complicated and not practical to elucidate since the purpose is to optimize the therapeutic efficacy.

Going forward, this formulation may be further developed into a “point-of-care” vaccine technology. Whole blood obtained from the patient can be immediately infused into an integrated microfluidic platform where the erythrocytes and leukocytes are separated into different channels, followed by flow electroporation within each channel (electroporated with cell-type optimized parameters) leading to optimal loading of mRNA into erythrocytes and leukocytes, respectively. Cells exiting the chip may be injected directly into the patient without further manipulation.

Appendix

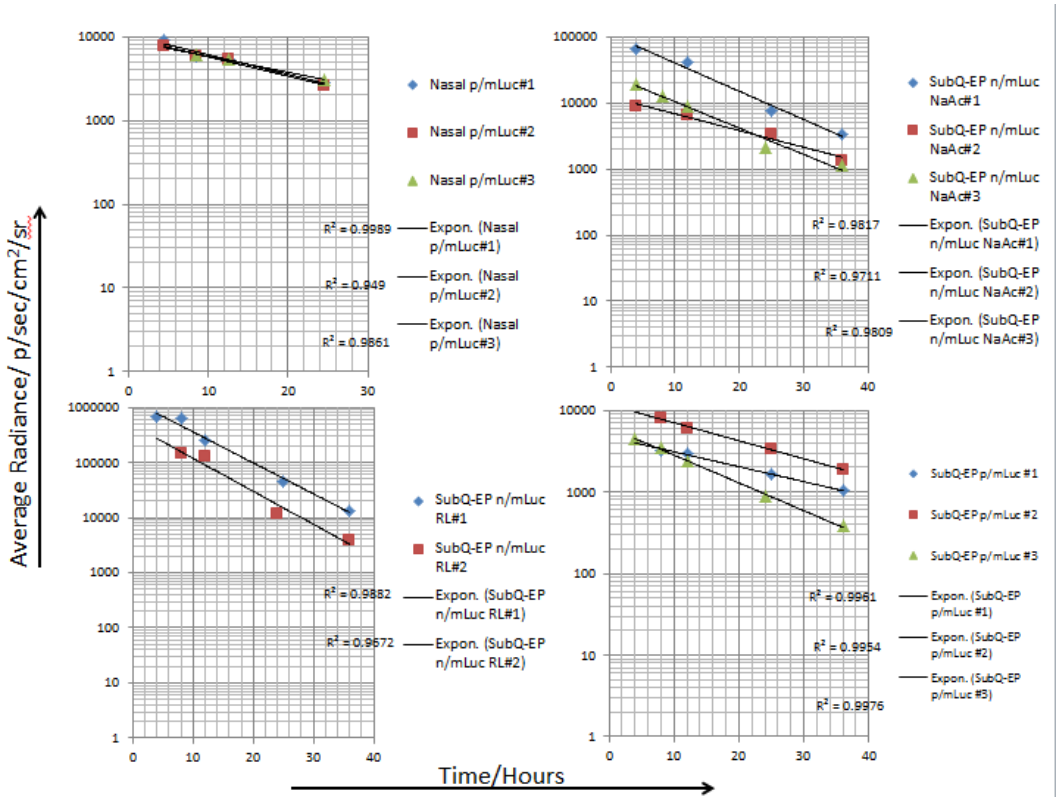

Supplementary Figure 1. Regression analysis of additional transgene expression kinetics experiment

	4h-n/mLuc	8h n/mLuc	12h n/mLuc	p/mOVA (4-36h)	NTC+ (4-36h)
4h-p/mLuc	**			**	
8h-p/mLuc		*		***	
12h-p/mLuc			**	***	
4h-n/mLuc (RL)	**				***
8h n/mLuc (RL)		ns			*
12h n/mLuc (RL			*		**
NTC+ (4-36h)	***	***	***	***	

Supplementary Figure 2. Detailed statistical analysis of data presented in Figure 11

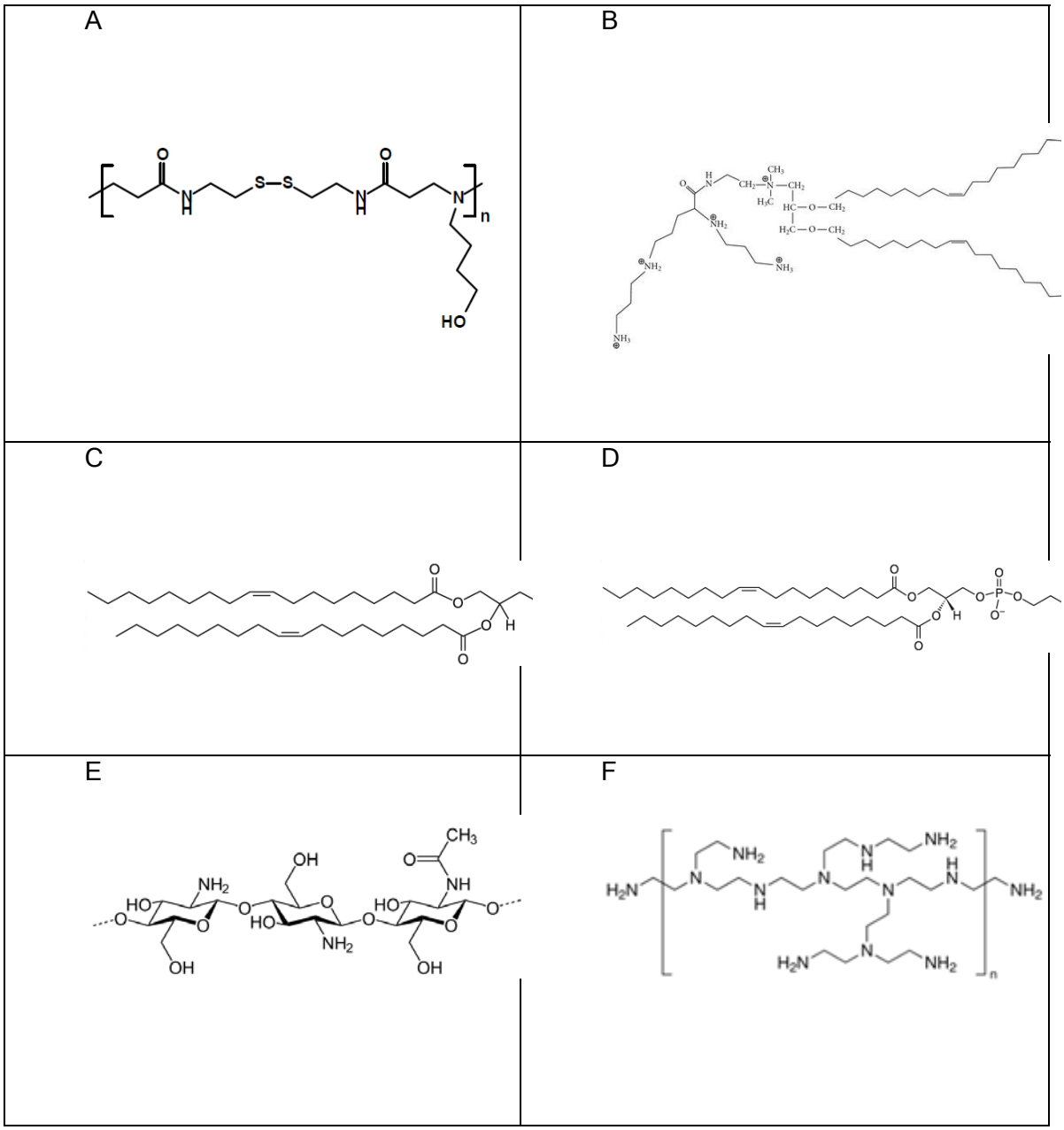

Supplementary Figure 3. Gene carriers preliminarily screened for mRNA nanoparticle transfection on JAWS II cell line.

A. CBA-ABOL, B. Lipofectamine, C. DOTAP (1,2-dioleoyl-3-trimethylammonium-propane), D. DOPE (1,2-dioleoyl-sn-glycero-3-phosphoethanolamine), E. Chitosan, F. PEI (25kda)

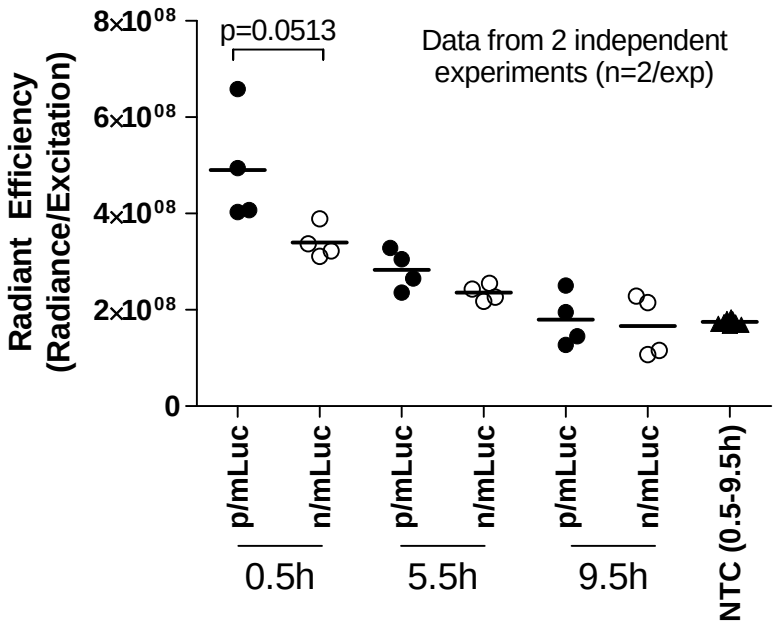

Supplementary Figure 4. 4 μg of Cy-5 labeled mLuc was administered intranasally into Balb/c mice.

Cy-5 fluorescence was monitored at indicated time points using IVIS Kinetics Imaging System. Results from 2 independent experiments (n=2/group) were normalized to respective non-transfected controls (NTC) and plotted on the same graph.

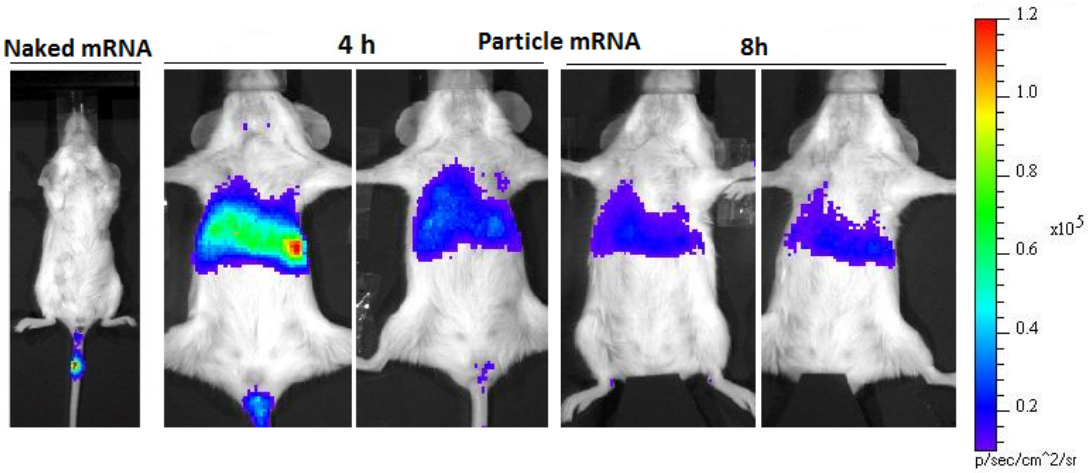

Supplementary Figure 5. Bioluminescence in BALB/c mice intravenously administered with 26 μg of partially aggregated p/mLuc at 4 and 8-hour post injection.

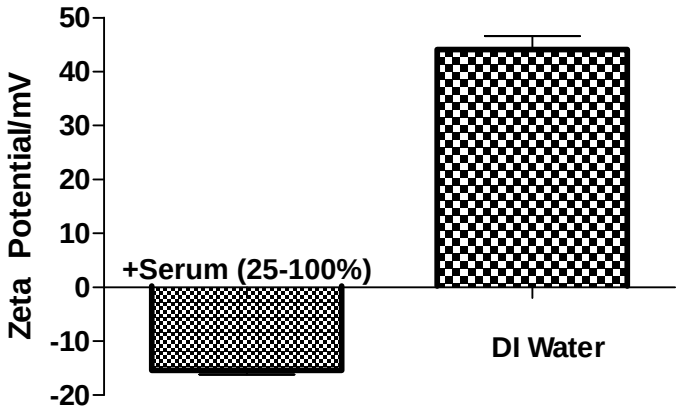

Supplementary Figure 6. Zeta potential of mRNA nanoparticles applied in this study.

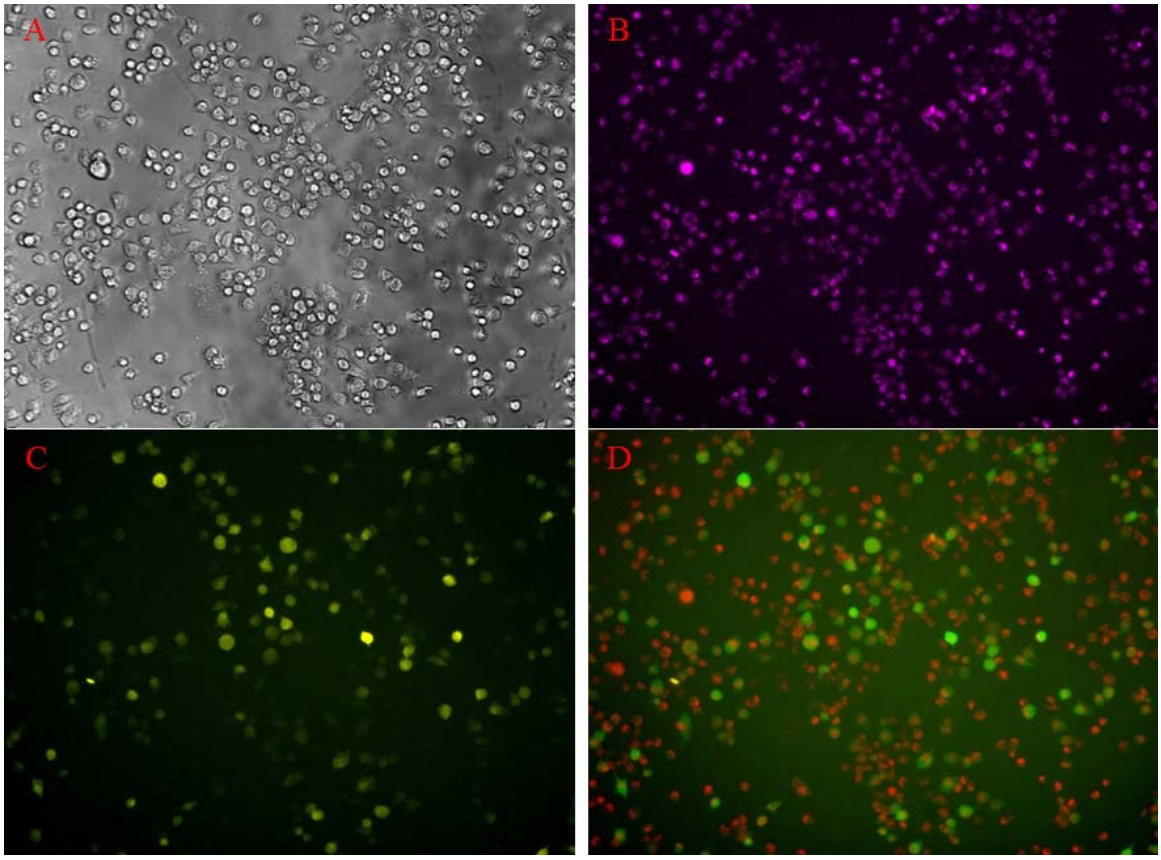

Supplementary Figure 7. Fluorescence microscope images of JAWS II cell transfected with nanoparticles co-encapsulating GFP and Cy5 labeled GFP mRNA.
A. Bright field. B. Cy5-labeled mGFP. C. GFP expression. D. GFP/Cy5 merge.

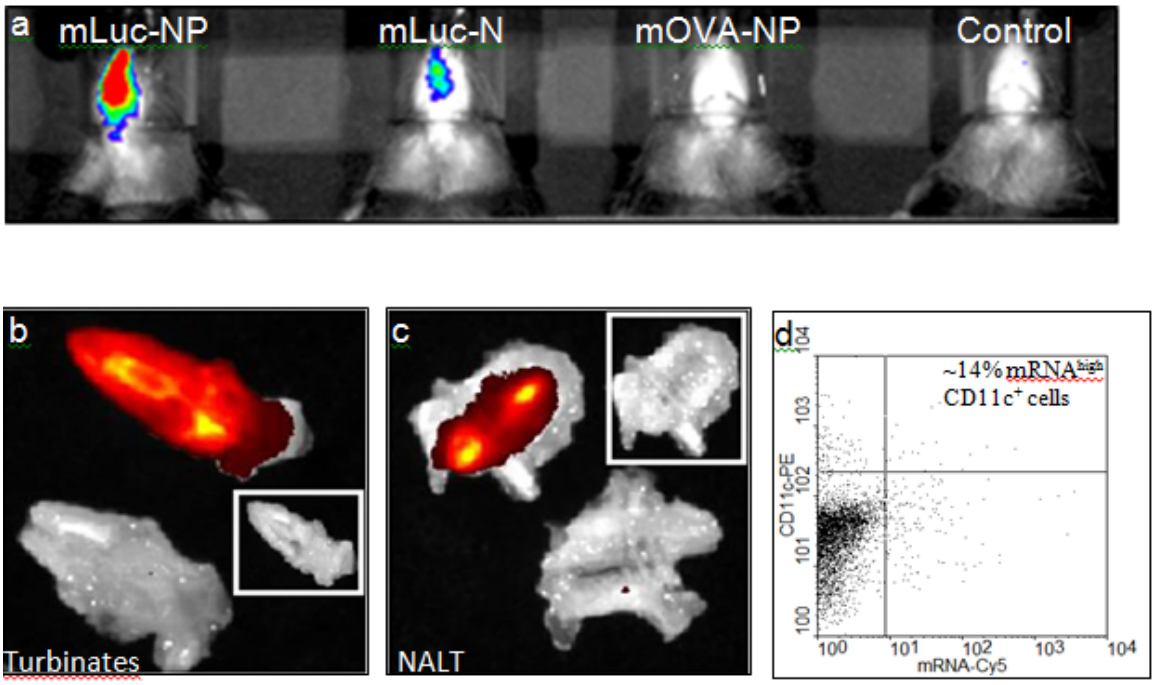

Supplementary Figure 8. Evaluating *in vivo* transfection efficiency of luciferase mRNA nanoparticle.

a) C57Bl/6 mice were administered intranasally with 6μg mRNA. From left: luciferase mRNA (mLuc-NP) nanoparticles, naked mLuc in Ringer's Lactate (mLuc-N), OVA mRNA (mOVA-NP) nanoparticles and non-transfected control (Control).

b-c) C57Bl/6 mice were administered intranasally with 4μg of Cy5-labeled green fluorescent protein mRNA (mGFP) encapsulated in nanoparticles. 30 minutes post-administration, nasal associated lymphoid tissue (NALT, b) and turbinate (c) were isolated, flushed 3 times with PBS and observed under IVIS (Kinetics, Caliper). Data is representative of 2 independent experiments.

d) Two female C57Bl/6 mice were administered intranasally with 6μg of Cy5-labeled mGFP encapsulated in nanoparticles. 4 hours post-administration, NALT from both mice were isolated and NALT cells were scraped off using a spatula. Cells were combined, blocked with CD16/32 (BioLegend), stained with CD11c-PE antibody (BioLegend), data acquired using flow cytometry (FACSCalibur) and analyzed using WinMDI 2.9 (freeware).

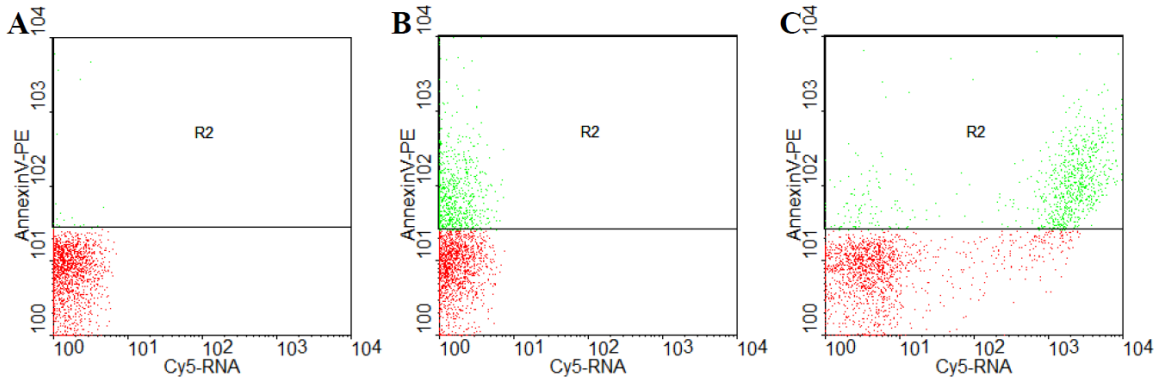

Supplementary Figure 9. Annexin V staining of Cy5-labeled GFP mRNA loaded leukocytes by electroporation.

(A) Non-electroporated cells.

(B) Cells electroporated without mRNA,

(C) Cells electroporated with mRNA. Cells were stained with PE-labeled Annexin V and analyzed using flow cytometry. Plots are gated for leukocytes based on forward scatter.

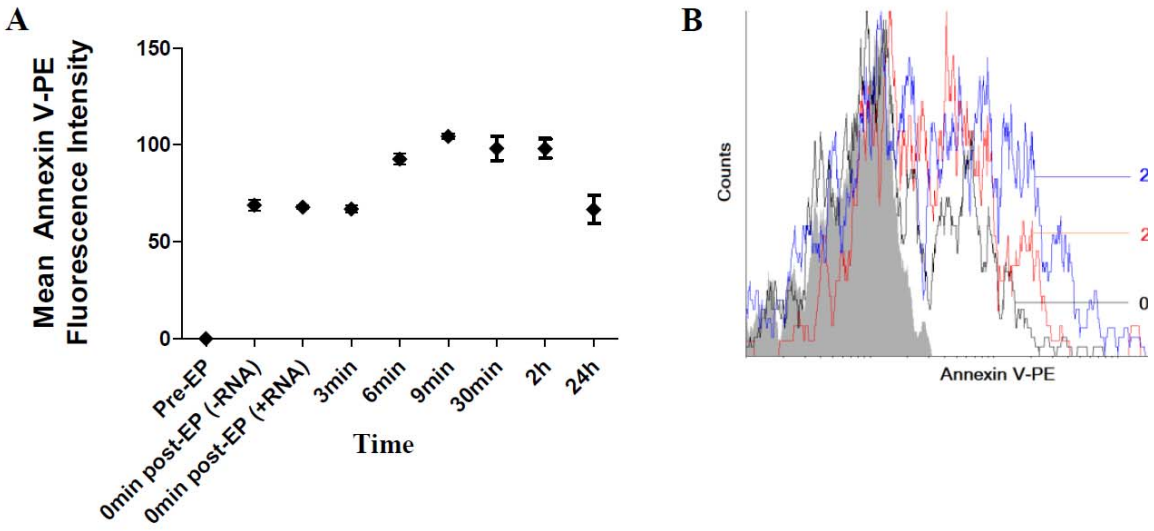

Supplementary Figure 10. Analysis of phosphatidylserine (PS) expression in electroporated leukocytes.

(A) Annexin V-PE staining of mRNA-loaded leukocytes (gated based on FSC) over 24 hours

(B) Histogram plot of annexin V+ cells at 0 min (black) 2 hours (blue) and 24 hours (red). Control (shaded grey) represents pre-electroporated FSC-gated leukocytes. EP: electroporation

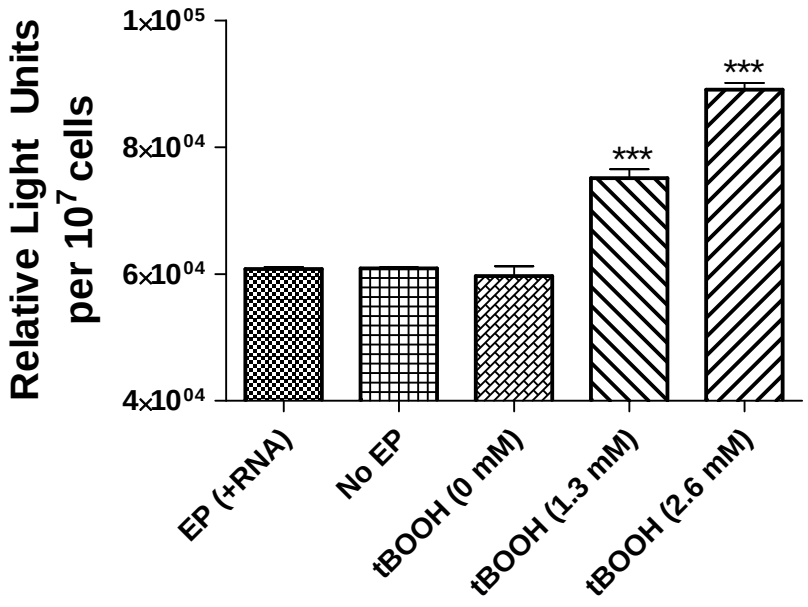

Supplementary Figure 11. Analysis of caspase 3 activation via luciferase activity mediated by release of aminoluciferin from caspase dependent DEVD cleavage.
(tBOOH: tert-butylhydrogen peroxide, DEVD: Asp-Glu-Val-Asp).

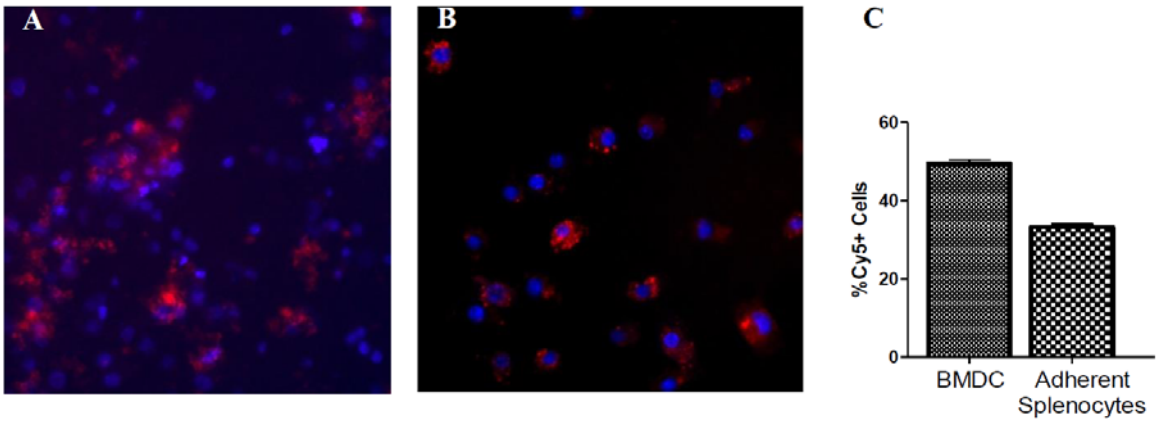

Supplementary Figure 12. Co-localization and uptake of whole blood cells loaded with Cy5-labeled GFP mRNA by antigen-presenting cells.

10^7 mRNA-loaded blood cells were co-cultured for 4 hours with 3x105 C57Bl/6 bone marrow-derived dendritic cells (BMDC) in a 24-well plate. Unattached cells were aspirated and adherent cells were rinsed with PBS. Fluorescence microscope images of bone marrow-derived dendritic cells 8 hours(A) and 24 hours (B) post-incubation with mRNA-loaded blood cells is shown.
(C) Flow cytometry quantification of Cy5+ dendritic cells or adherent splenocytes 24 hours post-incubation with mRNA-loaded blood cells.

Red: Cy5-RNA loaded blood cells. Blue: Hoechst stains for DC nuclei.

Kyle Phua

From: Blow, Nathan <Nathan.Blow@informausa.com>
Sent: Tuesday, March 25, 2014 6:48 PM
To: Kyle Phua
Subject: Permission to reuse figures

Dear Kyle,

We grant you permission to reuse Figure 2 from BioTechniques Vol 43, No 5, November 2007, pp.675-681. Please properly reference both the authors and journal within the figure legend and reference section of the article.

Please let me know if you have any additional questions or concerns.

Best regards,

Nathan

Nathan Blow, PhD. | Editor-in-Chief, *BioTechniques* | Mobile: 1-646-651-9084

ELSEVIER LICENSE
TERMS AND CONDITIONS

Jan 13, 2014

This is a License Agreement between Kyle Phua ("You") and Elsevier ("Elsevier") provided by Copyright Clearance Center ("CCC"). The license consists of your order details, the terms and conditions provided by Elsevier, and the payment terms and conditions.

All payments must be made in full to CCC. For payment instructions, please see information listed at the bottom of this form.

Supplier	Elsevier Limited The Boulevard,Langford Lane Kidlington,Oxford,OX5 1GB,UK
Registered Company Number	1982084
Customer name	Kyle Phua
Customer address	101 Science Drive CIEMAS 1228 DURHAM, NC 27708
License number	3307231370752
License date	Jan 13, 2014
Licensed content publisher	Elsevier
Licensed content publication	Journal of Controlled Release
Licensed content title	Non-viral vector delivery from PEG-hyaluronic acid hydrogels
Licensed content author	Julie A. Wieland,Tiffany L. Houchin-Ray,Lonnie D. Shea
Licensed content date	31 July 2007
Licensed content volume number	120
Licensed content issue number	3
Number of pages	9
Start Page	233
End Page	241
Type of Use	reuse in a journal/magazine
Requestor type	author of new work
Intended publisher of new work	Royal Society of Chemistry
Portion	figures/tables/illustrations
Number of figures/tables /illustrations	1
Format	both print and electronic
Are you the author of this Elsevier article?	No
Will you be translating?	No

ELSEVIER LICENSE
TERMS AND CONDITIONS

Jan 13, 2014

This is a License Agreement between Kyle Phua ("You") and Elsevier ("Elsevier") provided by Copyright Clearance Center ("CCC"). The license consists of your order details, the terms and conditions provided by Elsevier, and the payment terms and conditions.

All payments must be made in full to CCC. For payment instructions, please see information listed at the bottom of this form.

Supplier	Elsevier Limited The Boulevard,Langford Lane Kidlington,Oxford,OX5 1GB,UK
Registered Company Number	1982084
Customer name	Kyle Phua
Customer address	101 Science Drive CIEMAS 1228 DURHAM, NC 27708
License number	3307240045005
License date	Jan 13, 2014
Licensed content publisher	Elsevier
Licensed content publication	Biomaterials
Licensed content title	Controlled release of plasmid DNA from photo-cross-linked pluronic hydrogels
Licensed content author	Ki Woo Chun,Jun Bae Lee,Sun Hwa Kim,Tae Gwan Park
Licensed content date	June 2005
Licensed content volume number	26
Licensed content issue number	16
Number of pages	8
Start Page	3319
End Page	3326
Type of Use	reuse in a journal/magazine
Requestor type	author of new work
Intended publisher of new work	Royal Society of Chemistry
Portion	figures/tables/illustrations
Number of figures/tables /illustrations	1
Format	both print and electronic
Are you the author of this Elsevier article?	No
Will you be translating?	No

SPRINGER LICENSE
TERMS AND CONDITIONS

Mar 21, 2014

This is a License Agreement between Kyle Phua ("You") and Springer ("Springer") provided by Copyright Clearance Center ("CCC"). The license consists of your order details, the terms and conditions provided by Springer, and the payment terms and conditions.

All payments must be made in full to CCC. For payment instructions, please see information listed at the bottom of this form.

License Number	3353901154543
License date	Mar 21, 2014
Licensed content publisher	Springer
Licensed content publication	The AAPS Journal
Licensed content title	Mechanistic Determinants of Biotherapeutics Absorption Following SC Administration
Licensed content author	Wolfgang F. Richter
Licensed content date	Jan 1, 2012
Volume number	14
Issue number	3
Type of Use	Journal/Magazine
Requestor type	Publisher
Publisher	Royal Society of Chemistry
Portion	Figures
Format	Print and Electronic
Number of figures	1
Print run	1
Author of this Springer article	No
Order reference number	
Original figure numbers	Figure 2
Title of new article	mRNA Nanoparticle TUmor Vaccination
Publication the new article is in	Nanoscale
Author of new article	Kyle Phua
Expected publication date of new article	May 2014
Estimated size of new article (pages)	10
Total	0.00 USD
Terms and Conditions	

ELSEVIER LICENSE
TERMS AND CONDITIONS

Mar 24, 2014

This is a License Agreement between Kyle Phua ("You") and Elsevier ("Elsevier") provided by Copyright Clearance Center ("CCC"). The license consists of your order details, the terms and conditions provided by Elsevier, and the payment terms and conditions.

All payments must be made in full to CCC. For payment instructions, please see information listed at the bottom of this form.

Supplier	Elsevier Limited The Boulevard,Langford Lane Kidlington,Oxford,OX5 1GB,UK
Registered Company Number	1982084
Customer name	Kyle Phua
Customer address	101 Science Drive CIEMAS 1228
	DURHAM, NC 27708
License number	3355660797470
License date	Mar 24, 2014
Licensed content publisher	Elsevier
Licensed content publication	Journal of Controlled Release
Licensed content title	PEGylated cationic liposomes robustly augment vaccine-induced immune responses: Role of lymphatic trafficking and biodistribution
Licensed content author	Yan Zhuang,Yifan Ma,Ce Wang,Luo Hai,Chao Yan,Yijuan Zhang,Fengzhi Liu,Lintao Cai
Licensed content date	10 April 2012
Licensed content volume number	159
Licensed content issue number	1
Number of pages	8
Start Page	135
End Page	142
Type of Use	reuse in a journal/magazine
Requestor type	author of new work
Intended publisher of new work	Royal Society of Chemistry
Portion	figures/tables/illustrations
Number of figures/tables /illustrations	1
Format	both print and electronic
Are you the author of this Elsevier article?	No

NATURE PUBLISHING GROUP LICENSE
TERMS AND CONDITIONS

Mar 24, 2014

This is a License Agreement between Kyle Phua ("You") and Nature Publishing Group ("Nature Publishing Group") provided by Copyright Clearance Center ("CCC"). The license consists of your order details, the terms and conditions provided by Nature Publishing Group, and the payment terms and conditions.

All payments must be made in full to CCC. For payment instructions, please see information listed at the bottom of this form.

License Number	3355661373499
License date	Mar 24, 2014
Licensed content publisher	Nature Publishing Group
Licensed content publication	Nature Materials
Licensed content title	Synthetic mast-cell granules as adjuvants to promote and polarize immunity in lymph nodes
Licensed content author	Ashley L. St. John, Cheryl Y. Chan, Herman F. Staats, Kam W. Leong, Soman N. Abraham
Licensed content date	Jan 22, 2012
Volume number	11
Issue number	3
Type of Use	reuse in a journal/magazine
Requestor type	academic/university or research institute
Format	print and electronic
Portion	figures/tables/illustrations
Number of figures/tables /illustrations	1
High-res required	no
Figures	3
Author of this NPG article	no
Your reference number	
Title of the article	mRNA Nanoparticle TUmor Vaccination
Publication the new article is in	Nanoscale
Publisher of your article	Royal Society of Chemistry
Author of the article	Kyle Phua
Expected publication date	May 2014
Estimated size of new article (number of pages)	10
Total	0.00 USD
Terms and Conditions	

ELSEVIER LICENSE
TERMS AND CONDITIONS

Mar 24, 2014

This is a License Agreement between Kyle Phua ("You") and Elsevier ("Elsevier") provided by Copyright Clearance Center ("CCC"). The license consists of your order details, the terms and conditions provided by Elsevier, and the payment terms and conditions.

All payments must be made in full to CCC. For payment instructions, please see information listed at the bottom of this form.

Supplier	Elsevier Limited The Boulevard,Langford Lane Kidlington,Oxford,OX5 1GB,UK
Registered Company Number	1982084
Customer name	Kyle Phua
Customer address	101 Science Drive CIEMAS 1228 DURHAM, NC 27708
License number	3355661473916
License date	Mar 24, 2014
Licensed content publisher	Elsevier
Licensed content publication	Journal of Controlled Release
Licensed content title	Transfection efficiency and transgene expression kinetics of mRNA delivered in naked and nanoparticle format
Licensed content author	Kyle K.L. Phua,Kam W. Leong,Smita K. Nair
Licensed content date	28 March 2013
Licensed content volume number	166
Licensed content issue number	3
Number of pages	7
Start Page	227
End Page	233
Type of Use	reuse in a journal/magazine
Requestor type	author of new work
Intended publisher of new work	Royal Society of Chemistry
Portion	figures/tables/illustrations
Number of figures/tables /illustrations	1
Format	both print and electronic
Are you the author of this Elsevier article?	Yes
Will you be translating?	No

NATURE PUBLISHING GROUP LICENSE
TERMS AND CONDITIONS

Mar 24, 2014

This is a License Agreement between Kyle Phua ("You") and Nature Publishing Group ("Nature Publishing Group") provided by Copyright Clearance Center ("CCC"). The license consists of your order details, the terms and conditions provided by Nature Publishing Group, and the payment terms and conditions.

All payments must be made in full to CCC. For payment instructions, please see information listed at the bottom of this form.

License Number	3355670604667
License date	Mar 24, 2014
Licensed content publisher	Nature Publishing Group
Licensed content publication	Mucosal Immunology
Licensed content title	Imaging murine NALT following intranasal immunization with flagellin-modified circumsporozoite protein malaria vaccines
Licensed content author	A Nacer, D Carapau, R Mitchell, A Meltzer, A Shaw et al.
Licensed content date	Mar 1, 2014
Volume number	7
Issue number	2
Type of Use	reuse in a journal/magazine
Requestor type	academic/university or research institute
Format	print and electronic
Portion	figures/tables/illustrations
Number of figures/tables /illustrations	1
High-res required	no
Figures	3
Author of this NPG article	no
Your reference number	
Title of the article	mRNA Nanoparticle TUmor Vaccination
Publication the new article is in	Nanoscale
Publisher of your article	Royal Society of Chemistry
Author of the article	Kyle Phua
Expected publication date	May 2014
Estimated size of new article (number of pages)	10
Total	0.00 USD
Terms and Conditions	

References

[1] Boczkowski, D., S.K. Nair, D. Snyder,E. Gilboa, Dendritic cells pulsed with RNA are potent antigen-presenting cells in vitro and in vivo, Journal of Experimental Medicine, 1996, 184 (2), 465-72.

[2] Nair, S.K., D. Boczkowski, S. Pruitt,J. Urban, RNA in cancer vaccine therapy, in CANCER VACCINES: FROM RESEARCH TO CLINICAL PRACTICE, A.B.M.O.F. Marincola, Editor 2011, Taylor & Francis.

[3] Van Lint, S., C. Heirman, K. Thielemans,K. Breckpot, mRNA: From a chemical blueprint for protein production to an off-the-shelf therapeutic, Hum Vaccin Immunother, 2013, 9 (2)

[4] Sheikh, N.A., D. Petrylak, P.W. Kantoff, C. Dela Rosa, F.P. Stewart, L.Y. Kuan, J.B. Whitmore, J.B. Trager, C.H. Poehlein, M.W. Frohlich,D.L. Urdal, Sipuleucel-T immune parameters correlate with survival: an analysis of the randomized phase 3 clinical trials in men with castration-resistant prostate cancer, Cancer Immunology, Immunotherapy, 2013, 62 (1), 137-47.

[5] Chambers, J.D.,P.J. Neumann, Listening to Provenge--what a costly cancer treatment says about future Medicare policy, New England Journal of Medicine, 2011, 364 (18), 1687-9.

[6] Jonsson, B.,N. Wilking, Cancer vaccines and immunotherapeutics: challenges for pricing, reimbursement and market access, Hum Vaccin Immunother, 2012, 8 (9), 1360-3.

[7] Lee, J., D. Boczkowski,S. Nair, Programming human dendritic cells with mRNA, Methods in Molecular Biology, 2013, 969, 111-25.

[8] Van Tendeloo, V.F., P. Ponsaerts, F. Lardon, G. Nijs, M. Lenjou, C. Van Broeckhoven, D.R. Van Bockstaele,Z.N. Berneman, Highly efficient gene delivery by mRNA electroporation in human hematopoietic cells: superiority to lipofection and passive pulsing of mRNA and to electroporation of plasmid cDNA for tumor antigen loading of dendritic cells, Blood, 2001, 98 (1), 49-56.

[9] Banchereau, J.,A.K. Palucka, Dendritic cells as therapeutic vaccines against cancer, Nature Reviews Immunology, 2005, 5 (4), 296-306.

[10] Boczkowski, D., J. Lee, S. Pruitt,S. Nair, Dendritic cells engineered to secrete anti-GITR antibodies are effective adjuvants to dendritic cell-based immunotherapy, Cancer Gene Therapy, 2009, 16 (12), 900-911.

[11] Boczkowski, D.,S. Nair, RNA as performance-enhancers for dendritic cells, Expert Opinion on Biological Therapy, 2010, 10 (4), 563-574.

[12] Bonehill, A., C. Heirman, S. Tuyaerts, A. Michiels, K. Breckpot, F. Brasseur, Y. Zhang, P. van der Bruggen,K. Thielemans, Messenger RNA-electroporated dendritic cells presenting MAGE-A3 simultaneously in HLA class I and class II molecules, Journal of Immunology, 2004, 172 (11), 6649-6657.

[13] Bonehill, A., S. Tuyaerts, A.M. Van Nuffel, C. Heirman, T.J. Bos, K. Fostier, B. Neyns,K. Thielemans, Enhancing the T-cell stimulatory capacity of human dendritic cells by co-electroporation with CD40L, CD70 and constitutively active TLR4 encoding mRNA, Molecular Therapy, 2008, 16 (6), 1170-1180.

[14] Chung, D.J., E. Romano, K.B. Pronschinske, J.A. Shyer, M. Mennecozzi, E.T. St Angelo,J.W. Young, Langerhans-type and monocyte-derived human dendritic cells have different susceptibilities to mRNA electroporation with distinct effects on maturation and activation: implications for immunogenicity in dendritic cell-based immunotherapy, J Transl Med, 2013, 11, 166.

[15] Dannull, J., N.R. Haley, G. Archer, S. Nair, D. Boczkowski, M. Harper, N. De Rosa, N. Pickett, P.J. Mosca, J. Burchette, M.A. Selim, D.A. Mitchell, J. Sampson, D.S. Tyler,S.K. Pruitt, Melanoma immunotherapy using mature DCs expressing the constitutive proteasome, Journal of Clinical Investigation, 2013, 123 (7), 3135-3145.

[16] de Saint-Vis, B., J. Vincent, S. Vandenabeele, B. Vanbervliet, J.J. Pin, S. Ait-Yahia, S. Patel, M.G. Mattei, J. Banchereau, S. Zurawski, J. Davoust, C. Caux,S. Lebecque, A novel lysosome-associated membrane glycoprotein, DC-LAMP, induced upon DC maturation, is transiently expressed in MHC class II compartment, Immunity, 1998, 9 (3), 325-336.

[17] Kreiter, S., M. Diken, A. Selmi, O. Tureci,U. Sahin, Tumor vaccination using messenger RNA: prospects of a future therapy, Current Opinion in Immunology, 2011, 23 (3), 399-406.

[18] Mitchell, D.A.,S.K. Nair, RNA-transfected dendritic cells in cancer immunotherapy, Journal of Clinical Investigation, 2000, 106 (9), 1065-1069.

[19] Van Lint, S., C. Goyvaerts, S. Maenhout, L. Goethals, A. Disy, D. Benteyn, J. Pen, A. Bonehill, C. Heirman, K. Breckpot,K. Thielemans, Preclinical evaluation of TriMix and antigen mRNA-based antitumor therapy, Cancer Research, 2012, 72 (7), 1661-71.

[20] Han, T.H., P. Jin, J. Ren, S. Slezak, F.M. Marincola,D.F. Stroncek, Evaluation of 3 clinical dendritic cell maturation protocols containing lipopolysaccharide and interferon-gamma, Journal of Immunotherapy, 2009, 32 (4), 399-407.

[21] Snijders, A., P. Kalinski, C.M.U. Hilkens,M.L. Kapsenberg, High-level IL-12 production by human dendritic cells requires two signals, International Immunology, 1998, 10 (11), 1593-1598.

[22] Albert, M.L., M. Jegathesan,R.B. Darnell, Dendritic cell maturation is required for the cross-tolerization of CD8(+) T cells, Nature Immunology, 2001, 2 (11), 1010-1017.

[23] Dieu, M.C., B. Vanbervliet, A. Vicari, J.M. Bridon, E. Oldham, S. Ait-Yahia, F. Briere, A. Zlotnik, S. Lebecque,C. Caux, Selective recruitment of immature and mature dendritic cells by distinct chemokines expressed in different anatomic sites, Journal of Experimental Medicine, 1998, 188 (2), 373-86.

[24] Nomura, T.,S. Sakaguchi, Naturally arising CD25(+)CD4(+) regulatory T cells in tumor immunity, Cd4-Pluscd25-Plus Regulatory T Cells: Origin, Function and Therapeutic Potential, 2005, 293, 287-302.

[25] Shevach, E.M.,G.L. Stephens, The GITR-GITRL interaction: co-stimulation or contrasuppression of regulatory activity?, Nature Reviews Immunology, 2006, 6 (8), 613-618.

[26] Nocentini, G., L. Giunchi, S. Ronchetti, L.T. Krausz, A. Bartoli, R. Moraca, G. Migliorati,C. Riccardi, A new member of the tumor necrosis factor nerve growth factor receptor family inhibits T cell receptor-induced apoptosis, Proceedings of the National Academy of Sciences of the United States of America, 1997, 94 (12), 6216-6221.

[27] Stephens, G.L., R.S. McHugh, M.J. Whitters, D.A. Young, D. Luxenberg, B.M. Carreno, M. Collins,E.M. Shevach, Engagement of glucocorticoid-induced TNFR family-related receptor on effector T cells by its ligand mediates resistance to suppression by CD4(+) CD25(+) T cells, Journal of Immunology, 2004, 173 (8), 5008-5020.

[28] Morse, M.A., R.E. Coleman, G. Akabani, N. Niehaus, D. Coleman,H.K. Lyerly, Migration of human dendritic cells after injection in patients with metastatic malignancies, Cancer Research, 1999, 59 (1), 56-58.

[29] Verdijk, P., E.H.J.G. Aarntzen, W.J. Lesterhuis, A.C.I. Boullart, E. Kok, M.M. van Rossum, S. Strijk, F. Eijckeler, J.J. Bonenkamp, J.F.M. Jacobs, W. Blokx, J.H.J.M. van Krieken, I. Joosten, O.C. Boerman, W.J.G. Oyen, G. Adema, C.J.A. Punt, C.G. Figdor,I.J.M. de Vries, Limited Amounts of Dendritic Cells Migrate into the T-Cell Area of Lymph Nodes but Have High Immune Activating Potential in Melanoma Patients, Clinical Cancer Research, 2009, 15 (7), 2531-2540.

[30] Schuurhuis, D.H., P. Verdijk, G. Schreibelt, E.H.J.G. Aarntzen, N. Scharenborg, A. de Boer, M.W.M.M. van de Rakt, M. Kerkhoff, M.J.P. Gerritsen, F. Eijckeler, J.J. Bonenkamp, W. Blokx, J.H. van Krieken, O.C. Boerman, W.J.G. Oyen, C.J.A. Punt, C.G. Figdor, G.J. Adema,I.J.M. de Vries, In situ Expression of Tumor Antigens by Messenger RNA-Electroporated Dendritic Cells in Lymph Nodes of Melanoma Patients, Cancer Research, 2009, 69 (7), 2927-2934.

[31] Lesterhuis, W.J., I.J.M. de Vries, G. Schreibelt, A.J.A. Lambeck, E.H.J.G. Aarntzen, J.F.M. Jacobs, N.M. Scharenborg, M.W.M.M. van de Rakt, A.J. de Boer, S. Croockewit, M.M. van Rossum, R. Mus, W.J.G. Oyen, O.C. Boerman, S. Lucas, G.J. Adema, C.J.A. Punt,C.G. Figdor, Route of Administration Modulates the Induction of Dendritic Cell Vaccine-Induced Antigen-Specific T Cells in Advanced Melanoma Patients, Clinical Cancer Research, 2011, 17 (17), 5725-5735.

[32] Wu, X.Y.,G. Brewer, The regulation of mRNA stability in mammalian cells: 2.0, Gene, 2012, 500 (1), 10-21.

[33] Grudzien-Nogalska, E., J. Kowalska, W. Su, A.N. Kuhn, S.V. Slepenkov, E. Darzynkiewicz, U. Sahin, J. Jemielity,R.E. Rhoads, Synthetic mRNAs with superior translation and stability properties, Methods in Molecular Biology, 2013, 969, 55-72.

[34] Phua, K.K., D. Boczkowski, J. Dannull, S. Pruitt, K.W. Leong,S.K. Nair, Whole Blood Cells Loaded with Messenger RNA as an Anti-Tumor Vaccine, Adv Healthc Mater, 2013,

[35] Walch, B., T. Breinig, M.J. Schmitt,F. Breinig, Delivery of functional DNA and messenger RNA to mammalian phagocytic cells by recombinant yeast, Gene Therapy, 2012, 19 (3), 237-45.

[36] Kreiter, S., A. Selmi, M. Diken, M. Koslowski, C.M. Britten, C. Huber, O. Tureci,U. Sahin, Intranodal vaccination with naked antigen-encoding RNA elicits potent prophylactic and therapeutic antitumoral immunity, Cancer Research, 2010, 70 (22), 9031-40.

[37] Hess, P.R., D. Boczkowski, S.K. Nair, D. Snyder,E. Gilboa, Vaccination with mRNAs encoding tumor-associated antigens and granulocyte-macrophage colony-stimulating factor efficiently primes CTL responses, but is insufficient to overcome tolerance to a model tumor/self antigen, Cancer Immunology, Immunotherapy, 2006, 55 (6), 672-83.

[38] Hoerr, I., R. Obst, H.G. Rammensee,G. Jung, In vivo application of RNA leads to induction of specific cytotoxic T lymphocytes and antibodies, European Journal of Immunology, 2000, 30 (1), 1-7.

[39] Mockey, M., E. Bourseau, V. Chandrashekhar, A. Chaudhuri, S. Lafosse, E. Le Cam, V.F. Quesniaux, B. Ryffel, C. Pichon,P. Midoux, mRNA-based cancer vaccine: prevention of B16 melanoma progression and metastasis by systemic injection of MART1 mRNA histidylated lipopolyplexes, Cancer Gene Therapy, 2007, 14 (9), 802-14.

[40] Perche, F., T. Benvegnu, M. Berchel, L. Lebegue, C. Pichon, P.A. Jaffres,P. Midoux, Enhancement of dendritic cells transfection in vivo and of vaccination against B16F10 melanoma with mannosylated histidylated lipopolyplexes loaded with tumor antigen messenger RNA, Nanomed-Nanotechnol, 2011, 7 (4), 445-53.

[41] Pollard, C., J. Rejman, W. De Haes, B. Verrier, E. Van Gulck, T. Naessens, S. De Smedt, P. Bogaert, J. Grooten, G. Vanham,S. De Koker, Type I IFN Counteracts the Induction of Antigen-Specific Immune Responses by Lipid-Based Delivery of mRNA Vaccines, Molecular Therapy, 2013, 21 (1), 251-259.

[42] Zhou, W.Z., D.S. Hoon, S.K. Huang, S. Fujii, K. Hashimoto, R. Morishita,Y. Kaneda, RNA melanoma vaccine: induction of antitumor immunity by human glycoprotein 100 mRNA immunization, Human Gene Therapy, 1999, 10 (16), 2719-24.

[43] Mockey, M., C. Goncalves, F.P. Dupuy, F.M. Lemoine, C. Pichon,P. Midoux, mRNA transfection of dendritic cells: Synergistic effect of ARCA mRNA capping with Poly(A) chains in cis and in trans for a high protein expression level, Biochem Bioph Res Co, 2006, 340 (4), 1062-1068.

[44] Zou, S., K. Scarfo, M.H. Nantz,J.G. Hecker, Lipid-mediated delivery of RNA is more efficient than delivery of DNA in non-dividing cells, International Journal of Pharmaceutics, 2010, 389 (1-2), 232-243.

[45] Yamamoto, A., M. Kormann, J. Rosenecker,C. Rudolph, Current prospects for mRNA gene delivery, European Journal of Pharmaceutics and Biopharmaceutics, 2009, 71 (3), 484-9.

[46] Tavernier, G., O. Andries, J. Demeester, N.N. Sanders, S.C. De Smedt,J. Rejman, mRNA as gene therapeutic: How to control protein expression, Journal of Controlled Release, 2011, 150 (3), 238-247.

[47] Kariko, K., M. Buckstein, H. Ni,D. Weissman, Suppression of RNA recognition by Toll-like receptors: the impact of nucleoside modification and the evolutionary origin of RNA, Immunity, 2005, 23 (2), 165-75.

[48] Kariko, K., H. Muramatsu, F.A. Welsh, J. Ludwig, H. Kato, S. Akira,D. Weissman, Incorporation of Pseudouridine Into mRNA Yields Superior Nonimmunogenic Vector With Increased Translational Capacity and Biological Stability, Molecular Therapy, 2008, 16 (11), 1833-1840.

[49] Jones, K.L., D. Drane,E.J. Gowans, Long-term storage of DNA-free RNA for use in vaccine studies, BioTechniques, 2007, 43 (5), 675-81.

[50] Wieland, J.A., T.L. Houchin-Ray,L.D. Shea, Non-viral vector delivery from PEG-hyaluronic acid hydrogels, J Control Release, 2007, 120 (3), 233-41.

[51] Chun, K.W., J.B. Lee, S.H. Kim,T.G. Park, Controlled release of plasmid DNA from photo-cross-linked pluronic hydrogels, Biomaterials, 2005, 26 (16), 3319-26.

[52] Kumar, A., P. Wonganan, M.A. Sandoval, X. Li, S. Zhu,Z. Cui, Microneedle-mediated transcutaneous immunization with plasmid DNA coated on cationic PLGA nanoparticles, J Control Release, 2012, 163 (2), 230-9.

[53] DeMuth, P.C., X. Su, R.E. Samuel, P.T. Hammond,D.J. Irvine, Nano-layered microneedles for transcutaneous delivery of polymer nanoparticles and plasmid DNA, Adv Mater, 2010, 22 (43), 4851-6.

[54] Kasper, F.K., S.K. Seidlits, A. Tang, R.S. Crowther, D.H. Carney, M.A. Barry,A.G. Mikos, In vitro release of plasmid DNA from oligo(poly(ethylene glycol) fumarate) hydrogels, J Control Release, 2005, 104 (3), 521-39.

[55] Phua, K.,K.W. Leong, Microscale oral delivery devices incorporating nanoparticles, Nanomedicine (Lond), 2010, 5 (2), 161-3.

[56] Tseng, Y.C., S. Mozumdar,L. Huang, Lipid-based systemic delivery of siRNA, Advanced Drug Delivery Reviews, 2009, 61 (9), 721-731.

[57] Owens, D.E.,N.A. Peppas, Opsonization, biodistribution, and pharmacokinetics of polymeric nanoparticles, International Journal of Pharmaceutics, 2006, 307 (1), 93-102.

[58] Kabanov, A.V., Taking polycation gene delivery systems from in vitro to in vivo, Pharmaceutical Science & Technology Today, 1999, 2 (9), 365-372.

[59] Ho, Y.P., C.L. Grigsby, F. Zhao,K.W. Leong, Tuning Physical Properties of Nanocomplexes through Microfluidics-Assisted Confinement, Nano Letters, 2011, 11 (5), 2178-2182.

[60] Merdan, T., K. Kunath, H. Petersen, U. Bakowsky, K.H. Voigt, J. Kopecek,T. Kissel, PEGylation of poly(ethylene imine) affects stability of complexes with plasmid DNA under in vivo conditions in a dose-dependent manner after intravenous injection into mice, Bioconjugate Chemistry, 2005, 16 (4), 785-92.

[61] Dileo, J., R. Banerjee, M. Whitmore, J.V. Nayak, L.D. Falo, Jr.,L. Huang, Lipid-protamine-DNA-mediated antigen delivery to antigen-presenting cells results in enhanced anti-tumor immune responses, Molecular Therapy, 2003, 7 (5 Pt 1), 640-8.

[62] Maemura, K., Q. Zheng, T. Wada, M. Ozaki, S. Takao, T. Aikou, G.B. Bulkley, A.S. Klein,Z. Sun, Reactive oxygen species are essential mediators in antigen presentation by Kupffer cells, Immunology and Cell Biology, 2005, 83 (4), 336-43.

[63] Medd, P.G.,B.M. Chain, Protein degradation in MHC class II antigen presentation: opportunities for immunomodulation, Seminars in Cell & Developmental Biology, 2000, 11 (3), 203-210.

[64] Allen, T.M., C.B. Hansen,L.S.S. Guo, Subcutaneous Administration of Liposomes - a Comparison with the Intravenous and Intraperitoneal Routes of Injection, Biochimica et Biophysica Acta, 1993, 1150 (1), 9-16.

[65] Weissman, D., H.P. Ni, D. Scales, A. Dude, J. Capodici, K. McGibney, A. Abdool, S.N. Isaacs, G. Cannon,K. Kariko, HIV gag mRNA transfection of dendritic cells (DC) delivers encoded antigen to MHC class I and II molecules, causes DC maturation, and induces a potent human in vitro primary immune response, Journal of Immunology, 2000, 165 (8), 4710-4717.

[66] Li, S.D.,L. Huang, Nanoparticles evading the reticuloendothelial system: role of the supported bilayer, Biochimica et Biophysica Acta, 2009, 1788 (10), 2259-66.

[67] Idoyaga, J.S., R. Immunology Image Resource.

[68] Richter, W.F., S.G. Bhansali,M.E. Morris, Mechanistic Determinants of Biotherapeutics Absorption Following SC Administration, Aaps Journal, 2012, 14 (3), 559-570.

[69] Reddy, S.T., A. Rehor, H.G. Schmoekel, J.A. Hubbell,M.A. Swartz, In vivo targeting of dendritic cells in lymph nodes with poly(propylene sulfide) nanoparticles, Journal of Controlled Release, 2006, 112 (1), 26-34.

[70] Manolova, V., A. Flace, M. Bauer, K. Schwarz, P. Saudan,M.F. Bachmann, Nanoparticles target distinct dendritic cell populations according to their size, European Journal of Immunology, 2008, 38 (5), 1404-1413.

[71] Zhuang, Y., Y.F. Ma, C. Wang, L. Hai, C. Yan, Y.J. Zhang, F.Z. Liu,L.T. Cai, PEGylated cationic liposomes robustly augment vaccine-induced immune responses: Role of lymphatic trafficking and biodistribution, Journal of Controlled Release, 2012, 159 (1), 135-142.

[72] Moghimi, S.M., The effect of methoxy-PEG chain length and molecular architecture on lymph node targeting of immuno-PEG liposomes, Biomaterials, 2006, 27 (1), 136-144.

[73] John, A.L.S., C.Y. Chan, H.F. Staats, K.W. Leong,S.N. Abraham, Synthetic mast-cell granules as adjuvants to promote and polarize immunity in lymph nodes, Nature Materials, 2012, 11 (3), 250-257.

[74] Daftarian, P., A.E. Kaifer, W. Li, B.B. Blomberg, D. Frasca, F. Roth, R. Chowdhury, E.A. Berg, J.B. Fishman, H.A. Al Sayegh, P. Blackwelder, L. Inverardi, V.L. Perez, V. Lemmon,P. Serafini, Peptide-Conjugated PAMAM Dendrimer as a Universal DNA Vaccine Platform to Target Antigen-Presenting Cells, Cancer Research, 2011, 71 (24), 7452-7462.

[75] Chen, W.S., W.L. Yan,L. Huang, A simple but effective cancer vaccine consisting of an antigen and a cationic lipid, Cancer Immunology Immunotherapy, 2008, 57 (4), 517-530.

[76] Witte, C.L., M.H. Witte, A.E. Dumont, W.R. Cole,J.R. Smith, Protein Content in Lymph and Edema Fluids in Congestive Heart Failure, Circulation, 1969, 40 (5), 623-&.

[77] Harrell, M.I., B.M. Iritani,A. Ruddell, Lymph node mapping in the mouse, Journal of Immunological Methods, 2008, 332 (1-2), 170-174.

[78] Phua, K.K.L., K.W. Leong,S.K. Nair, Transfection efficiency and transgene expression kinetics of mRNA delivered in naked and nanoparticle format, Journal of Controlled Release, 2013, 166 (3), 227-233.

[79] Cesta, M.F., Normal structure, function, and histology of mucosa-associated lymphoid tissue, Toxicologic Pathology, 2006, 34 (5), 599-608.

[80] Miller, H., J. Zhang, R. Kuolee, G.B. Patel,W. Chen, Intestinal M cells: the fallible sentinels?, World J Gastroenterol, 2007, 13 (10), 1477-86.

[81] Vila, A., A. Sanchez, C. Evora, I. Soriano, O. McCallion,M.J. Alonso, PLA-PEG particles as nasal protein carriers: the influence of the particle size, International Journal of Pharmaceutics, 2005, 292 (1-2), 43-52.

[82] Rajapaksa, T.E., K.M. Bennett, M. Hamer, C. Lytle, V.G.J. Rodgers,D.D. Lo, Intranasal M Cell Uptake of Nanoparticles Is Independently Influenced by Targeting Ligands and Buffer Ionic Strength, Journal of Biological Chemistry, 2010, 285 (31), 23739-23746.

[83] Matsuo, K., H. Koizumi, M. Akashi, S. Nakagawa, T. Fujita, A. Yamamoto,N. Okada, Intranasal immunization with poly(gamma-glutamic acid) nanoparticles entrapping antigenic proteins can induce potent tumor immunity, Journal of Controlled Release, 2011, 152 (2), 310-316.

[84] Southam, D.S., M. Dolovich, P.M. O'Bryne,M.D. Inman, Distribution of intranasal instillations in mice: effects of volume, time, body position, and anesthesia, American Journal of Physiology-Lung Cellular and Molecular Physiology, 2002, 282 (4), L833-L839.

[85] Xu, J.H., W.J. Dai, Z.M. Wang, B. Chen, Z.M. Li,X.Y. Fan, Intranasal Vaccination with Chitosan-DNA Nanoparticles Expressing Pneumococcal Surface Antigen A Protects Mice against Nasopharyngeal Colonization by Streptococcus pneumoniae, Clinical and Vaccine Immunology, 2011, 18 (1), 75-81.

[86] Roy, K., H.Q. Mao, S.K. Huang,K.W. Leong, Oral gene delivery with chitosan-DNA nanoparticles generates immunologic protection in a murine model of peanut allergy, Nature Medicine, 1999, 5 (4), 387-391.

[87] Lai, S.K., Y.Y. Wang,J. Hanes, Mucus-penetrating nanoparticles for drug and gene delivery to mucosal tissues, Advanced Drug Delivery Reviews, 2009, 61 (2), 158-171.

[88] Su, X., J. Fricke, D.G. Kavanagh,D.J. Irvine, In vitro and in vivo mRNA delivery using lipid-enveloped pH-responsive polymer nanoparticles, Mol Pharm, 2011, 8 (3), 774-87.

[89] Frey, A., K.T. Giannasca, R. Weltzin, P.J. Giannasca, H. Reggio, W.I. Lencer,M.R. Neutra, Role of the glycocalyx in regulating access of microparticles to apical plasma membranes of intestinal epithelial cells: Implications for microbial attachment and oral vaccine targeting, Journal of Experimental Medicine, 1996, 184 (3), 1045-1059.

[90] Nacer, A., D. Carapau, R. Mitchell, A. Meltzer, A. Shaw, U. Frevert,E.H. Nardin, Imaging murine NALT following intranasal immunization with flagellin-modified circumsporozoite protein malaria vaccines, Mucosal Immunol, 2013,

[91] Hartmann, E., H. Graefe, A. Hopert, R. Pries, S. Rothenfusser, H. Poeck, B. Mack, S. Endres, G. Hartmann,B. Wollenberg, Analysis of plasmacytoid and myeloid dendritic cells in nasal epithelium, Clinical and Vaccine Immunology, 2006, 13 (11), 1278-1286.

[92] Shen, Z.H., G. Reznikoff, G. Dranoff,K.L. Rock, Cloned dendritic cells can present exogenous antigens on both MHC class I and class II molecules, Journal of Immunology, 1997, 158 (6), 2723-2730.

[93] Gao, X.,L. Huang, Potentiation of cationic liposome-mediated gene delivery by polycations, Biochemistry, 1996, 35 (3), 1027-36.

[94] Cheng, C., A.J. Convertine, P.S. Stayton,J.D. Bryers, Multifunctional triblock copolymers for intracellular messenger RNA delivery, Biomaterials, 2012, 33 (28), 6868-6876.

[95] Singh, M., M. Briones, G. Ott,D. O'Hagan, Cationic microparticles: A potent delivery system for DNA vaccines, Proceedings of the National Academy of Sciences of the United States of America, 2000, 97 (2), 811-6.

[96] Blum, J.S., P.A. Wearsch,P. Cresswell, Pathways of Antigen Processing, Annual Review of Immunology, Vol 31, 2013, 31, 443-473.

[97] Kurts, C., B.W.S. Robinson,P.A. Knolle, Cross-priming in health and disease, Nature Reviews Immunology, 2010, 10 (6), 403-414.

[98] Nair, S.K., D. Boczkowski, M. Morse, R.I. Cumming, H.K. Lyerly,E. Gilboa, Induction of primary carcinoembryonic antigen (CEA)-specific cytotoxic T lymphocytes in vitro using human dendritic cells transfected with RNA, Nature Biotechnology, 1998, 16 (4), 364-369.

[99] Valencia, P.M., O.C. Farokhzad, R. Karnik,R. Langer, Microfluidic technologies for accelerating the clinical translation of nanoparticles, Nat Nanotechnol, 2012, 7 (10), 623-9.

[100] Hornung, V., J. Ellegast, S. Kim, K. Brzozka, A. Jung, H. Kato, H. Poeck, S. Akira, K.K. Conzelmann, M. Schlee, S. Endres,G. Hartmann, 5 '-triphosphate RNA is the ligand for RIG-I, Science, 2006, 314 (5801), 994-997.

[101] Geall, A.J., A. Verma, G.R. Otten, C.A. Shaw, A. Hekele, K. Banerjee, Y. Cu, C.W. Beard, L.A. Brito, T. Krucker, D.T. O'Hagan, M. Singh, P.W. Mason, N.M. Valiante, P.R. Dormitzer, S.W. Barnett, R. Rappuoli, J.B. Ulmer,C.W. Mandl, Nonviral delivery of self-amplifying RNA vaccines, Proceedings of the National Academy of Sciences of the United States of America, 2012, 109 (36), 14604-9.

[102] Uchida, S., K. Itaka, H. Uchida, K. Hayakawa, T. Ogata, T. Ishii, S. Fukushima, K. Osada,K. Kataoka, In Vivo Messenger RNA Introduction into the Central Nervous System Using Polyplex Nanomicelle, Plos One, 2013, 8 (2)

[103] Lund, J.M., L. Alexopoulou, A. Sato, M. Karow, N.C. Adams, N.W. Gale, A. Iwasaki,R.A. Flavell, Recognition of single-stranded RNA viruses by Toll-like receptor 7, Proceedings of the National Academy of Sciences of the United States of America, 2004, 101 (15), 5598-5603.

[104] Scheel, B., S. Braedel, J. Probst, J.P. Carralot, H. Wagner, H. Schild, G. Jung, H.G. Rammensee,S. Pascolo, Immunostimulating capacities of stabilized RNA molecules, European Journal of Immunology, 2004, 34 (2), 537-547.

[105] Scheel, B., R. Teufel, J. Probst, J.P. Carralot, J. Geginat, M. Radsak, D. Jarrossay, H. Wagner, G. Jung, H.G. Rammensee, I. Hoerr,S. Pascolo, Toll-like receptor-dependent activation of several human blood cell types by protamine-condensed mRNA, European Journal of Immunology, 2005, 35 (5), 1557-1566.

[106] Diebold, S.S., T. Kaisho, H. Hemmi, S. Akira,C.R.E. Sousa, Innate antiviral responses by means of TLR7-mediated recognition of single-stranded RNA, Science, 2004, 303 (5663), 1529-1531.

[107] Su, X.F., J. Fricke, D.G. Kavanagh,D.J. Irvine, In Vitro and in Vivo mRNA Delivery Using Lipid-Enveloped pH-Responsive Polymer Nanoparticles, Molecular Pharmaceutics, 2011, 8 (3), 774-787.

[108] L. M. Kranz, M.D., M. Holzmann, K. Reuter, A. Selmi, D. Fritz, M. Meng,,P.B.G. I. Esparza, H. Haas, S. Kreiter, Ö. Türeci, U. Sahin, Induction of potent anti-tumoral immunity via systemic delivery of antigen-encoding RNA-lipoplexes, in 11th Annual Meeting of the Association for Cancer Immunotherapy2013: Mainz, Germany. p. 281.

[109] Watson, D.S., A.N. Endsley,L. Huang, Design considerations for liposomal vaccines: Influence of formulation parameters on antibody and cell-mediated

immune responses to liposome associated antigens (vol 30, pg 2256, 2012), Vaccine, 2012, 30 (39), 5799-5799.

[110] Andries, O., M. De Filette, S.C. De Smedt, J. Demeester, M. Van Poucke, L. Peelman,N.N. Sanders, Innate immune response and programmed cell death following carrier-mediated delivery of unmodified mRNA to respiratory cells, J Control Release, 2013, 167 (2), 157-66.

[111] Martinon, F., S. Krishnan, G. Lenzen, R. Magne, E. Gomard, J.G. Guillet, J.P. Levy,P. Meulien, Induction of virus-specific cytotoxic T lymphocytes in vivo by liposome-entrapped mRNA, European Journal of Immunology, 1993, 23 (7), 1719-22.

[112] Yan, W.,L. Huang, The effects of salt on the physicochemical properties and immunogenicity of protein based vaccine formulated in cationic liposome, International Journal of Pharmaceutics, 2009, 368 (1-2), 56-62.

[113] Regelin, A.E., S. Fankhaenel, L. Gurtesch, C. Prinz, G. von Kiedrowski,U. Massing, Biophysical and lipofection studies of DOTAP analogs, Biochimica et Biophysica Acta, 2000, 1464 (1), 151-64.

[114] Perche, F., D. Gosset, M. Mevel, M.L. Miramon, J.J. Yaouanc, C. Pichon, T. Benvegnu, P.A. Jaffres,P. Midoux, Selective gene delivery in dendritic cells with mannosylated and histidylated lipopolyplexes, Journal of Drug Targeting, 2011, 19 (5), 315-25.

[115] Wakim, L.M.,M.J. Bevan, Cross-dressed dendritic cells drive memory CD8+ T-cell activation after viral infection, Nature, 2011, 471 (7340), 629-32.

[116] Yewdall, A.W., S.B. Drutman, F. Jinwala, K.S. Bahjat,N. Bhardwaj, CD8+ T cell priming by dendritic cell vaccines requires antigen transfer to endogenous antigen presenting cells, Plos One, 2010, 5 (6), e11144.

[117] Aarntzen, E.H., G. Schreibelt, K. Bol, W.J. Lesterhuis, A.J. Croockewit, J.H. de Wilt, M.M. van Rossum, W.A. Blokx, J.F. Jacobs, T. Duiveman-de Boer, D.H. Schuurhuis, R. Mus, K. Thielemans, I.J. de Vries, C.G. Figdor, C.J. Punt,G.J. Adema, Vaccination with mRNA-Electroporated Dendritic Cells Induces Robust Tumor Antigen-Specific CD4+ and CD8+ T Cells Responses in Stage III and IV Melanoma Patients, Clinical Cancer Research, 2012, 18 (19), 5460-5470.

[118] Holtkamp, S., S. Kreiter, A. Selmi, P. Simon, M. Koslowski, C. Huber, O. Tureci,U. Sahin, Modification of antigen-encoding RNA increases stability, translational efficacy, and T-cell stimulatory capacity of dendritic cells, Blood, 2006, 108 (13), 4009-17.

[119] Kuhn, A.N., M. Diken, S. Kreiter, A. Selmi, J. Kowalska, J. Jemielity, E. Darzynkiewicz, C. Huber, O. Tureci,U. Sahin, Phosphorothioate cap analogs increase stability and translational efficiency of RNA vaccines in immature

dendritic cells and induce superior immune responses in vivo, Gene Therapy, 2010, 17 (8), 961-71.

[120] Probst, J., B. Weide, B. Scheel, B.J. Pichler, I. Hoerr, H.G. Rammensee,S. Pascolo, Spontaneous cellular uptake of exogenous messenger RNA in vivo is nucleic acid-specific, saturable and ion dependent, Gene Therapy, 2007, 14 (15), 1175-80.

[121] Wurtele, H., K.C. Little,P. Chartrand, Illegitimate DNA integration in mammalian cells, Gene Therapy, 2003, 10 (21), 1791-9.

[122] Nair, S.K., A. Heiser, D. Boczkowski, A. Majumdar, M. Naoe, J.S. Lebkowski, J. Vieweg,E. Gilboa, Induction of cytotoxic T cell responses and tumor immunity against unrelated tumors using telomerase reverse transcriptase RNA transfected dendritic cells, Nature Medicine, 2000, 6 (9), 1011-7.

[123] Lin, C., Z. Zhong, M.C. Lok, X. Jiang, W.E. Hennink, J. Feijen,J.F. Engbersen, Novel bioreducible poly(amido amine)s for highly efficient gene delivery, Bioconjugate Chemistry, 2007, 18 (1), 138-45.

[124] Torrieri-Dramard, L., B. Lambrecht, H.L. Ferreira, T. Van den Berg, D. Klatzmann,B. Bellier, Intranasal DNA vaccination induces potent mucosal and systemic immune responses and cross-protective immunity against influenza viruses, Mol Ther, 2011, 19 (3), 602-11.

[125] Leuschner, F., P. Dutta, R. Gorbatov, T.I. Novobrantseva, J.S. Donahoe, G. Courties, K.M. Lee, J.I. Kim, J.F. Markmann, B. Marinelli, P. Panizzi, W.W. Lee, Y. Iwamoto, S. Milstein, H. Epstein-Barash, W. Cantley, J. Wong, V. Cortez-Retamozo, A. Newton, K. Love, P. Libby, M.J. Pittet, F.K. Swirski, V. Koteliansky, R. Langer, R. Weissleder, D.G. Anderson,M. Nahrendorf, Therapeutic siRNA silencing in inflammatory monocytes in mice, Nature Biotechnology, 2011, 29 (11), 1005-10.

[126] Yu, B., J. Zhu, W. Xue, Y. Wu, X. Huang, L.J. Lee,R.J. Lee, Microfluidic assembly of lipid-based oligonucleotide nanoparticles, Anticancer Research, 2011, 31 (3), 771-6.

[127] Hung, L.H., S.Y. Teh, J. Jester,A.P. Lee, PLGA micro/nanosphere synthesis by droplet microfluidic solvent evaporation and extraction approaches, Lab Chip, 2010, 10 (14), 1820-5.

[128] Wang, J., P.C. Zhang, H.Q. Mao,K.W. Leong, Enhanced gene expression in mouse muscle by sustained release of plasmid DNA using PPE-EA as a carrier, Gene Therapy, 2002, 9 (18), 1254-61.

[129] Wang, J., P.C. Zhang, H.F. Lu, N. Ma, S. Wang, H.Q. Mao,K.W. Leong, New polyphosphoramidate with a spermidine side chain as a gene carrier, Journal of Controlled Release, 2002, 83 (1), 157-168.

[130] Caruso, D.A., L.M. Orme, A.M. Neale, F.J. Radcliff, G.M. Amor, W. Maixner, P. Downie, T.E. Hassall, M.L. Tang,D.M. Ashley, Results of a phase 1 study utilizing monocyte-derived dendritic cells pulsed with tumor RNA in children and young adults with brain cancer, Neuro Oncol, 2004, 6 (3), 236-46.

[131] Coosemans, A., M. Wolfl, Z.N. Berneman, V. Van Tendeloo, I. Vergote, F. Amant,S.W. Van Gool, Immunological response after therapeutic vaccination with WT1 mRNA-loaded dendritic cells in end-stage endometrial carcinoma, Anticancer Research, 2010, 30 (9), 3709-14.

[132] Morse, M.A., S.K. Nair, P.J. Mosca, A.C. Hobeika, T.M. Clay, Y. Deng, D. Boczkowski, A. Proia, D. Neidzwiecki, P.A. Clavien, H.I. Hurwitz, J. Schlom, E. Gilboa,H.K. Lyerly, Immunotherapy with autologous, human dendritic cells transfected with carcinoembryonic antigen mRNA, Cancer Investigation, 2003, 21 (3), 341-9.

[133] Rains, N., R.J. Cannan, W. Chen,R.S. Stubbs, Development of a dendritic cell (DC)-based vaccine for patients with advanced colorectal cancer, Hepato-Gastroenterology, 2001, 48 (38), 347-51.

[134] Steitz, J., C.M. Britten, T. Wolfel,T. Tuting, Effective induction of anti-melanoma immunity following genetic vaccination with synthetic mRNA coding for the fusion protein EGFP.TRP2, Cancer Immunology, Immunotherapy, 2006, 55 (3), 246-53.

[135] Su, Z., J. Dannull, B.K. Yang, P. Dahm, D. Coleman, D. Yancey, S. Sichi, D. Niedzwiecki, D. Boczkowski, E. Gilboa,J. Vieweg, Telomerase mRNA-transfected dendritic cells stimulate antigen-specific CD8+ and CD4+ T cell responses in patients with metastatic prostate cancer, Journal of Immunology, 2005, 174 (6), 3798-807.

[136] Nair, S., D. Boczkowski, S. Pruitt,J. Urban, RNA in cancer vaccine therapy, in Cancer Vaccines: From Research To Clinical Practice, A. Bot, Obrocea, M., Marincola, F. , Editor 2011, Informa Healthcare: Switzerland. p. 217-231.

[137] Kariko, K., H. Muramatsu, J.M. Keller,D. Weissman, Increased Erythropoiesis in Mice Injected With Submicrogram Quantities of Pseudouridine-containing mRNA Encoding Erythropoietin, Molecular Therapy, 2012, 20 (5), 948-953.

[138] Zohra, F.T., E.H. Chowdhury, M. Nagaoka,T. Akaike, Drastic effect of nanoapatite particles on liposome-mediated mRNA delivery to mammalian cells, Analytical Biochemistry, 2005, 345 (1), 164-166.

[139] Phua, K.K., K.W. Leong,S.K. Nair, Transfection efficiency and transgene expression kinetics of mRNA delivered in naked and nanoparticle format, J Control Release, 2013, 166 (3), 227-33.

[140] Nochi, T., Y. Yuki, H. Takahashi, S. Sawada, M. Mejima, T. Kohda, N. Harada, I.G. Kong, A. Sato, N. Kataoka, D. Tokuhara, S. Kurokawa, Y. Takahashi, H. Tsukada, S. Kozaki, K. Akiyoshi,H. Kiyono, Nanogel antigenic protein-delivery system for adjuvant-free intranasal vaccines, Nature Materials, 2010, 9 (7), 572-578.

[141] Lorenzi, J.C., A.P. Trombone, C.D. Rocha, L.P. Almeida, R.L. Lousada, T. Malardo, I.C. Fontoura, R.A. Rossetti, A.F. Gembre, A.M. Silva, C.L. Silva,A.A. Coelho-Castelo, Intranasal vaccination with messenger RNA as a new approach in gene therapy: use against tuberculosis, BMC Biotechnol, 2010, 10, 77.

[142] Porgador, A., H.F. Staats, B. Faiola, E. Gilboa,T.J. Palker, Intranasal immunization with CTL epitope peptides from HIV-1 or ovalbumin and the mucosal adjuvant cholera toxin induces peptide-specific CTLs and protection against tumor development in vivo, Journal of Immunology, 1997, 158 (2), 834-41.

[143] Gwinn, W.M., S.M. Kirwan, S.H. Wang, K.A. Ashcraft, N.L. Sparks, C.R. Doil, T.G. Tlusty, L.S. Casey, S.K. Hollingshead, D.E. Briles, R.S. Dondero, A.J. Hickey, W.M. Foster,H.F. Staats, Effective induction of protective systemic immunity with nasally administered vaccines adjuvanted with IL-1, Vaccine, 2010, 28 (42), 6901-14.

[144] Nair, S., C. McLaughlin, A. Weizer, Z. Su, D. Boczkowski, J. Dannull, J. Vieweg,E. Gilboa, Injection of immature dendritic cells into adjuvant-treated skin obviates the need for ex vivo maturation, Journal of Immunology, 2003, 171 (11), 6275-82.

[145] Mehrara, E., E. Forssell-Aronsson, H. Ahlman,P. Bernhardt, Specific growth rate versus doubling time for quantitative characterization of tumor growth rate, Cancer Research, 2007, 67 (8), 3970-3975.

[146] Antonia, S.J., M. Extermann,R.A. Flavell, Immunologic nonresponsiveness to tumors, Critical Reviews in Oncogenesis, 1998, 9 (1), 35-41.

[147] Dunn, G.P., A.T. Bruce, H. Ikeda, L.J. Old,R.D. Schreiber, Cancer immunoediting: from immunosurveillance to tumor escape, Nat Immunol, 2002, 3 (11), 991-8.

[148] Marincola, F.M., E.M. Jaffee, D.J. Hicklin,S. Ferrone, Escape of human solid tumors from T-cell recognition: molecular mechanisms and functional significance, Advances in Immunology, 2000, 74, 181-273.

[149] Bodmer, W.F., M.J. Browning, P. Krausa, A. Rowan, D.C. Bicknell,J.G. Bodmer, Tumor escape from immune response by variation in HLA expression and other mechanisms, Annals of the New York Academy of Sciences, 1993, 690, 42-9.

[150] Baumgartner, J., C. Wilson, B. Palmer, D. Richter, A. Banerjee,M. McCarter, Melanoma induces immunosuppression by up-regulating FOXP3(+) regulatory T cells, Journal of Surgical Research, 2007, 141 (1), 72-7.

[151] Rabinovich, G.A., D. Gabrilovich,E.M. Sotomayor, Immunosuppressive strategies that are mediated by tumor cells, Annual Review of Immunology, 2007, 25, 267-96.

[152] Aptsiauri, N., T. Cabrera, R. Mendez, A. Garcia-Lora, F. Ruiz-Cabello,F. Garrido, Role of altered expression of HLA class I molecules in cancer progression, Advances in Experimental Medicine and Biology, 2007, 601, 123-31.

[153] Restifo, N.P., Y. Kawakami, F. Marincola, P. Shamamian, A. Taggarse, F. Esquivel,S.A. Rosenberg, Molecular mechanisms used by tumors to escape immune recognition: immunogenetherapy and the cell biology of major histocompatibility complex class I, Journal of Immunotherapy With Emphasis on Tumor Immunology, 1993, 14 (3), 182-90.

[154] Paschen, A., R.M. Mendez, P. Jimenez, A. Sucker, F. Ruiz-Cabello, M. Song, F. Garrido,D. Schadendorf, Complete loss of HLA class I antigen expression on melanoma cells: a result of successive mutational events, International Journal of Cancer, 2003, 103 (6), 759-67.

[155] Fernandez, S., E.D. Cisney,R.G. Ulrich, Enhancement of Serum and Mucosal Immune Responses to a Haemophilus influenzae Type B Vaccine by Intranasal Delivery, Clinical and Vaccine Immunology, 2013, 20 (11), 1690-1696.

[156] Li, Y.H., J. Jin, Y.P. Yang, Z.A. Bian, Z. Chen,M.W. Fan, Enhanced immunogenicity of an anti-caries vaccine encoding a cell-surface protein antigen of Streptococcus mutans by intranasal DNA prime-protein boost immunization, Journal of Gene Medicine, 2009, 11 (11), 1039-1047.

[157] Mohan, T., D. Mitra,D.N. Rao, Nasal delivery of PLG microparticle encapsulated defensin peptides adjuvanted gp41 antigen confers strong and long-lasting immunoprotective response against HIV-1, Immunologic Research, 2014, 58 (1), 139-153.

[158] Nguyen, C.T., S.Y. Kim, M.S. Kim, S.E. Lee,J.H. Rhee, Intranasal immunization with recombinant PspA fused with a flagellin enhances cross-protective immunity against Streptococcus pneumoniae infection in mice, Vaccine, 2011, 29 (34), 5731-5739.

[159] Pontes, D., M. Azevedo, S. Innocentin, S. Blugeon, F. Lefevre, V. Azevedo, A. Miyoshi, P. Courtin, M.P. Chapot-Chartier, P. Langella,J.M. Chatel, Immune Response Elicited by DNA Vaccination Using Lactococcus lactis Is Modified by the Production of Surface Exposed Pathogenic Protein, Plos One, 2014, 9 (1)

[160] Wu, Y.B., W. Wei, M. Zhou, Y.Q. Wang, J. Wu, G.H. Ma,Z.G. Su, Thermal-sensitive hydrogel as adjuvant-free vaccine delivery system for H5N1 intranasal immunization, Biomaterials, 2012, 33 (7), 2351-2360.

[161] Yao, W., Y. Peng, M. Du, J. Luo,L. Zong, Preventative vaccine-loaded mannosylated chitosan nanoparticles intended for nasal mucosal delivery enhance immune responses and potent tumor immunity, Mol Pharm, 2013, 10 (8), 2904-14.

[162] Boczkowski, D., S.K. Nair, J.H. Nam, H.K. Lyerly,E. Gilboa, Induction of tumor immunity and cytotoxic T lymphocyte responses using dendritic cells transfected with messenger RNA amplified from tumor cells, Cancer Research, 2000, 60 (4), 1028-34.

[163] Rittig, S.M., M. Haentschel, K.J. Weimer, A. Heine, M.R. Muller, W. Brugger, M.S. Horger, O. Maksimovic, A. Stenzl, I. Hoerr, H.G. Rammensee, T.A. Holderried, L. Kanz, S. Pascolo,P. Brossart, Intradermal vaccinations with RNA coding for TAA generate CD8+ and CD4+ immune responses and induce clinical benefit in vaccinated patients, Mol Ther, 2011, 19 (5), 990-9.

[164] Russo, V., A. Cipponi, L. Raccosta, C. Rainelli, R. Fontana, D. Maggioni, F. Lunghi, S. Mukenge, F. Ciceri, M. Bregni, C. Bordignon,C. Traversari, Lymphocytes genetically modified to express tumor antigens target DCs in vivo and induce antitumor immunity, Journal of Clinical Investigation, 2007, 117 (10), 3087-96.

[165] Murray, A.M., I.F. Pearson, L.D. Fairbanks, R.A. Chalmers, M.D. Bain,B.E. Bax, The mouse immune response to carrier erythrocyte entrapped antigens, Vaccine, 2006, 24 (35-36), 6129-39.

[166] Lee, J., C.M. Dollins, D. Boczkowski, B.A. Sullenger,S. Nair, Activated B cells modified by electroporation of multiple mRNAs encoding immune stimulatory molecules are comparable to mature dendritic cells in inducing in vitro antigen-specific T-cell responses, Immunology, 2008, 125 (2), 229-240.

[167] Hamidi, M., N. Zarei, A.H. Zarrin,S. Mohammadi-Samani, Preparation and in vitro characterization of carrier erythrocytes for vaccine delivery, International Journal of Pharmaceutics, 2007, 338 (1-2), 70-8.

[168] Chiarantini, L., D. Matteucci, M. Pistello, U. Mancini, P. Mazzetti, C. Massi, S. Giannecchini, I. Lonetti, M. Magnani,M. Bendinelli, AIDS vaccination studies using an ex vivo feline immunodeficiency virus model: Homologous erythrocytes as a delivery system for preferential immunization with putative protective antigens, Clinical and Diagnostic Laboratory Immunology, 1998, 5 (2), 235-241.

[169] Banz, A., M. Cremel, A. Mouvant, N. Guerin, F. Horand,Y. Godfrin, Tumor Growth Control Using Red Blood Cells as the Antigen Delivery System and Poly(I:C), Journal of Immunotherapy, 2012, 35 (5), 409-417.

[170] Burch, P.A., G.A. Croghan, D.A. Gastineau, L.A. Jones, J.S. Kaur, J.W. Kylstra, R.L. Richardson, F.H. Valone,S. Vuk-Pavlovic, Immunotherapy (APC8015, Provenge) targeting prostatic acid phosphatase can induce durable remission of metastatic androgen-independent prostate cancer: a Phase 2 trial, Prostate, 2004, 60 (3), 197-204.

[171] Rowley, P.T.,J.A. Morris, Protein synthesis in the maturing reticulocyte, Journal of Biological Chemistry, 1967, 242 (7), 1533-40.

[172] Moenner, M., M. Vosoghi, S. Ryazantsev,D.G. Glitz, Ribonuclease inhibitor protein of human erythrocytes: characterization, loss of activity in response to oxidative stress, and association with Heinz bodies, Blood Cells, Molecules, and Diseases, 1998, 24 (2), 149-64.

[173] Porgador, A., E. Tzehoval, E. Vadai, M. Feldman,L. Eisenbach, Combined vaccination with major histocompatibility class I and interleukin 2 gene-transduced melanoma cells synergizes the cure of postsurgical established lung metastases, Cancer Research, 1995, 55 (21), 4941-9.

[174] Nair, S., D. Boczkowski, B. Moeller, M. Dewhirst, J. Vieweg,E. Gilboa, Synergy between tumor immunotherapy and antiangiogenic therapy, Blood, 2003, 102 (3), 964-71.

[175] Blomberg, K., C. Granberg, I. Hemmila,T. Lovgren, Europium-labelled target cells in an assay of natural killer cell activity. I. A novel non-radioactive method based on time-resolved fluorescence, Journal of Immunological Methods, 1986, 86 (2), 225-9.

[176] Porgador, A., D. Snyder,E. Gilboa, Induction of antitumor immunity using bone marrow-generated dendritic cells, Journal of Immunology, 1996, 156 (8), 2918-26.

[177] Wink, D.A., H.B. Hines, R.Y. Cheng, C.H. Switzer, W. Flores-Santana, M.P. Vitek, L.A. Ridnour,C.A. Colton, Nitric oxide and redox mechanisms in the immune response, Journal of Leukocyte Biology, 2011, 89 (6), 873-91.

[178] Tekle, E., M.D. Wolfe, H. Oubrahim,P.B. Chock, Phagocytic clearance of electric field induced 'apoptosis-mimetic' cells, Biochemical and Biophysical Research Communications, 2008, 376 (2), 256-60.

[179] Berg, C.P., I.H. Engels, A. Rothbart, K. Lauber, A. Renz, S.F. Schlosser, K. Schulze-Osthoff,S. Wesselborg, Human mature red blood cells express caspase-3 and caspase-8, but are devoid of mitochondrial regulators of apoptosis, Cell Death and Differentiation, 2001, 8 (12), 1197-206.

[180] Lui, J.C., J.W. Wong, Y.K. Suen, T.T. Kwok, K.P. Fung,S.K. Kong, Cordycepin induced eryptosis in mouse erythrocytes through a Ca2+-dependent pathway without caspase-3 activation, Archives of Toxicology, 2007, 81 (12), 859-65.

[181] Siniscalco, D., A. Sapone, C. Giordano, A. Cirillo, V. de Novellis, L. de Magistris, F. Rossi, A. Fasano, S. Maione,N. Antonucci, The Expression of Caspases is Enhanced in Peripheral Blood Mononuclear Cells of Autism Spectrum Disorder Patients, Journal of Autism and Developmental Disorders, 2012, 42 (7), 1403-1410.

[182] Schroit, A.J., J.W. Madsen,Y. Tanaka, In vivo recognition and clearance of red blood cells containing phosphatidylserine in their plasma membranes, Journal of Biological Chemistry, 1985, 260 (8), 5131-8.

[183] Uggeri, J., R. Gatti, S. Belletti, R. Scandroglio, R. Corradini, B.M. Rotoli,G. Orlandini, Calcein-AM is a detector of intracellular oxidative activity, Histochemistry and Cell Biology, 2004, 122 (5), 499-505.

[184] Kim, S.H., E.J. Kim, J.H. Hou, J.M. Kim, H.G. Choi, C.K. Shim,Y.K. Oh, Opsonized erythrocyte ghosts for liver-targeted delivery of antisense oligodeoxynucleotides, Biomaterials, 2009, 30 (5), 959-67.

Biography

Born on December 7, 1976. Singapore

Education

2008 – 2014	Ph.D (Biomedical Engineering), May 2014. Duke University. Durham, NC
2001 – 2002	Joint M.S (Chemical Engineering), Dec 2002. NUS and U of Illinois (Champaign-Urbana).
1997 – 2001	B.Eng (Chemical) 1st Class Honors, July 2001. National University of Singapore

Honors, Prizes and Awards

2013 Gordon Research Seminar Registration Award
2013 National Sigma-Xi Grant-in-Aid Research Award
2013 11th Association for Cancer Immunotherapy (CIMT) Travel Award
2013 Duke University Conference Travel Fellowship
2013 R&D Systems Travel Award
2012 National University of Singapore Field Work Grant
2012 National University of Singapore Travel Grant
2012 National Sigma-Xi Grant-in-Aid Research Award
2012 Duke University Medical Center Core Facility Voucher Award
2011 Biolegend Young Investigator Travel Award
2010 Mirus Research Award
2009 Graduate Research Assistantship. Duke University
2008 NUS Overseas Graduate (Ph.D) Scholarship

PUBLICATIONS

Phua K.L, Chiew YC. 2002. A Perturbed Yukawa Chain Equation of State for Real Non-Associating Fluids. . Journal of the Institution of Engineers Singapore 41 - 9

Phua K, Leong KW. 2010. Microscale oral delivery devices incorporating nanoparticles. Nanomedicine (Lond) 5:161-3.

Phua K.K.L, Roberts ERH, Leong KW. 2011. Degradable Polymers. In Comprehensive Biomaterials, 1:381-415 Elsevier.

Phua K.K., Boczkowski D, Dannull J, Pruitt S, Leong KW, Nair SK. 2013. Whole Blood Cells Loaded with Messenger RNA as an Anti-Tumor Vaccine. Advanced Healthcare Materials .

Phua K.K.L., Leong KW, Nair SK. 2013. Transfection efficiency and transgene expression kinetics of mRNA delivered in naked and nanoparticle format. Journal of Controlled Release 166:227-33.

Chiu Y, Chen HF, **Phua K.K.L.**, Zhang Y, Juul S, *et al.* 2014. Synthesis of Fluorosurfactants for Emulsion-Based Biological Applications. ACS Nano. (Accepted).

Phua K.K.L., Nair SK, Leong KW. 2014. mRNA Nanoparticle Tumor Vaccination. Nanoscale. (Submitted).

Phua K.K.L, Staats HF, Nair SK, Leong KW. 2014. Intranasal mRNA Nanoparticle Vaccination Induces Prophylactic and Therapeutic Anti-Tumor Immunity. Scientific Reports. (Revising).

US Provisional Appln No. 61/750,979 filed January 10, 2013. “Vaccinating with RNA-Loaded Blood Cells”.

POSTER PRESENTATIONS

Phua, K.K.L.,Leong K.W., Transfecting JAWS II Cells with Ternary-Core mRNA Lipopolyplexes, in Biomedical Engineering Society Conference, 2010: Austin, TX.

K.K.L Phua, K.W. Leong, Chemically Modified mRNA and "Trans-Effect" Together Enhances Transfection On Dendritic Cells, in NC ACS, 2011: Raleigh, NC.

Urban, J., D. Boczkwoski, **K.K.L. Phua**, S.K. Nair, Targeting Tumor Antigens To Dendritic Cells In Vivo Using Receptor-Specific Aptamers Conjugated To Tumor Antigen, in 7th Annual Meeting of The Oligonucleotide-Therapeutics Society, 2011: Copenhagen, Denmark.

Friede, K., M. Smith, Z. Zhang, Q. Ma, **K.K.L. Phua**, K.W. Leong, M. Podgoreanu, Experimental Circulation: Ischemia and Reperfusion Injury: MicroRNA-146b Attenuates Myocardial NF-kB Signaling Following Ischemia-Reperfusion: Early Translation to Perioperative Cardioprotection, in Anesthesiology, 2012: Washington, DC.

K.K.L Phua, K.W. Leong, S.K. Nair, Insights Into A New Treatment Strategy: Delivering mRNA Vaccines Using Synthetic And Natural Materials, in Duke University Center For AIDs Research Annual Retreat, 2012: Durham, NC.

K.K.L Phua, D. Boczkwoski, K.W. Leong, S.K. Nair, Using Synthetic and Natural Carriers To Deliver mRNA Cancer Vaccine, in Duke Center For Biomaterials & Tissue Engineering (CBTE) Kewaunee Event, 2013: Durham, NC.

K.K.L Phua, D. Boczkwoski, K.W. Leong, S.K. Nair, Using Synthetic and Natural Carriers To Deliver mRNA Cancer Vaccine, in 1st Duke-NUS Symposium, 2013: Durham, NC.

K.K.L Phua, D. Boczkwoski, K.W. Leong, S.K. Nair, Induction of Anti-Tumor Immunity With mRNA-loaded Apoptotic Cell and Gene Therapy, in Gordon Research Conference: Apoptotic Cell Recognition & Clearance , 2013: Biddeford, ME.

ORAL PRESENTATIONS

K.K.L Phua, K.W. Leong, S.K. Nair, In vivo Transfection Efficiencies and Pharmacokinetics of mRNA Delivered In Naked and Nanoparticle Format, in International Conference on Genetic Syndromes & Gene Therapy, 2012: San Antonio, TX. p. 227-233.

K.K.L Phua, D. Boczkowski, J. Dannull, S. Pruitt, K.W. Leong, S.K. Nair, Therapeutic Vaccination with mRNA-loaded Whole Blood Cells, in 11th Association for Cancer Immunotherapy (CIMT) Annual Meeting, 2013: Mainz, Germany.

K.K.L Phua, mRNA & Immunotherapy, in Invited Seminar, 2013: Singapore General Hospital.

K.K.L Phua, RNA therapy: Present Impact, Future Potential, in Invited Seminar, 2013: Department of Chemical & Biomolecular Engineering. NUS. Singapore.

K.K.L Phua, D. Boczkwoski, K.W. Leong, S.K. Nair, Induction of Anti-Tumor Immunity With mRNA-loaded Apoptotic Cell and Gene Therapy, in Gordon Research Seminar: Apoptotic Cell Recognition & Clearance , 2013: Biddeford, ME.

K.K.L Phua, D. Boczkwoski, K.W. Leong, S.K. Nair, Delivering mRNA Vaccines Using Synthetic and Natural Materials, in 1st IBN International Symposium, 2013: Singapore.

K.K.L Phua, D. Boczkwoski, K.W. Leong, S.K. Nair, Using Synthetic and Natural Materials to Deliver Messenger RNA and Confer Cancer Immunity, in 3rd Molecular Materials Meeting, 2013: Singapore.